

FUSION OF TARGET DENSITY AND INTENSITY FUNCTIONS BASED
ON CHERNOFF FUSION USING SIGMA POINTS

A THESIS SUBMITTED TO
THE GRADUATE SCHOOL OF NATURAL AND APPLIED SCIENCES
OF
MIDDLE EAST TECHNICAL UNIVERSITY

BY
MELİH GÜNAY

IN PARTIAL FULFILLMENT OF THE REQUIREMENTS
FOR
THE DEGREE OF DOCTOR OF PHILOSOPHY
IN
ELECTRICAL AND ELECTRONICS ENGINEERING

FEBRUARY 2015

Approval of the thesis:

**FUSION OF TARGET DENSITY AND INTENSITY FUNCTIONS
BASED ON CHERNOFF FUSION USING SIGMA POINTS**

submitted by **MELİH GÜNEY** in partial fulfillment of the requirements for
the degree of **Doctor of Philosophy in Electrical and Electronics Engineering**
Department, Middle East Technical University by,

Prof. Dr. Gülbin Dural Ünver _____
Dean, Graduate School of **Natural and Applied Sciences**

Prof. Dr. Gönül Turhan Sayan _____
Head of Department, **Electrical and Electronics Eng.**

Prof. Dr. Mübeccel Demirekler _____
Supervisor, **Electrical and Electronics Eng. Dept.,** _____
METU

Assoc. Prof. Dr. Umut Orguner _____
Co-supervisor, **Electrical and Electronics Eng. Dept.,** _____
METU

Examining Committee Members:

Prof. Dr. Orhan Arıkan _____
Electrical and Electronics Eng. Dept., Bilkent University

Prof. Dr. Mübeccel Demirekler _____
Electrical and Electronics Eng. Dept., METU

Assoc. Prof. Dr. Afşar Saranlı _____
Electrical and Electronics Eng. Dept., METU

Assoc. Prof. Dr. Asım Egemen Yılmaz _____
Electrical and Electronics Eng. Dept., Ankara University

Assoc. Prof. Dr. Çağatay Candan _____
Electrical and Electronics Eng. Dept., METU

Date: _____

I hereby declare that all information in this document has been obtained and presented in accordance with academic rules and ethical conduct. I also declare that, as required by these rules and conduct, I have fully cited and referenced all material and results that are not original to this work.

Name, Last Name: MELİH GÜNEY

Signature :

ABSTRACT

FUSION OF TARGET DENSITY AND INTENSITY FUNCTIONS BASED ON CHERNOFF FUSION USING SIGMA POINTS

GÜNAY, MELİH

Ph.D., Department of Electrical and Electronics Engineering

Supervisor : Prof. Dr. Mübeccel Demirekler

Co-Supervisor : Assoc. Prof. Dr. Umut Orguner

February 2015, 151 pages

Handling of unknown correlation in the target information obtained from different sources is an important problem for consistent track fusion. Chernoff fusion technique is one of the popular approaches which produce conservative fusion results to bring this consistency. This method is based on exponential scaling of the input functions and it provides an analytical solution when input functions are Gaussian densities. The thesis mainly discusses the extension of the Chernoff fusion method to Gaussian Mixtures in a consistent and robust way and proposes an approximate approach for the computation of the fused output. The exponential scaling, required for Chernoff fusion, is based on a sigma-point approximation of the underlying functions. The resulting general fusion rule yields a closed form problem formulation that gives the fused function as a Gaussian mixture. Effectiveness of the fusion method is presented for simple but illustrative density fusion problems and compared to the optimal solutions and exact numerical Chernoff fusion. The technique is applied to the

IMM filter used in target tracking problems. The results show the effectiveness of the method. The second application of the method is to fuse the PHD filter outputs that are Gaussian Mixture intensities. PHD filters are again used in target tracking. Different fusion architectures are investigated and their results are compared with each other. The comparison is also made with other available methods whenever they are applicable.

Keywords: Handling unknown correlation, Chernoff fusion of Gaussian mixtures, Single-target IMM track density fusion, Multi-target PHD target intensity fusion

ÖZ

SİGMA NOKTALARLA YAPILAN CHERNOFF BİRLEŞTİRME KURALINA DAYALI HEDEF OLASILIK DAĞILIM VE YOĞUNLUK FONKSİYONLARININ BİRLEŞTİRİLMESİ

GÜNAY, MELİH

Doktora, Elektrik ve Elektronik Mühendisliği Bölümü

Tez Yöneticisi : Prof. Dr. Mübeccel Demirekler

Ortak Tez Yöneticisi : Doç. Dr. Umut Orguner

Şubat 2015 , 151 sayfa

Farklı kaynaklardan elde edilen hedef bilgilerindeki bilinmeyen korelasyonun ele alınması tutarlı bir iz füzyonu yapılması açısından önemli bir problemdir. Chernoff birleştirme tekniği bu tutarlılığı sağlamak adına önerilen popüler yöntemlerden biridir. Bu yöntem girdi fonksiyonlarının üstel olarak ağırlıklandırılmasına dayanmakta ve Gauss dağılımlı fonksiyonlar için analitik çözüm önermektedir. Bu tezde Gauss Karışımli fonksiyonlar için Chernoff birleştirme yönteminin geliştirilmesi ve tutarlı ve gürbüz sonuçlar elde edilmesine yönelik çözüm önerilmektedir. Önerilen teknik Gauss karışım fonksiyonunun yaklaşık üstel değerini bulmayı gerektirir. Üstel değer bulma işlemi girdi fonksiyonlara sigma nokta yaklaştırmı uygulanması ile sağlanmaktadır. Sonuçta, Gauss karışımli fonksiyonlar için kapalı formda bir maliyet fonksiyonu üretilmekte ve füzyon sonucu yeni bir Gauss karışımı olarak elde edilmektedir. Önerilen yöntemin etkinliği

basit ve aydınlatıcı örneklerde gösterilmiştir. Bu örneklerde olasılık yoğunluk fonksiyonlarının birleştirilmesi problemi ele alınmış ve önerilen yöntem optimal çözüm ve nümerik Chernoff birleştirme çözümleri ile kıyaslanmıştır. Bu teknik, hedef izlemede güncel bir problem olan IMM süzgeci içeren füzyon mimarilerinin çıktılarının birleştirilmesi amacı ile kullanılmıştır. Diğer bir güncel problem olan PHD filtresi içeren füzyon mimarilerinin çıktılarının birleştirilmesi problemi için de aynı yöntem kullanılmıştır. Sonuçlar gerek değişik füzyon mimarileri için gerekse, olabildiği durumlarda, değişik füzyon yöntemleri için karşılaştırılmıştır.

Anahtar Kelimeler: Bilinmeyen korelasyonun ele alınması, Gauss karışımlarının Chernoff birleştirme tekniği ile birleştirilmesi, Tek hedef IMM iz olasılık dağılım fonksiyonu birleştirimi, Çoklu-hedef PHD hedef yoğunluk fonksiyonu birleştirimi

To my wife “Elif” and my daughter “Ada”...

ACKNOWLEDGMENTS

I would like to thank my supervisor Professor Demirekler for her constant support, guidance and friendship. It was a great honor to work with her for the last ten years and our cooperation influenced my academical and world view highly. I also would like to thank Assoc. Prof. Orguner for his strong support and guidance during all phases of this thesis study.

This thesis is also supported by my company, ASELSAN, and I would like to thank all of my managers and colleagues there because of their patience and understanding me throughout this very long and challenging period of study time.

A lot of people from ASELSAN influenced and supported this work but Hüseyin Yavuz is the one who directed me to start this Ph.D. program, and always understood and encouraged me in this period, so I would like to thank specially to him a lot.

Many thanks goes to Prof. Akar for allowing me to study in the excellent multimedia research laboratory which helped me very much during the writing phase of this thesis.

My parents also has provided invaluable support for this work. I would like to thank specially to my mother Vildan, my mother-in law Gülbeyaz, my father Mehmet, my sister Melike and brother-in-law Emre who always make me feel loved and cared.

Last words goes to my family, my wife Elif and my daughter Ada. This thesis would not appear in this way without their endless love...

TABLE OF CONTENTS

ABSTRACT	v
ÖZ	vii
ACKNOWLEDGMENTS	x
TABLE OF CONTENTS	xi
LIST OF TABLES	xvi
LIST OF FIGURES	xviii
LIST OF ABBREVIATIONS	xxiv
CHAPTERS	
1 INTRODUCTION	1
1.1 Introduction to Data Fusion	4
1.2 Elimination of Unknown Correlation in Decentralized Fusion Systems	6
1.2.1 Channel Filter Fusion	8
1.2.2 Naïve Fusion	8
1.2.3 Chernoff Fusion	9
1.2.4 Shannon Fusion	10
1.2.5 Bhattacharyya Fusion	10

1.3	Elimination of Unknown Correlation in Track Fusion Problems	11
1.4	State-Of-The Art Fusion Techniques for Gaussian Densities and Gaussian Mixture Densities	12
1.5	Analysis and Comparison of the Existing Studies for Track Fusion Architectures	13
2	SIGMA POINT CHERNOFF FUSION	17
2.1	Introduction	17
2.2	Covariance Intersection and Chernoff Fusion	18
2.3	Chernoff Fusion of Gaussian Mixtures Using Sigma-Points	19
2.3.1	Taking the w^{th} Power of a Gaussian Mixture .	20
2.3.2	Chernoff Fusion of Gaussian Mixtures	23
2.4	Comparison of Different Fusion Techniques with Optimum Fusion Based on Simulations	24
2.4.1	1D-Case	27
2.4.1.1	Parameter Selection I	27
2.4.1.2	Parameter Selection II	29
2.4.2	2D-Case	30
2.5	Comparison of Different Fusion Techniques with Numeric Chernoff Fusion Based on Simulations	33
2.6	Discussions	37
3	FUSION OF IMM'S IN A DECENTRALIZED RADAR SYSTEM	39
3.1	Introduction	39
3.2	Short Description of IMM (Adopted from [5])	40

3.3	Fusion Strategies Regarding the Fusion of Information Produced by Local and Remote IMM's	43
3.3.1	Fusion Strategy-1	44
3.3.1.1	Implementation of Naive Fusion Tech- nique	45
3.3.1.2	Implementation of SPCF Technique	48
3.3.2	Fusion Strategy-2	50
3.3.3	Fusion Strategy-3	53
3.3.4	Fusion Strategy-4	56
3.4	Performance Evaluation	57
3.4.1	Ideal System Scenarios	59
3.4.1.1	Selection of the Target and the Radar Characteristics	59
3.4.1.2	Analysis of the IMM Filter to be Used	61
3.4.1.3	Fusion Experiments	62
3.4.2	Realistic System Scenarios	70
3.4.2.1	Selection of Targets	71
3.4.2.2	Radar Model	73
3.4.2.3	Filter Parameters	76
3.4.2.4	Fusion Experiments	77
3.5	Discussions	82
4	FUSION OF PHD'S IN A DECENTRALIZED RADAR SYSTEM	87
4.1	Introduction	87

4.2	The PHD Filter	88
4.2.1	PHD Filter Stages	92
4.2.2	Basic PHD Implementations	94
4.2.2.1	Gaussian Mixture PHD Filter	94
4.2.2.2	Particle PHD Filter	96
4.3	Multisensor PHD Fusion	96
4.3.1	Centralized PHD Fusion	96
4.3.2	Decentralized PHD Fusion	98
4.4	Fusion of Multiple PHD Filters with Unknown Correlation	98
4.4.1	PHD Fusion Strategies	99
4.4.2	Derivations for SPCF Fusion of Local and Remote PHD Filters	102
4.5	Performance Evaluation	104
4.5.1	OSPA(Optimal SubPattern Assignment) Metric	105
4.5.2	Experiment Set-up	106
4.5.3	Target Scenarios	107
4.5.4	Target Model and Related Parameters	108
4.5.5	Radar Model	109
4.5.6	PHD Filter	111
4.5.7	Fusion Results	112
4.6	Discussions	116
5	CONCLUSION	135

REFERENCES	139
APPENDICES	
A EK-GMPHD FILTER PSEUDO CODE	145
CURRICULUM VITAE	149

LIST OF TABLES

TABLES

Table 1.1	Existence analysis of state-of-the art fusion techniques to Gaussian densities and Gaussian mixture densities.	13
Table 2.1	Cost of different approximations. Results of PCCI and Pseudo Chernoff-1 techniques are adopted from [26].	36
Table 2.2	Approximate computation times for numeric Chernoff, Pseudo Chernoff and SPCF techniques.	37
Table 3.1	Experiments designed to understand performance boundaries of the strategies.	63
Table 3.2	Summary of the fusion techniques to be analyzed.	64
Table 3.3	Radar parameters selected for the experiments.	75
Table 3.4	Average computation times for each strategy.	82
Table 4.1	Some concepts in the single sensor/target domain and their correspondence in the multi one (adopted from the reference [39]). . .	90
Table 4.2	Average computation times in seconds for PHD fusion techniques.	116
Table A.1	EK-GMPHD filter (Prediction of birth targets, prediction of existing targets, construction of PHD update components steps),(adopted from [47]).	146

Table A.2 EK-GMPHD filter (Measurement update and outputting steps), (adopted from [47]).	147
Table A.3 EK-GMPHD filter (Pruning step), (adopted from [47]). . . .	148
Table A.4 EK-GMPHD filter (Multitarget state extraction), (adopted from [47]).	148

LIST OF FIGURES

FIGURES

Figure 1.1	Suspect list for the robbery.	2
Figure 1.2	Unknown conversation made before the interrogation day. . .	3
Figure 1.3	Some examples to radar communication structures.	15
Figure 1.4	Cyclic communication scenario (adopted from [10]).	16
Figure 1.5	Track fusion architecture based on IMM filter in which Gaussian densities are exchanged.	16
Figure 1.6	Track fusion architecture based on PHD filter in which Gaussian mixture intensities are exchanged.	16
Figure 2.1	Covariance intersection algorithm in two dimensional case ($n = 2$). Similar figures also appear in [23, 25].	20
Figure 2.2	The densities $p(\cdot)$, $p_1(\cdot)$, $p_2(\cdot)$ and $p_{\text{optimal}}(\cdot)$ for parameter selection I.	28
Figure 2.3	The fused densities $p_{\text{optimal}}(\cdot)$, $p_{\text{naive}}(\cdot)$, $p_{\text{CF}}(\cdot)$ and $p_{\text{scaling}}(\cdot)$ for parameter selection I.	29
Figure 2.4	The cdfs for e_{mean} for parameter selection I.	30
Figure 2.5	The cdfs for e_{std} for parameter selection I.	31
Figure 2.6	The cdfs for e_{mean} for parameter selection II.	32
Figure 2.7	The cdfs for e_{std} for parameter selection II.	33

Figure 2.8 The cdfs for e_{mean} for parameter selection for 2D.	34
Figure 2.9 The cdfs for e_{std} for parameter selection for 2D.	35
Figure 2.10 Input estimates for the benchmark scenario.	36
Figure 2.11 Fusion results for the benchmark scenario. Results of PCCI and Pseudo Chernoff-1 techniques are adopted from [26].	38
Figure 3.1 Block diagram of the IMM for two models.	40
Figure 3.2 IMM fusion structure in which Gaussian mixtures are ex- changed and Naive/SPCF methods are applicable.	45
Figure 3.3 IMM fusion structure in which Gaussian mixtures are ex- changed and SPCF method is used.	51
Figure 3.4 IMM fusion structure in which Gaussian densities are ex- changed and CI method is applied in a feedback mechanism.	54
Figure 3.5 IMM fusion structure in which only state estimates are ex- changed and CI method is applicable.	57
Figure 3.6 Experimental set-up to analyze different fusion approaches. .	59
Figure 3.7 Markov chain for the selection of the process noise model. . .	61
Figure 3.8 One of the generated targets and related radar measurements.	62
Figure 3.9 Radar measurements and IMM tracker outputs on the zoomed version of Figure 3.8.	63
Figure 3.10 IMM weights for different models (belonging to the IMM ex- ample in Figure 3.9).	64
Figure 3.11 Ensemble average of NIS values and required boundaries. . .	65
Figure 3.12 Ensemble average of NEES values and required boundaries. .	66

Figure 3.13 Ensemble average of the fusion results for the parameters $\sigma_{p1} = 1$, $\sigma_{p2} = 35$ and $\sigma_r = 50$. Dashed lines represent the mean lines for each result.	67
Figure 3.14 Zoomed version of Figure 3.13.	68
Figure 3.15 Mean of L2 Norm error of the ensemble averages vs different measurement noise standard deviations for $\sigma_{p1} = 1$ and $\sigma_{p2} = 35$. . .	69
Figure 3.16 Zoomed version of Figure 3.15 to exclude Naive fusion. . . .	70
Figure 3.17 Zoomed version of Figure 3.15 focusing in the measurement noise standard deviation margin [10-50].	71
Figure 3.18 Mean of L2 Norm error of the ensemble averages vs. alpha parameter ($\sigma_{p1} = 1 \times \alpha$, $\sigma_{p2} = 35 \times \alpha$ and $\sigma_r = 25$).	72
Figure 3.19 Zoomed version of Figure 3.18 to exclude Naive fusion. . . .	73
Figure 3.20 Trajectory of Target-2 and deployment of radars.	74
Figure 3.21 Trajectory of Target-6 and deployment of radars.	75
Figure 3.22 Experimental set-up adapted to radar simulator to pick-up the target related measurements.	76
Figure 3.23 Fusion performances of the techniques at the “local radar” for target-2. Dashed gray line corresponds to the maneuver of the target and other dashed lines represent the mean lines for each result. . . .	78
Figure 3.24 Fusion performances of the techniques at the “remote radar” for target-2. Dashed gray line corresponds to the maneuver of the target and other dashed lines represent the mean lines for each result. . . .	79
Figure 3.25 Fusion performances of the techniques at the “local radar” for Target-6. Dashed gray line corresponds to the maneuver of the target and other dashed lines represent the mean lines for each result. . . .	80
Figure 3.26 Zoomed version of Figure 3.25.	81

Figure 3.27 Fusion performances of the techniques at the “remote radar” for Target-6. Dashed gray line corresponds to the maneuver of the target and other dashed lines represent the mean lines for each result.	82
Figure 3.28 Zoomed version of Figure 3.27.	83
Figure 3.29 An adaptive hybrid fusion structure which includes SPCF and Naive techniques.	84
Figure 3.30 Target-6 results for the hybrid structure together with those of SPCF and Naive techniques. Dashed gray line corresponds to the maneuver of the target and other dashed lines represent the mean lines for each result.	85
Figure 4.1 Transforming multitarget/sensor world into a meta world (adopted from the reference [2]).	89
Figure 4.2 Basic steps in the PHD filtering process.	93
Figure 4.3 GMPHD Implementation.	95
Figure 4.4 Iterated-corrector approximation technique for two sensor case.	97
Figure 4.5 GMPHD fusion structure in which Gaussian mixtures are ex- changed and SPCF/Pseudo Chernoff-2 methods are used.	100
Figure 4.6 Experimental set-up to analyze different fusion approaches. .	106
Figure 4.7 Trajectories of Scenario-1. Start points of the red and blue trajectories are marked by circles. Radar positions are denoted by magenta and yellow squares. Large circles at the starting point show the “birth” regions.	107
Figure 4.8 Trajectories of Scenario-2. Start points of the red and blue trajectories are marked by circles. Radar positions are denoted by magenta and yellow squares. Large circles at the starting point show the “birth” regions.	108

Figure 4.9 Measurements generated by the local radar for a single run. “x” and “o”s correspond to the measurements related to the clutter and the targets, respectively.	110
Figure 4.10 State estimates of the EK-GMPHD filter together with true target trajectories for Scenario-1. “o”s correspond to the filter state estimates.	111
Figure 4.11 Representation of the state estimates of EK-GMPHD filter in terms of x and y coordinates. “o”s correspond to the filter state estimates.	112
Figure 4.12 Estimated number of targets with respect to time for the same single run.	113
Figure 4.13 “Scenario-1”, “Method-1 with feedback”: Ensemble averaged OSPA distances of the trackers and the fusion techniques.	114
Figure 4.14 “Scenario-1”, “Method-1 with feedback”: Ensemble averaged expected number of targets of the trackers and the fusion techniques.	118
Figure 4.15 “Scenario-1”, “Method-2 with feedback”: Ensemble averaged OSPA distances of the trackers and the fusion techniques.	119
Figure 4.16 “Scenario-1”, “Method-2 with feedback”: Ensemble averaged expected number of targets of the trackers and the fusion techniques.	120
Figure 4.17 “Scenario-1”, “Method-1 without feedback”: Ensemble averaged OSPA distances of the trackers and the fusion techniques.	121
Figure 4.18 “Scenario-1”, “Method-1 without feedback”: Ensemble averaged expected number of targets of the trackers and the fusion techniques.	122
Figure 4.19 “Scenario-1”, “Method-2 without feedback”: Ensemble averaged OSPA distances of the trackers and the fusion techniques.	123
Figure 4.20 “Scenario-1”, “Method-2 without feedback”: Ensemble averaged expected number of targets of the trackers and the fusion techniques.	124

Figure 4.21 “Scenario-2”, “Method-1 with feedback”: Ensemble averaged OSPA distances of the trackers and the fusion techniques.	125
Figure 4.22 “Scenario-2”, “Method-1 with feedback”: Ensemble averaged expected number of targets of the trackers and the fusion techniques.	126
Figure 4.23 “Scenario-2”, “Method-2 with feedback”: Ensemble averaged OSPA distances of the trackers and the fusion techniques.	127
Figure 4.24 “Scenario-2”, “Method-2 with feedback”: Ensemble averaged expected number of targets of the trackers and the fusion techniques.	128
Figure 4.25 “Scenario-2”, “Method-1 without feedback”: Ensemble averaged OSPA distances of the trackers and the fusion techniques.	129
Figure 4.26 “Scenario-2”, “Method-1 without feedback”: Ensemble averaged expected number of targets of the trackers and the fusion techniques.	130
Figure 4.27 “Scenario-2”, “Method-2 without feedback”: Ensemble averaged OSPA distances of the trackers and the fusion techniques.	131
Figure 4.28 “Scenario-2”, “Method-2 without feedback”: Ensemble averaged expected number of targets of the trackers and the fusion techniques.	132
Figure 4.29 “Scenario-1”, “Method-2 with and without feedback”: Ensemble averaged number of Gaussians generated in SPCF fusion technique.	133
Figure 4.30 “Scenario-1”, “Method-2 with and without feedback”: Ensemble averaged number of Gaussians generated in Pseudo Chernoff-2 fusion technique.	134

LIST OF ABBREVIATIONS

CI	Covariance Intersection
EK-GMPHD	Extended Kalman Gaussian Mixture Probability Hypothesis Density
FOV	Field of View
FISST	Finite Set Statistics
GMPHD	Gaussian Mixture Probability Hypothesis Density
IG	Information Graph
IMM	Interacting Multiple Model
JPDA	Joint Probabilistic Data Association
KF	Kalman Filter
LEA	Largest Ellipsoid Algorithm
NEES	Normalized Estimate Error Squared
NIS	Normalized Innovations Squared
PCCI	Pairwise Component Covariance Intersection
PHD	Probability Hypothesis Density
SMC	Sequential Monte Carlo
SNR	Signal to Noise Ratio
SPCF	Sigma Point Chernoff Fusion
UKF	Unscented Kalman Filter

CHAPTER 1

INTRODUCTION

*“... That night, detective went to bed early but he could not fall asleep. He was still thinking about the recent investigation on the robbery taken place at one of the most popular museums in the capital city. Thieves had stolen the “Golden Circuit”, one of the most valuable paintings of the world, a week ago. This painting was in oil on a golden plate, describing the equivalent circuit of a vacuum tube operational amplifier designed by the Bell Labs in 1941. He was never good at electricity at the school but he had to learn that this picture represented the first version of an operational amplifier which was very important to today’s technology world. Then, he got out of his bed and stood up by the window. He looked at the colorful lights of the city and thought that he would not sleep without reaching a conclusion on this robbery. He was sure that without any internal support from the museum staff, that would not happen. He went over his suspect list in his mind again (Figure 1.1) and he decided that the thief had to be John since all the signs were directing himself towards this old security officer. He was **quite sure**...”*

Leaving the detective with his own responsibilities, there is an important question that we need to ask as the readers of this story: Should the detective be **so much sure** about his decision? Since most of the suspects of the event say that John is the criminal, detective naturally thinks in this way. However, if there exist some “unknown factors” that build up a correlation between what the suspects tell and, that the detective would never know, all the conclusions may totally be changed (Figure 1.2).

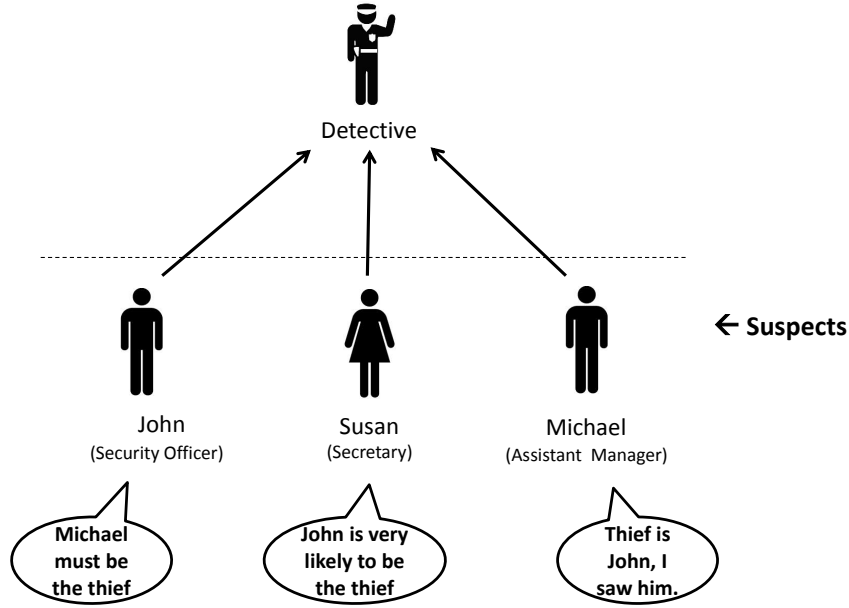


Figure 1.1: Suspect list for the robbery.

Hopefully, the detective reconsiders “his confidence” on his decision and also thinks about the unknown correlation in the information at hand. This story is dreamed up to express the vitality of handling the unknown correlation between data obtained from different sources which is, actually, the main topic of this thesis.

Recently, importance of information fusion concept has significantly raised for several disciplines of the technology. Together with the development of the “**system of systems**” approach, which includes several fusion systems, it become necessary to generate various fusion levels and methods in a decentralized framework. This basically requires continuous research and development activities to integrate these systems with each other effectively. For this aim, researchers study for designing more and more robust and accurate fusion algorithms. Generally, these algorithms and the architecture of the system affects each other in both ways based on the requirements and the communication capacity of the system. Various aspects of data fusion will be provided briefly in Section 1.1.

One of the decentralized fusion applications is the combination of the information

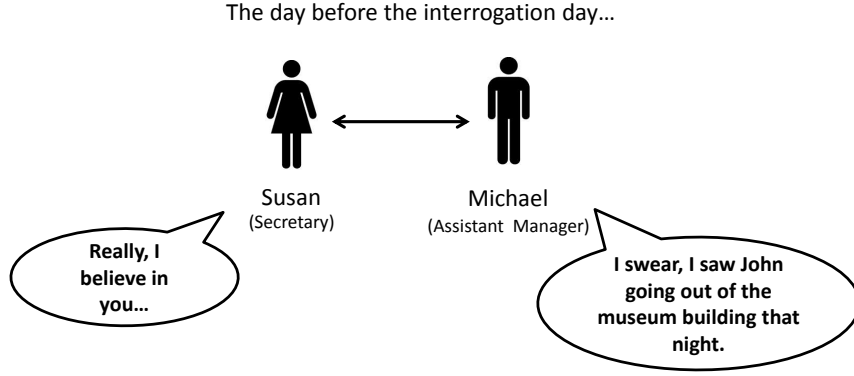


Figure 1.2: Unknown conversation made before the interrogation day.

obtained from various types and number of radars. In such applications, the degree of the correlation is unknown because of the unknown target dynamics and it has to be approximated to achieve a consistent fusion result. In case the radar information to be fused is in the form of Gaussian Mixtures, the fusion problem turns out to be much more difficult when compared with the single Gaussian case since dimension of the state space does not allow numerical methods. This thesis proposes to use a novel method called Sigma Point Chernoff Fusion (SPCF) technique to overcome the difficulties of Chernoff fusion, which is one of these numerical methods.

Additionally, performance of SPCF is analyzed for two different architectures in which Gaussian mixtures has to be exchanged and the fusion operation has to be performed. These two architectures contain different types of radars whose association and tracking mechanisms differ from each other. While the first architecture includes Interacting Multiple Model (IMM) tracker following Joint Probabilistic Data Association (JPDA) algorithm, the second one uses Extended Kalman Gaussian Mixture Probability Hypothesis Density (EK-GMPHD) filter for both tracking and association steps. Both of the architectures produce Gaussian mixture information regarding the targets of interest and this information should be communicated to other radars in the architecture to perform the fusion operation at the receiver side.

To sum up, this thesis mainly brings the contributions stated below to the data fusion area:

- Sigma Point Chernoff Fusion (SPCF)
- Fusion of target density functions (In IMM framework)
- Fusion of target intensity functions (In EK-GMPHD framework)

This thesis first provides some general information regarding data fusion problems and, specifically decentralized data fusion algorithms in this chapter. Then, problem definition of this thesis is also given in the same chapter to draw the boundaries of the thesis study. In Chapter 2, theory for the proposed technique SPCF will be discussed in detail and its performance will be analyzed based on simple benchmarks scenarios. Chapter 3 will rely on the application of SPCF technique in a radar network in which the radars have IMM trackers. Fusion analysis and performance comparison of different fusion strategies including the methods SPCF, Naive and Covariance Intersection (CI), will be performed. PHD fusion application based on fusion of target intensity functions will be investigated in Chapter 4, next. Proposals for the fusion strategies will be given together with their analytical analysis. Finally, the thesis will end up with the conclusions that discusses about the contributions of it to the data fusion world.

1.1 Introduction to Data Fusion

The aim of data fusion is to achieve better situation awareness by combining the data obtained from various number and type of sensors. Connections of the sensors and the fusion nodes may vary depending on the specific system requirements or the design decisions. These connections define the architectural framework of the fusion system and this framework is categorized into two: centralized and decentralized fusion. In centralized fusion, sensors are directly connected to a single node and fusion is performed only at that node. On the other hand, in the decentralized data fusion, the connection schemes may be complex and there may be several fusion nodes performing the fusion simultaneously. Within this

scheme, the fusion is performed locally at each node on the basis of local observations and the information communicated from the neighboring nodes. There may be several connection schemes of the sensors in a fusion system. For instance, Figure 1.3 describes various possible radar communication structures in which the arrows represent the track/measurement/density exchange direction. Fusion process is performed at each radar site when remote target information is received and each unit separately generates the fused track.

The following are the natural problems of a sensor fusion system which have to be solved to achieve the desired over-all system performance.

- **Distribution or management model of the system:** Data exchange mechanism of the overall fusion system must be designed (e.g. decision on which node will send to or receive from which node), if needed, management and control signals must be determined and the fusion must support these commands.
- **Data alignment:** Especially, when the system is heterogeneous, i.e., composed of various types of sensors, data produced by those sensors must be interpreted appropriately so that all information are referenced to a common reference unit.
- **Adaptation of fusion to communication or bandwidth constraints:** The fusion architecture must be designed according to the the communication infrastructure of the over-all system.
- **Handle of asynchronous or delayed data:** Since the sensors in the system may not produce the target data at the same time, the measurements incoming to a node may belong to different time instances of the target whose state is changing dynamically. The possible delay in the communication channels may cause deficiency in the data obtained for which precaution must be taken in the system design.
- **Association:** Data from different sources must be correlated and unique and correct target picture must be obtained. Association must be designed in the way that it must provide correct identification of the targets

continuously.

- **Tracking:** Information belonging to the same target must be processed so as to fuse and track that target and the target state must be estimated.
- **Elimination of unknown correlation:** Information gathered from different information sources at a given node is very likely to possess commonalities. The common information in the data must be eliminated so as to prevent the fusion system from producing inconsistent results.

All of these problems are important to the performance of a fusion system and there are numerous completed/ongoing studies on all of these areas. Main focus of the thesis will just rely on “elimination of unknown correlation in decentralized fusion systems” and techniques proposed to solve other problems of the fusion systems will be used, if it is required. Following section will now provide basic information regarding the techniques proposed to perform the fusion operation of correlated data.

1.2 Elimination of Unknown Correlation in Decentralized Fusion Systems

A decentralized data fusion system is composed of sensors and processors. Processors fuse local sensor data and remote data obtained from other sensor systems. Characteristics of a decentralized fusion system are described by the network architecture, communication links and fusion algorithms. A three sensor cyclic communication structure is provided in Figure 1.4 as an example. This structure has an optimal analytical solution yet it is a complex structure because of multiple paths resulting in information propagation.

Following resultant formulae (1.1) for the first fusion step is proved to be the optimal decentralized fusion for three sensor cyclic communication network shown in Figure 1.4.

$$p(x) = \frac{1}{c} \frac{p_{1,k}(x)p_{2,k}(x)p_{1,k-3}(x)}{p_{1,k-2}(x)p_{2,k-1}(x)} \quad (1.1)$$

where c is the normalization constant, $p(x)$ is the conditional probability at node S_1 after the fusion operation, and $p_{i,k}(x)$ is the conditional probability at node S_i at time k before the fusion.

This approach is called the Information Graph (IG) approach and [10] shows us that the application of the optimal decentralized fusion techniques to obtain optimal results must be supported by carrying information belonging to the previous steps via communication links which may be undesirable and expensive for most fusion systems.

The idea of obtaining the optimal fusion must take into account the fact that the decentralized fusion problem is characterized by the unknown correlation of the information gathered from the different sensors. The correlation in the data must be eliminated in order to avoid over-confident results and obtain much more consistent ones. In the literature, there are several scalable fusion techniques which do not demand previous step's information and propose some approximations for the fusion of the densities gathered from these sensors. Detailed information on these techniques and comparison of them are provided in [10]. A list and summary on the most commonly used fusion methods are listed below to provide the completeness of the thesis report :

- Channel Filter Fusion
- Naïve Fusion
- Chernoff Fusion
- Shannon Fusion
- Bhattacharyya Fusion

1.2.1 Channel Filter Fusion

Channel Filter approach is a first order approximation of IG method and only the first order redundant information is aimed to be eliminated. Channel Filter fusion equation is given in equation (1.2).

$$p_{\text{ChF}}(x) = \frac{p_{1,k}(x)p_{2,k}(x)/p_{2,k-1}(x)}{\int p_{1,k}(x)p_{2,k}(x)/p_{2,k-1}(x)dx} \quad (1.2)$$

where $p_1(x)$ and $p_2(x)$ are the two probability density functions belonging to the local and remote densities, respectively. The subscript ChF is for the channel filter. When both densities are Gaussian, fusion formulae for Channel Filter Fusion becomes as the equations (1.3).

$$P_k^{-1} = P_{1,k}^{-1} + P_{2,k}^{-1} - P_{2,k-1}^{-1} \quad (1.3a)$$

$$P_k^{-1}\hat{x}_k = P_{1,k}^{-1}\hat{x}_{1,k} + P_{2,k}^{-1}\hat{x}_{2,k} - P_{2,k-1}^{-1}\hat{x}_{2,k-1} \quad (1.3b)$$

where, $p_k(x) = \mathcal{N}(x, \hat{x}_k, P_k)$, $p_{1,k}(x) = \mathcal{N}(x, \hat{x}_{1,k}, P_{1,k})$ and $p_{2,k}(x) = \mathcal{N}(x, \hat{x}_{2,k}, P_{2,k})$. It is obvious that this is an approximation and the performance is not expected to be satisfactory when compared to that of IG approach.

1.2.2 Naïve Fusion

Naïve fusion is the simplest fusion approach and it assumes that there is no dependency between the densities to be fused. Its general fusion formulae and formulae for Gaussian case is provided in the equations (1.4) and (1.5), respectively.

$$p_{\text{NF}}(x) = \frac{p_1(x)p_2(x)}{\int p_1(x)p_2(x)dx} \quad (1.4)$$

$$P^{-1} = P_1^{-1} + P_2^{-1} \quad (1.5a)$$

$$P^{-1}\hat{x} = P_1^{-1}\hat{x}_1 + P_2^{-1}\hat{x}_2 \quad (1.5b)$$

1.2.3 Chernoff Fusion

Another idea is to define a notion of “conservativeness” that is used to avoid overconfidence. The main problem is then to obtain a measure of conservativeness, i.e., how to say one pdf is “more conservative” than another. One option is to utilize the entropy measure concept which will produce the level of an uncertainty for a given pdf. For this aim, Chernoff information measure has been proposed and Chernoff Information fusion has been defined. The reader is referred to [2] for further information and a comprehensive understanding of Chernoff Fusion. Given two density functions $p_{x,1}(\cdot)$ and $p_{x,2}(\cdot)$ representing the same random variable x , the fused density $p_{x,\text{CF}}(\cdot)$ is obtained as

$$p_{x,\text{CF}}(x) = \frac{p_{x,1}^{w^*}(x)p_{x,2}^{1-w^*}(x)}{\int p_{x,1}^{w^*}(x)p_{x,2}^{1-w^*}(x)dx} \quad (1.6)$$

where the subscript CF stands for Chernoff fusion and w^* is selected as below

$$w^* = \arg \min_{w \in [0,1]} \mathcal{L} \left(\frac{p_{x,1}^w(x)p_{x,2}^{1-w}(x)}{\int p_{x,1}^w(x)p_{x,2}^{1-w}(x)dx} \right). \quad (1.7)$$

Here, the function $\mathcal{L}(\cdot)$ represents an uncertainty measure from the space of density functions into real numbers. See [2] for details about the consistency and conservativeness properties of Chernoff fusion formula (1.6).

When the input densities are Gaussian, this approach corresponds to Covariance Intersection (CI) technique [23, 25] which is one of the main approaches to decentralized fusion [10]. Detailed information about this fusion method is given in section 2.2 and analytic expression of the mean and covariance of the fused density is provided in the Equations (1.8) and (1.9).

$$P_{\text{CI}}^{-1}x_{\text{CI}} = w^*P_1^{-1}x_1 + (1 - w^*)P_2^{-1}x_2 \quad (1.8a)$$

$$P_{\text{CI}}^{-1} = w^*P_1^{-1} + (1 - w^*)P_2^{-1} \quad (1.8b)$$

where $w^* \in [0, 1]$ is calculated using the following optimization

$$w^* \triangleq \arg \min_{w \in [0, 1]} \mathcal{L} \left((wP_1^{-1} + (1 - w)P_2^{-1})^{-1} \right) \quad (1.9)$$

1.2.4 Shannon Fusion

Shannon fusion is a special case of Chernoff fusion when w is selected for the minimum value of the determinant of the fused density covariance, i.e., the function \mathcal{L} in the cost (1.7) is selected to be the determinant of the fused covariance. For the Gaussian case, this turns out to be minimizing the Shannon Information of the fused density. Shannon information for the Gaussian density case is calculated as $I_s = \int p(x) \ln p(x) dx = \frac{1}{2} \ln (2\pi)^n |P|^{1/2} + n/2$, where P is the covariance of $p(x)$. Fusion of two Gaussians utilizing the Shannon technique requires solving the optimization problem defined in (1.10) and (1.11).

$$P_{\text{SF}}^{-1}x_{\text{SF}} = w^*P_1^{-1}x_1 + (1 - w^*)P_2^{-1}x_2 \quad (1.10a)$$

$$P_{\text{SF}}^{-1} = w^*P_1^{-1} + (1 - w^*)P_2^{-1} \quad (1.10b)$$

where $w^* \in [0, 1]$ is calculated using the following optimization

$$w^* \triangleq \arg \min_{w \in [0, 1]} I_s. \quad (1.11)$$

1.2.5 Bhattacharyya Fusion

Similar to Shannon fusion, this fusion technique is again a special case of Chernoff Fusion. The parameter w is selected as 0.5 and the equations get similar to those of Naïve Fusion for the Gaussian case. The covariance and mean of the fused density is provided in (1.13) and (1.15), respectively.

$$P_{\text{BF}}^{-1} = \frac{1}{2} (P_1^{-1} + P_2^{-1}) \quad (1.12)$$

$$= (P_1^{-1} + P_2^{-1}) - \frac{1}{2} (P_1^{-1} + P_2^{-1}) \quad (1.13)$$

$$P_{\text{BF}}^{-1} \hat{x}_{\text{BF}} = \frac{1}{2} (P_1^{-1} \hat{x}_1 + P_2^{-1} \hat{x}_2) \quad (1.14)$$

$$= (P_1^{-1} \hat{x}_1 + P_2^{-1} \hat{x}_2) - \frac{1}{2} (P_1^{-1} \hat{x}_1 + P_2^{-1} \hat{x}_2) \quad (1.15)$$

Note that in this case, common prior information corresponds to the average of the two sets of information to be fused in the fusion equations.

1.3 Elimination of Unknown Correlation in Track Fusion Problems

The area of track fusion is mainly concerned about the correlation between the estimates to be fused. Even if the sensors used in a network collect measurements which are conditionally independent of each other, local processing of the measurements in the presence of common process noise in the target dynamics makes the local estimation errors correlated [3]. Moreover, the existence of data feedback loops can cause rumor propagation all over the network, which would result in inconsistencies, overconfidence and in turn even filter divergence. The proposed solutions for the track correlation problem range from the ones requiring extra information transmission (e.g. Kalman filter gains [4]) or extra processing (e.g. information decorrelation [32, 12]) to compensate for the correlation, like the Covariance Intersection (CI) [23, 25] and the Largest Ellipsoid Algorithm (LEA) [6, 52]. An analysis with a survey and comparison of the possible approaches is presented in [9, 10].

The early approaches to track fusion considered only the fusion of locally estimated means and covariances due to the ubiquitous use of Gaussian density based state estimators (e.g. Kalman filter (KF), extended KF (EKF), unscented KF (UKF) [24]). This was indeed a manifestation of the computational restrictions of the era which made such filters actually the only possible choices. With

the advent of more sophisticated state estimators like Gaussian sum filters [44], multiple model filters [8], [5, Section 11.6] and particle filters [20, 1], the need for fusing density functions became more apparent. Similarly, in multiple target tracking, the consideration of local multiple hypothesis trackers (MHT) which inherently hold mixtures for targets directly leads to the problem of fusing local mixtures for a single target (even if Gaussian based state estimators are used in local trackers). The recent developments in multiple target tracking leading to the extensive use of probability hypothesis density (PHD) filters [34] made the need for density/intensity fusion methods even more significant.

1.4 State-Of-The Art Fusion Techniques for Gaussian Densities and Gaussian Mixture Densities

Because of the reasons depicted in Section 1.3, consistent and optimum fusion of density functions is investigated in detail in [13]. The generalization of CI to probability density functions was first proposed by Mahler in [40] and two years later, independently, by Hurley in [22]. This generalization is called by different names by different authors: Chernoff fusion [10]; geometric mean density [2]; exponential mixture densities [27]. In [40], Mahler also proposed the application of both the optimal approach [13] and Chernoff fusion to multitarget densities. The consistency and conservativeness properties of Chernoff fusion are investigated in [2]. Explicit formulae are derived for Chernoff fusion of Bernoulli, Poisson and independent cluster process multitarget densities in [15].

Table 1.1 demonstrates the applicable fusion techniques to both Gaussian densities and Gaussian mixture densities and clearly reveals the point that has to be studied in detail. Although there has been several studies on the aspects of Chernoff fusion, there does not exist satisfactory approaches in the literature that enable to apply Chernoff fusion to Gaussian Mixtures. According to our knowledge, the only solution proposed for this problem is by [26] and this work makes an analysis on the existing fusion technique Pairwise Component Covariance Intersection (PCCI) and proposes two other different methods, Pseudo Chernoff-1 and Pseudo Chernoff-2 which are derived from first order approxima-

tion of w^{th} power of the mixture. Comparison of these techniques are performed and Pseudo Chernoff-2 algorithm is found as the best among all. Notice that the first order approximation of the exponent of a given mixture sounds as a weak assumption and its weakness will be demonstrated by comparing these techniques with the one proposed in the thesis in Section 2.5.

Table 1.1: Existence analysis of state-of-the art fusion techniques to Gaussian densities and Gaussian mixture densities.

Density Fusion techniques	Fusion Formulae	Existence Analysis for fusion of «Gaussian Densities»	Existence Analysis for fusion of «Gaussian Mixtures»
Channel Filter	$p(x) = \frac{p_{1,k}(x)p_{2,k}(x)/p_{2,k-1}(x)}{\int [p_{1,k}(x)p_{2,k}(x)/p_{2,k-1}(x)]dx}$	OK	NO
Naive Fusion	$p_N(x) = \frac{p_1(x)p_2(x)}{\int p_1(x)p_2(x)dx}$	OK	OK
Chernoff Fusion	$p_{CF}(x) = \frac{p_1^{w^*}(x)p_2^{1-w^*}(x)}{\int p_1^{w^*}(x)p_2^{1-w^*}(x)dx}$	OK	Not satisfactory
Shannon Fusion	Same as that of Chernoff Fusion	OK	Not satisfactory
Bhattacharyya Fusion	Special Case of Chernoff Fusion	OK	Not satisfactory

As a result, this thesis aims to fill the gap on performing Chernoff fusion of Gaussian mixtures. The proposed method called Sigma Point Chernoff Fusion (SPCF) is given in Chapter 2 with some analysis.

1.5 Analysis and Comparison of the Existing Studies for Track Fusion Architectures

Although some work is done for different fusion techniques, it seems that there does not exist sufficient study on the performances of different decentralized fusion techniques applied to track fusion problems. For instance, even for CI technique, there is no study clearly showing its benefits over Naive fusion when only state estimates are fused. Additionally, performance of Chernoff fusion could not be evaluated on a track fusion system because of the difficulty of the implementation of Chernoff fusion for high state dimensions, which is the

general case. This study claims to fill this gap and allows to implement Chernoff fusion technique for fusion of track density/intensity functions in the form Gaussian Mixture. Specifically, this thesis aims to propose some fusion strategies and to compare these strategies in case the radars possesses IMM and PHD filters, which corresponds to the fusion of target density and intensity functions, respectively.

Focusing on a track fusion system based on IMM filter, the only analysis in the literature is the fusion of the state estimates with Gaussian densities. There does not exist any study that inspects using Gaussian mixture densities internally produced by an IMM filter for fusion purposes. This requires consistent fusion of two Gaussian mixture densities which was not that practical and efficient up to this thesis. For instance, at an architecture like the one given in Figure 1.5, fusion operation should be performed at each radar site, and the fusion problem of IMM output density functions in the form of Gaussian mixtures are to be analyzed. The problem is elaborated in Chapter 3.

Another area that requires the fusion of Gaussian mixtures is the PHD filter, in particular GMPHD filtering (Figure 1.6). GMPHD filters generate Gaussian Mixture intensity functions. There is no work in the literature that fuses the PHD's without referring to the measurements that generate them. The thesis focuses on proposing different fusion strategies enabling the fusion and demonstrate some results for comparing them. Chapter 4 is devoted to this track fusion problem.

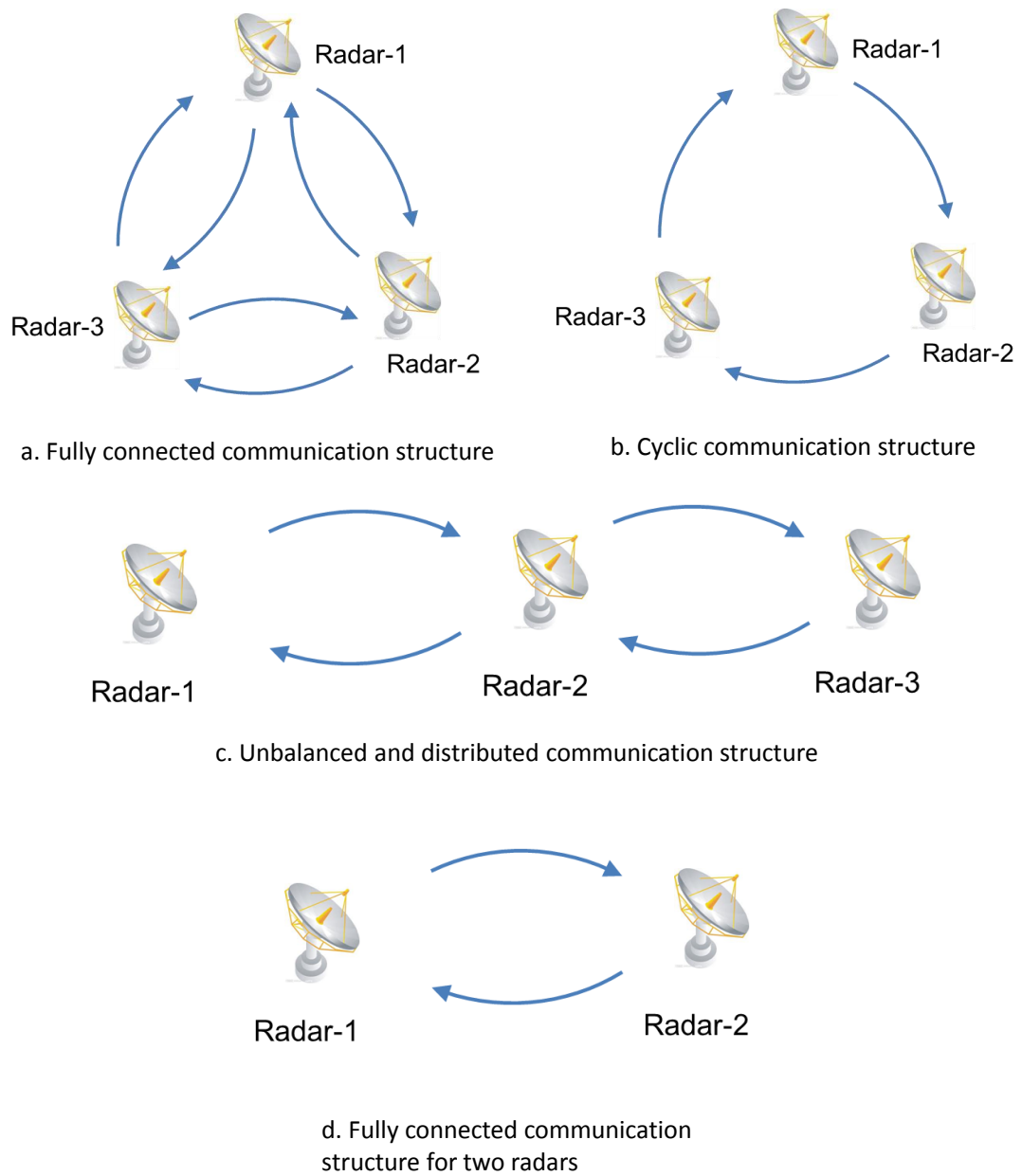


Figure 1.3: Some examples to radar communication structures.

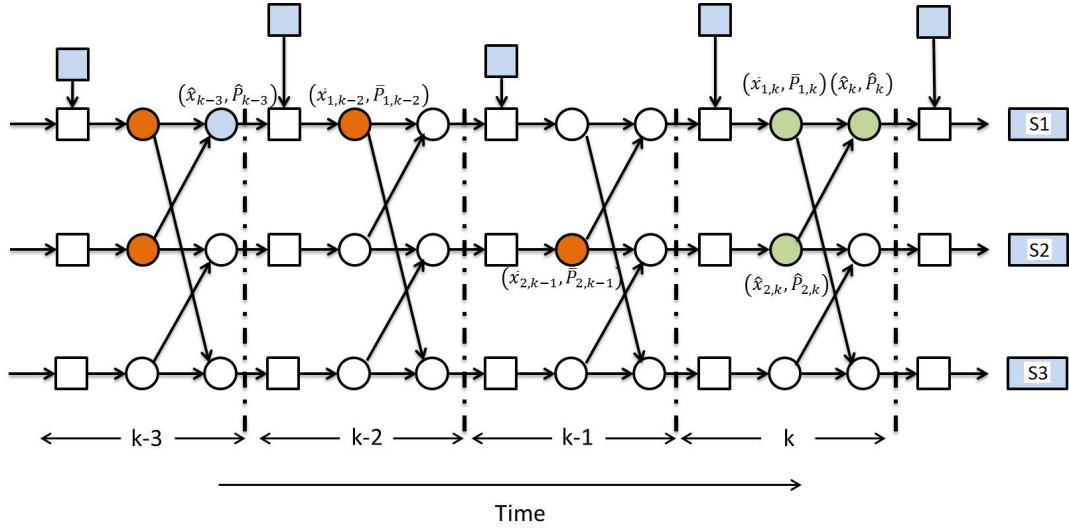


Figure 1.4: Cyclic communication scenario (adopted from [10]).

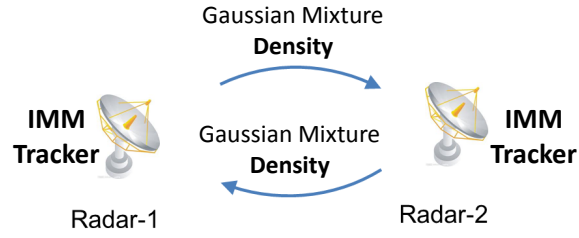


Figure 1.5: Track fusion architecture based on IMM filter in which **Gaussian densities** are exchanged.

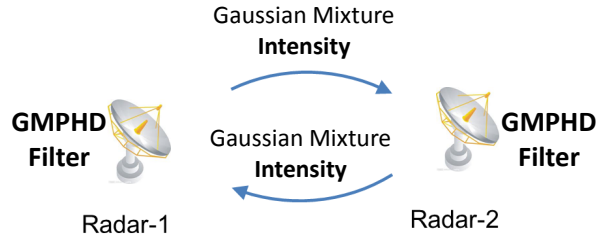


Figure 1.6: Track fusion architecture based on PHD filter in which **Gaussian mixture intensities** are exchanged.

CHAPTER 2

SIGMA POINT CHERNOFF FUSION

2.1 Introduction

In this chapter, we propose an approximate approach for the Chernoff fusion of Gaussian mixtures. As indicated in Section 1.4, the existing literature on this subject is not mature. Our methodology starts by approximating an arbitrary power of a Gaussian mixture with an unnormalized Gaussian mixture whose weights are to be found by using a weighted least squares formulation. The instrumental weighted least squares problem that gives the weights is constructed by approximating the original Gaussian mixture with its sigma-point approximation. Such an approximation can lead to a density fusion which no longer involves powers of the densities to be fused. An important merit of the proposed fusion rule is that it yields a closed form problem formulation including the cost function and the fused density in the form of a Gaussian mixture. We illustrate the performance of the proposed generalization on a density fusion scenario and on a benchmark scenario where Gaussian mixtures are required to be fused.

The organization of the chapter is as follows: A brief overview of CI and Chernoff fusion is presented in Section 2.2. Section 2.3.1 first establishes the approximation of the density powers appearing in Chernoff fusion for Gaussian mixtures and then presents the proposed new version of Chernoff fusion for Gaussian mixtures, which is the main result of this chapter. The explicit fused density formula resulting from the application of the proposed fusion rule to Gaussian mixtures is obtained in Section 2.3.2. The simulation results are given in Sections 2.4 and

2.5. The chapter is finalized with discussions in Section 2.6.

2.2 Covariance Intersection and Chernoff Fusion

Covariance Intersection (CI) [23, 25] is one of the main approaches to decentralized fusion [10]. Its main advantage is that it enables consistent fusion under unknown correlation information. The consistency in this context is defined as the fused covariance being always larger than or equal to the optimally fused covariance that would be obtained if the correlation information was available. For more details about the optimality and consistency properties of CI, see [11].

The main idea of CI is to combine the estimates and their covariances as a weighted sum of them. Assume two local estimates $x_1 \in \mathbb{R}^n$ and $x_2 \in \mathbb{R}^n$ and their positive definite covariances $P_1 \in \mathbb{R}^{n \times n}$ and $P_2 \in \mathbb{R}^{n \times n}$. Then the fused estimate x_{CI} and covariance P_{CI} are calculated as

$$P_{\text{CI}}^{-1} x_{\text{CI}} = w^* P_1^{-1} x_1 + (1 - w^*) P_2^{-1} x_2 \quad (2.1a)$$

$$P_{\text{CI}}^{-1} = w^* P_1^{-1} + (1 - w^*) P_2^{-1} \quad (2.1b)$$

where $w^* \in [0, 1]$ is calculated using the following optimization

$$w^* \triangleq \arg \min_{w \in [0, 1]} L \left((w P_1^{-1} + (1 - w) P_2^{-1})^{-1} \right). \quad (2.2)$$

Here, the function $L : \mathbb{S}_{\geq 0}^{n \times n} \rightarrow \mathbb{R}_{\geq 0}$ represents an uncertainty measure from the space of symmetric positive semi-definite matrices ($\mathbb{S}_{\geq 0}^{n \times n}$) into non-negative real numbers ($\mathbb{R}_{\geq 0}$) and usually selected either as the trace or the determinant of the matrix argument. Define the ellipsoid \mathcal{E}_P , as

$$\mathcal{E}_P \triangleq \{x | x^T P^{-1} x < 1\} \quad (2.3)$$

Above approach generates the fused covariance P_{CI} as “the smallest” ellipsoid containing the intersection $\mathcal{E}_{P_1} \cap \mathcal{E}_{P_2}$ of the ellipsoids \mathcal{E}_{P_1} and \mathcal{E}_{P_2} corresponding to the local covariances P_1 and P_2 respectively. See Figure 2.1 for an illustration of this property in two dimensions.

A very attractive property of CI is that it is generalizable to the fusion of density functions [40, 22]. The corresponding generalization is called *Chernoff fusion* [10]. Given two density functions $p_{x,1}(\cdot)$ and $p_{x,2}(\cdot)$ representing the same random variable x , the fused density $p_{x,\text{CF}}(\cdot)$ is obtained as

$$p_{x,\text{CF}}(x) = \frac{p_{x,1}^{w^*}(x)p_{x,2}^{1-w^*}(x)}{\int p_{x,1}^{w^*}(x)p_{x,2}^{1-w^*}(x)dx} \quad (2.4)$$

where the subscript CF stands for Chernoff fusion and w^* is selected as below

$$w^* = \arg \min_{w \in [0,1]} \mathcal{L} \left(\frac{p_{x,1}^w(x)p_{x,2}^{1-w}(x)}{\int p_{x,1}^w(x)p_{x,2}^{1-w}(x)dx} \right). \quad (2.5)$$

Here, the function $\mathcal{L}(\cdot)$ represents an uncertainty measure from the space of density functions into real numbers. For example, the matrix uncertainty measure trace in CI corresponds to the uncertainty measure variance ($E_x[x^T x] - E_x[x^T]E_x[x]$) in Chernoff fusion and the matrix uncertainty measure, determinant in CI, corresponds to the uncertainty measure entropy ($E_x[-\log p(x)]$) in Chernoff fusion. See [2] for details about the consistency and conservativeness properties of Chernoff fusion formula (2.4).

2.3 Chernoff Fusion of Gaussian Mixtures Using Sigma-Points

When the densities $p_{x,1}(\cdot)$ and $p_{x,2}(\cdot)$ in (2.4) are selected to be Gaussian Mixtures as:

$$p_{x,1}(x) = \sum_{i=1}^M \mu_i \mathcal{N}(x; \phi_i, \Phi_i) \quad (2.6a)$$

$$p_{x,2}(x) = \sum_{j=1}^N \nu_j \mathcal{N}(x; \psi_j, \Psi_j) \quad (2.6b)$$

application of Chernoff fusion formula (2.4) requires the exponentiation of the Gaussian mixtures for exponent values in $[0,1]$.

Starting with the single Gaussian case, the exponentiation results in the scaled Gaussian given below.

$$\mathcal{N}^w(x; \phi, \Phi) = c(w, \Phi) \mathcal{N}(x; \phi, w^{-1}\Phi) \quad (2.7)$$

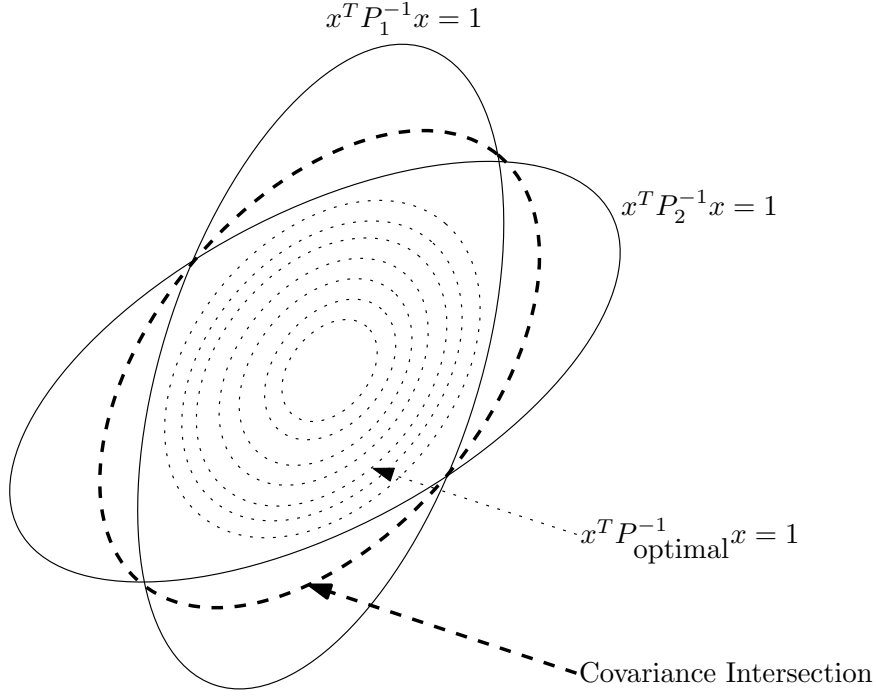


Figure 2.1: Covariance intersection algorithm in two dimensional case ($n = 2$). Similar figures also appear in [23, 25].

for $w \in (0, 1)$ where $c(w, \Phi)$ is a scalar independent of x . Later, the expression above will be the basis for some assumptions in this chapter. Notice that the mean of the Gaussian density does not change after the exponentiation and the covariance is multiplied simply by w^{-1} .

2.3.1 Taking the w^{th} Power of a Gaussian Mixture

For the Gaussian mixture case, the Chernoff fusion formula requires the w^{th} power of the Gaussian mixture where $w \in (0, 1)$. We call the w^{th} power of a Gaussian mixture $p(x) = \sum_{i=1}^N w_i \mathcal{N}(x; x_i, P_i)$ as $q(x) \triangleq p^w(x)$. Note that $q(\cdot)$ is not necessarily a Gaussian mixture but one can intuitively say that its shape would be similar to a Gaussian mixture. Assuming that $q(\cdot)$ can be approximated as a (unnormalized) Gaussian mixture, estimation of the number of mixture components, weights, means and covariances of the components of $q(\cdot)$ becomes the main concern. Defining an optimization problem over all of these parameters to find $q(x)$ is possible, however even numerical solutions may not be feasible for

real-time applications. Therefore, we make the following assumptions utilizing the interpretation for the single Gaussian case given in (2.7).

- $q(\cdot)$ has the same number of components as $p(\cdot)$.
- The means of the components of $q(\cdot)$ are equal to those of $p(\cdot)$.
- The covariances of the components of $q(\cdot)$ are equal to the covariances of the components of $p(\cdot)$ scaled by $1/w$

The assumptions listed above results in the following expression for $q(\cdot)$.

$$q(x) \approx \sum_{i=1}^N \beta_i \mathcal{N}(x; x_i, w^{-1} P_i) \quad (2.8)$$

Note that the only unknown variables in (2.8) are the weights $\{\beta_i\}_{i=1}^N$ of the components of $q(x)$ which can be found by solving the following optimization problem.

$$\underset{\beta}{\text{minimize}} \int (q(x) - p^w(x))^2 p(x) dx \quad (2.9a)$$

$$\text{subject to } 0 \leq \beta_i, i = 1, \dots, N. \quad (2.9b)$$

where $\beta = [\beta_1, \beta_2, \dots, \beta_N]^T$. In the optimization problem defined above the cost function (2.9a) is quadratic and the constraint (2.9b) is linear in the unknown weights $\{\beta_i\}_{i=1}^N$. Hence we have a quadratic optimization problem which is relatively easy to solve. An important drawback is that the analytic evaluation of the integral in the cost (2.9a) is not possible. Notice that the optimization problem has to be solved for every candidate exponent w for the Chernoff fusion which would lead to extreme amount of computations, especially in high dimensions. Therefore we choose here to approximate the optimization problem above by the following optimization problem.

$$\underset{\beta}{\text{minimize}} \sum_{i=1}^N w_i \sum_{j=1}^{2n+1} \pi_i^j (q(s_i^j) - p^w(s_i^j))^2 \quad (2.10a)$$

$$\text{subject to } 0 \leq \beta_i, i = 1, \dots, N. \quad (2.10b)$$

where $\{s_i^j\}_{j=1}^{2n+1}$ are the sigma-points for the i th component of $p(\cdot)$ generated by unscented transform [24] and $\{\pi_i^j\}_{j=1}^{2n+1}$ are their weights. Note that the approximate optimization problem given above follows simply from the approximation

of $p(\cdot)$ given as

$$p(x) \approx \sum_{i=1}^N w_i \underbrace{\sum_{j=1}^{2n+1} \pi_i^j \delta_{s_i^j}(x)}_{\approx \mathcal{N}(x; x_i, P_i)} \quad (2.11)$$

where $\delta_s(\cdot)$ denotes the Dirac delta function placed at s .

The new optimization problem (2.10a) can simply be written as the following weighted non-negative least squares problem.

$$\underset{\beta}{\text{minimize}} \quad (\mathbf{M}\beta - \mathbf{b})^T \mathbf{W}(\mathbf{M}\beta - \mathbf{b}) \quad (2.12a)$$

$$\text{subject to } 0 \leq \beta_i, \quad i = 1, \dots, N. \quad (2.12b)$$

where the elements of the vector $\mathbf{b} \in \mathbb{R}^{N(2n+1) \times 1}$, the matrix $\mathbf{M} \in \mathbb{R}^{N(2n+1) \times N}$ and the diagonal matrix $\mathbf{W} \in \mathbb{R}^{N(2n+1) \times N(2n+1)}$ are defined as

$$[\mathbf{M}]_{(2n+1)(i-1)+j,m} \triangleq \mathcal{N}(s_i^j; x_m, w^{-1}P_m), \quad (2.13)$$

$$[\mathbf{b}]_{(2n+1)(i-1)+j,1} \triangleq p^w(s_i^j) \quad (2.14)$$

$$[\mathbf{W}]_{(2n+1)(i-1)+j,(2n+1)(i-1)+j} = w_i \pi_i^j \quad (2.15)$$

for $i, m = 1, \dots, N$ and $j = 1, \dots, 2n + 1$ where the notation $[\cdot]_{i,j}$ denotes the i, j th element of the argument matrix. The solution for the weighted least squares problem (when the constraints are neglected) is given as

$$\hat{\beta} = (\mathbf{M}^T \mathbf{W} \mathbf{M})^{-1} \mathbf{M}^T \mathbf{W} \mathbf{b}. \quad (2.16)$$

Note that the problem defined as (2.12a) and (2.12b) is a weighted non-negative least squares problem. There are existing simple solutions to the original weighted non-negative least squares problem like Lawson-Hanson algorithm given in [28] which may require some computational power. To speed up the process to find the optimal solution, first we propose to solve the problem ignoring the non-negativity constraint, and then in case the solution turns out to with negative weights, Lawson-Hanson algorithm is used.

The approach described above provides a fast and scalable (with the dimension of x) way for approximating the w^{th} power of a Gaussian Mixture as another Gaussian Mixture which is going to be instrumental in the Chernoff fusion of Gaussian mixtures.

2.3.2 Chernoff Fusion of Gaussian Mixtures

In this section, we are going to investigate the fusion of Gaussian mixtures by Chernoff Fusion technique using the results of the previous subsection. In order to find the fused density given in (2.4), the w^{th} and $(1 - w)^{\text{th}}$ powers of $p_{x,1}(x)$ and $p_{x,2}(x)$ should be found, respectively. The approximate solution proposed in the previous subsection, generates functions $q_{x,1}(\cdot)$ and $q_{x,2}(\cdot)$ that are also (unnormalized) Gaussian mixtures given as

$$q_{x,1}(x) = \sum_{i=1}^M \hat{\mu}_i(w) \mathcal{N}(x; \phi_i, w^{-1} \Phi_i) \quad (2.17)$$

$$q_{x,2}(x) = \sum_{j=1}^N \hat{\nu}_j(w) \mathcal{N}(x; \psi_j, (1 - w)^{-1} \Psi_j) \quad (2.18)$$

where the dependency of the weights on w is emphasized. Given $q_{x,1}(\cdot)$ and $q_{x,2}(\cdot)$, the rest of the fusion amounts to nothing but applying the so called “naive” fusion formula [10] (i.e., the fusion formula that would be valid if the local quantities were independent.¹) to fuse the resultant mixtures (2.17) and (2.18).

Multiplication of the Gaussian Mixtures $q_{x,1}(\cdot)$ and $q_{x,2}(\cdot)$ results in

$$\begin{aligned} q_{x,1}(x) q_{x,2}(x) &= \sum_{i=1}^M \sum_{j=1}^N \hat{\mu}_i \hat{\nu}_j \mathcal{N}\left(x; \phi_i, \frac{\Phi_i}{w}\right) \mathcal{N}\left(x; \psi_j, \frac{\Psi_j}{1 - w}\right) \end{aligned} \quad (2.20)$$

$$= \sum_{i=1}^M \sum_{j=1}^N \hat{\mu}_i \hat{\nu}_j \pi_{ij}(w) \mathcal{N}\left(x; \tilde{x}_{ij}(w), \tilde{P}_{ij}(w)\right) \quad (2.21)$$

where

$$\pi_{ij}(w) \triangleq \mathcal{N}\left(\phi_i; \psi_j, \frac{\Phi_i}{w} + \frac{\Psi_j}{1 - w}\right) \quad (2.22)$$

$$\tilde{P}_{ij}^{-1}(w) = w \Phi_i^{-1} + (1 - w) \Psi_j^{-1} \quad (2.23)$$

$$\tilde{P}_{ij}^{-1}(w) \tilde{x}_{i,j}(w) = w \Phi_i^{-1} \phi_i + (1 - w) \Psi_j^{-1} \psi_j. \quad (2.24)$$

¹ The naive fusion formulae is given as

$$p_{\text{naive}}(x) = \frac{p_{x,1}(x) p_{x,2}(x)}{\int p_{x,1}(x) p_{x,2}(x) dx}. \quad (2.19)$$

Therefore, we have

$$p_{x,\text{SPCF}}(x) = \frac{\left(\sum_{i=1}^M \sum_{j=1}^N \hat{\mu}_i(w) \hat{\nu}_j(w) \pi_{ij}(w^*) \right) \times \mathcal{N}\left(x; \tilde{x}_{ij}(w^*), \tilde{P}_{ij}(w^*)\right)}{\sum_{i=1}^M \sum_{j=1}^N \hat{\mu}_i \hat{\nu}_j \pi_{ij}(w^*)} \quad (2.25)$$

where

$$w^* = \arg \min_{w \in [0,1]} \mathcal{L} \left(\frac{\sum_{i=1}^M \sum_{j=1}^N \hat{\mu}_i(w) \hat{\nu}_j(w) \pi_{ij}(w) \mathcal{N}\left(x; \tilde{x}_{ij}(w), \tilde{P}_{ij}(w)\right)}{\sum_{i=1}^M \sum_{j=1}^N \hat{\mu}_i(w) \hat{\nu}_j(w) \pi_{ij}(w)} \right). \quad (2.26)$$

In this work we are going to use the variance as the optimizing criterion since it is analytically computable for Gaussian mixtures, i.e., $\mathcal{L}(p_x(x)) = E_x[x^T x] - E_x[x^T] E_x[x]$, which gives

$$w^* = \arg \min_{w \in [0,1]} \frac{\left(\sum_{i=1}^M \sum_{j=1}^N \hat{\mu}_i(w) \hat{\nu}_j(w) \pi_{ij}(w) \times \left[\text{tr} \left(\tilde{P}_{ij}(w) \right) + \|\tilde{x}_{ij}(w) - \tilde{x}(w)\|_2^2 \right] \right)}{\sum_{i=1}^M \sum_{j=1}^N \hat{\mu}_i(w) \hat{\nu}_j(w) \pi_{ij}(w)} \quad (2.27)$$

where

$$\tilde{x}(w) \triangleq \sum_{i=1}^M \sum_{j=1}^N \hat{\mu}_i(w) \hat{\nu}_j(w) \pi_{ij}(w) \tilde{x}_{ij}(w), \quad (2.28)$$

and the notation $\|\cdot\|_2$ denotes the Euclidean norm of the argument vector; the operator $\text{tr}(\cdot)$ is the trace of the argument matrix.

Notice that while the cost function and the fused density for Chernoff fusion can only be obtained with resort to numerical optimization due to the exponentiation of the Gaussian mixtures, the sigma-point Chernoff fusion enables the analytical evaluation of the cost function and provides an explicit formula for the fused density once the optimization problem (with respect to w) is solved.

2.4 Comparison of Different Fusion Techniques with Optimum Fusion Based on Simulations

In this section, we are going to present the results obtained by applying the sigma-point Chernoff fusion to univariate and bivariate density fusion problems

and comparing the results to those of exact numerical Chernoff fusion and optimum fusion. The case study given here considers a fusion scenario where we have two local agents, called A_1 and A_2 , which process both conditionally independent and common information about a random variable $x \in \mathbb{R}^n$. Both agents assume common prior information about x given as

$$x \sim p(x) \triangleq \sum_{i=1}^2 \pi_i \mathcal{N}(x; \mu_i, M_i). \quad (2.29)$$

We consider three conditionally independent measurements z_1 , z_2 and z_3 of x which are related to x with the simple noisy measurement relation

$$z_j = x + v_j \quad (2.30)$$

where $v_j \sim \mathcal{N}(v_j; 0, R_j)$ for $i = 1, 2, 3$. We suppose that the measurement pairs $Z_1 \triangleq \{z_1, z_2\}$ and $Z_2 \triangleq \{z_2, z_3\}$ are available to agents A_1 and A_2 respectively. When the agents get their respective information, Z_1 and Z_2 , they calculate the posterior densities $p_1(\cdot)$ and $p_2(\cdot)$ defined as

$$p_1(x) \triangleq p(x|Z_1) \propto p(Z_1|x)p(x) \quad (2.31)$$

$$p_2(x) \triangleq p(x|Z_2) \propto p(Z_2|x)p(x) \quad (2.32)$$

respectively. The task is then going to be the fusion of $p_1(\cdot)$ and $p_2(\cdot)$ under unknown correlations. Note here that the common information in this case is the common prior information that the agents use and the information of the measurement z_2 . It is obvious that the optimal fused density would be given as

$$p_{\text{opt}}(x) \triangleq p(x|z_1, z_2, z_3) \propto p(z_1|x)p(z_2|x)p(z_3|x)p(x). \quad (2.33)$$

A point to be emphasized here is that the densities $p_1(\cdot)$, $p_2(\cdot)$ and $p_{\text{opt}}(\cdot)$ can all be calculated exactly using the Kalman filter update formulae. We below give the analytical formula only for $p(x|z_1)$ and the others can be calculated similarly.

$$p(x|z_1) = \sum_{i=1}^2 \bar{\pi}_i \mathcal{N}(x; \bar{\mu}_i, \bar{M}_i) \quad (2.34)$$

where

$$\bar{\mu}_i = \mu_i + K_i(z_i - \mu_i) \quad (2.35a)$$

$$\bar{M}_i = M_i - K_i S_i K_i^T \quad (2.35b)$$

$$\bar{\pi}_i \propto \pi_i \mathcal{N}(z_i; \mu_i, S_i) \quad (2.35c)$$

$$S_i = M_i + R_i \quad (2.35d)$$

$$K_i = M_i S_i^{-1} \quad (2.35e)$$

For this case study, the fused density results of 4 different density fusion methods are presented for different scenarios. The 4 methods are:

- **Optimal:** The optimal result calculated using (2.33).
- **Naive:** The fused density obtained assuming independence between the two local densities. This method gives highly overconfident results since it totally neglects the existent dependence between the local quantities.
- **Chernoff:** Chernoff fusion formula (2.4) is applied. In this case, the optimization (2.5) is carried out on a grid of 100 uniformly placed w -values in the interval $[0, 1]$. The variance of the fused density is used as the objective function. The integrals involved for calculating both the cost function and the normalization constant for the resulting density were taken numerically using a uniform grid of all components of the x vector placed in the interval $[-400\text{m}, 400\text{m}]$ with a spacing of h meters.
- **Sigma Point Chernoff:** The method proposed in this work is applied. As in Chernoff fusion, the optimization is carried out on a grid of 100 uniformly placed w -values in the interval $[0, 1]$. The variance of the fused density is used as the objective function. The cost function is calculated analytically using the formula (2.27).

A total of 10000 Monte Carlo runs are made, where in each run different realizations of x , z_1 , z_2 and z_3 are used. As the comparison metrics, we calculate the means and the standard deviations of the components of x corresponding to the resulting fused densities for each run. For each algorithm (naive fusion,

Chernoff fusion, sigma-point Chernoff fusion), we calculate the distance from the mean and the standard deviation obtained by the algorithm to the mean and the standard deviation of the optimally fused density $p_{\text{optimal}}(\cdot)$, i.e., we calculate

$$e_{\text{mean}} = \left\| \text{mean}[p_{\text{algorithm}}(\cdot)] - \text{mean}[p_{\text{optimal}}(\cdot)] \right\|_2 \quad (2.36)$$

$$e_{\text{std}} = \left\| \text{std}[p_{\text{algorithm}}(\cdot)] - \text{std}[p_{\text{optimal}}(\cdot)] \right\|_2 \quad (2.37)$$

where “algorithm” can be one of naive fusion, Chernoff fusion and sigma-point Chernoff fusion and the notation $\text{std}[\cdot]$ denotes the vector composed of the standard deviations of components of x distributed with the argument density. After calculating the error metrics for each Monte Carlo run, we calculate the empirical estimate of the cumulative distribution function of each error metric.

2.4.1 1D-Case

In the following, we are going to make two parameter selections for the scenario described above when $x \in \mathbb{R}$, i.e., $n = 1$, and then present the results.

2.4.1.1 Parameter Selection I

In this case we select the parameters of the scenario as below.

$$\pi_1 = 0.8 \quad \pi_2 = 0.2 \quad (2.38a)$$

$$\mu_1 = -50\text{m} \quad \mu_2 = 50\text{m} \quad (2.38b)$$

$$M_1 = 100^2\text{m}^2 \quad M_2 = 20^2\text{m}^2. \quad (2.38c)$$

$$R_1 = R_2 = R_3 = 100^2\text{m}^2. \quad (2.39)$$

In Figures 2.2 and 2.3 we show the result of the single run where the sampled x value is $x = -36.1141\text{m}$ and the sampled measurements are given as $z_1 = 59.9\text{m}$, $z_2 = -112.6\text{m}$ and $z_3 = -22.1\text{m}$. The densities $p(\cdot)$, $p_1(\cdot)$, $p_2(\cdot)$ and $p_{\text{optimal}}(\cdot)$ are illustrated in Figure 2.2. In Figure 2.3, we show the fused densities $p_{\text{optimal}}(\cdot)$, $p_{\text{naive}}(\cdot)$, $p_{\text{CF}}(\cdot)$ and $p_{\text{SPCF}}(\cdot)$. For this example, the Chernoff fusion selects the exponent $w = 1$ while sigma-point Chernoff fusion selects the scaling factor

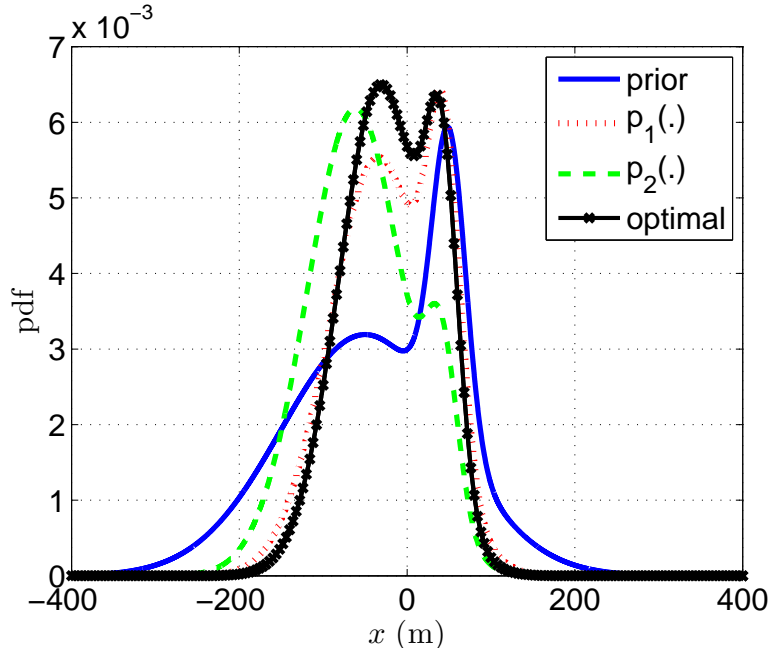


Figure 2.2: The densities $p(\cdot)$, $p_1(\cdot)$, $p_2(\cdot)$ and $p_{\text{optimal}}(\cdot)$ for parameter selection I.

$w = 0.9394$. Note that for this specific case, the fused densities $p_{\text{SPCF}}(\cdot)$ and $p_{\text{CF}}(\cdot)$ seem to be quite similar and they fit better to $p_{\text{optimal}}(\cdot)$ than $p_{\text{naive}}(\cdot)$ does. It must be noted that, for exactly the same example, it is easy to find the reverse case if other samples are generated from the random variables x , z_1 , z_2 and z_3 . We show the error cdfs for the means and the standard deviations in Figures 2.4 and 2.5 respectively. The results show that for this example, sigma-point Chernoff fusion is a little better than Chernoff fusion on the average in terms of both mean error and standard deviation error. Note that the mean error of both algorithms are worse than naive fusion whose mean estimates are surprisingly close to the optimal means. However, as can be observed, the naive fusion standard deviation errors are much worse than the other algorithms which is expected.

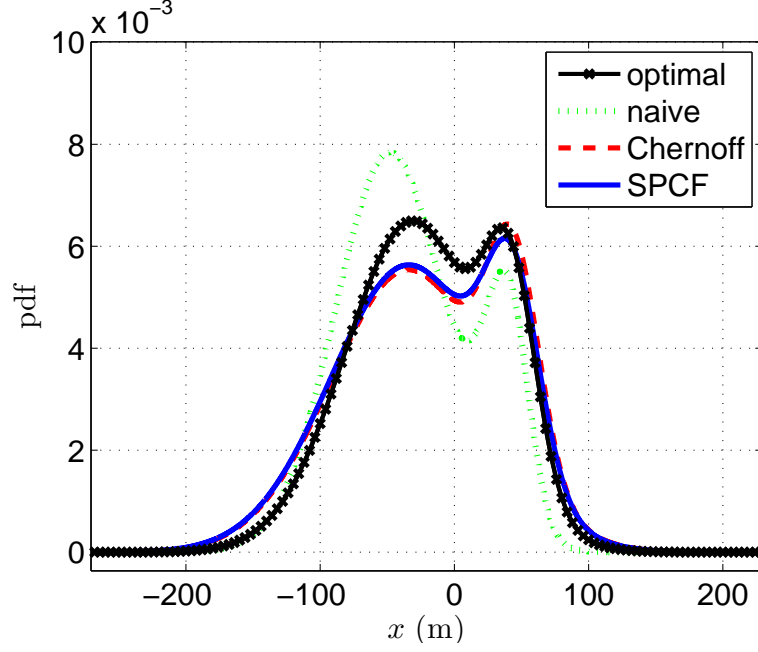


Figure 2.3: The fused densities $p_{\text{optimal}}(\cdot)$, $p_{\text{naive}}(\cdot)$, $p_{\text{CF}}(\cdot)$ and $p_{\text{scaling}}(\cdot)$ for parameter selection I.

2.4.1.2 Parameter Selection II

In this case we select the parameters of the scenario as below.

$$\pi_1 = 0.5 \quad \pi_2 = 0.5 \quad (2.40a)$$

$$\mu_1 = -20\text{m} \quad \mu_2 = 20\text{m} \quad (2.40b)$$

$$M_1 = 10^2 \text{m}^2 \quad M_2 = 10^2 \text{m}^2. \quad (2.40c)$$

$$R_1 = R_2 = R_3 = 100^2 \text{m}^2. \quad (2.41)$$

The error cdfs for the means and the standard deviations are given in Figures 2.6 and 2.7 respectively. For this example, the results show that the differences of the obtained means and covariances from the optimal mean and covariances are much smaller compared to the previous parameter set. For a better visual comparison, the axes limits are selected same in Figures 2.6 and 2.7 and in Figures 2.4 and 2.5. The mean errors of the sigma-point Chernoff fusion for the current parameter selection are on average similar to those of Chernoff fusion and Naive fusion. Nevertheless, the sigma-point Chernoff fusion still seems to be considerably more consistent than naive fusion.

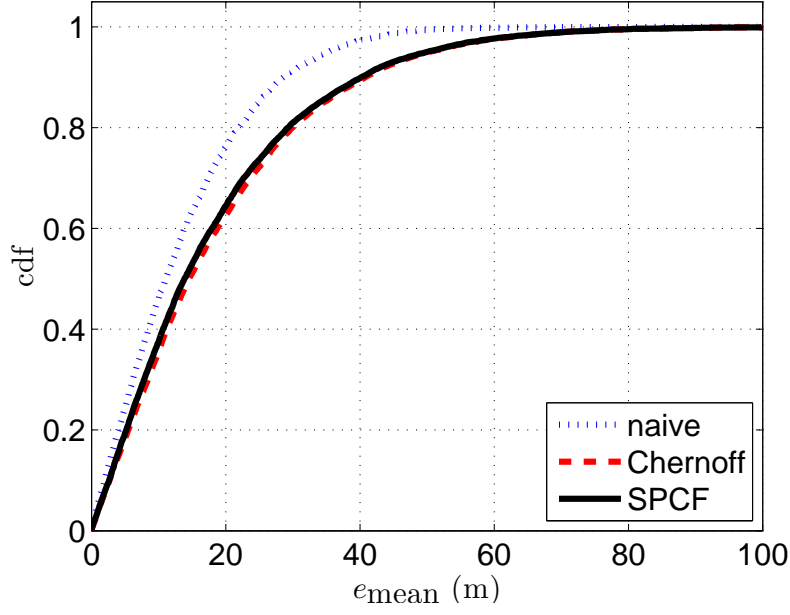


Figure 2.4: The cdfs for e_{mean} for parameter selection I.

The above case study gives some preliminary information about the performance of SPCF compared to Chernoff. SPCF is an approximation to Chernoff and the case study demonstrates that this approximation is reasonable. Two different parameter sets are selected with different characteristics: first is anti-symmetric, the second one is symmetric. For both cases, SPCF's performance is close to Chernoff.

2.4.2 2D-Case

The aim of this part is to give some idea about the computational power requirement of the algorithms. Comparison of the methods from a computational point of view is much more meaningful when the problem is defined in a higher dimensional space. For this aim, 2D example is generated. The new problem is analyzed in terms of the performances of different fusion techniques, as well. One-dimensional simulations presented in the previous subsection are extended

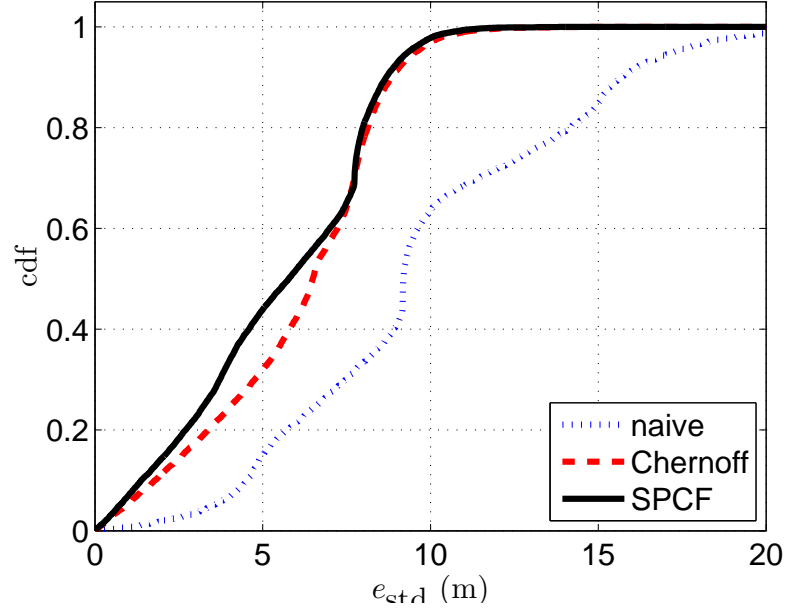


Figure 2.5: The cdfs for e_{std} for parameter selection I.

to the 2D space in which the parameters of the scenario are selected as below.

$$\pi_1 = 0.8 \quad \pi_2 = 0.2 \quad (2.42a)$$

$$\mu_1 = [-50\text{m}; -50\text{m}] \quad \mu_2 = [50\text{m}; 50\text{m}] \quad (2.42b)$$

$$M_1 = \text{diag}(100^2\text{m}^2, 100^2\text{m}^2) \quad M_2 = \text{diag}(20^2\text{m}^2, 20^2\text{m}^2) \quad (2.42c)$$

$$R_1 = R_2 = R_3 = \text{diag}(100^2\text{m}^2, 100^2\text{m}^2) \quad (2.43)$$

The results of performance analysis are represented in the figures 2.8 and 2.9. In parallel with the earlier findings, mean estimates of the sigma-point Chernoff fusion are very similar to those of Chernoff and Naive fusion methods while it has better covariance characteristics than these two methods. These results are an indication of the effectiveness of the proposed technique in a higher dimension.

From computational point of view, for the 1D case, when the discretization interval length h is equal to 0.1m for the Chernoff fusion, the computation times of the proposed technique and the Chernoff fusion method were, more or less, similar on the average and both run 100 times slower than naive fusion. This is

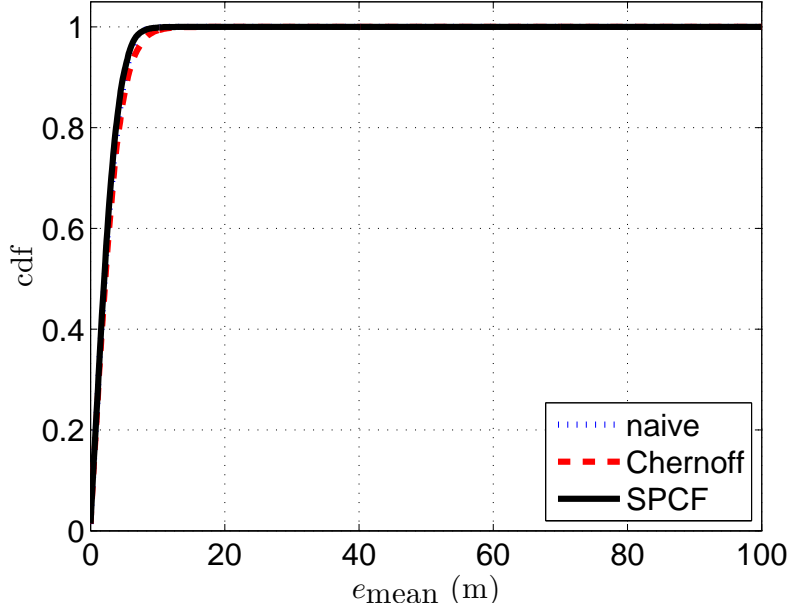


Figure 2.6: The cdfs for e_{mean} for parameter selection II.

reasonable since the fused density computation is carried out 100 times for the optimization involved in the method. On the other hand, when the dimension is increased to 2, the sigma-point Chernoff fusion is approximately 350 times faster than the Chernoff fusion due to the numerical integral taken in the Chernoff fusion while calculating the objective function and the normalization constants. This difference is expected to increase drastically with multivariate densities in higher dimensions where taking numerical integrals would be much more difficult. Note that the discretization interval length h for the 2D case is taken as 1m and reducing this length further will certainly increase the computation difference between the sigma-point Chernoff fusion and the Chernoff fusion. Also note that while the Chernoff fusion spends a lot of time in the objective function evaluation, it still cannot provide an analytical fused density estimate at the end of the optimization which is not the case with the sigma-point Chernoff fusion.

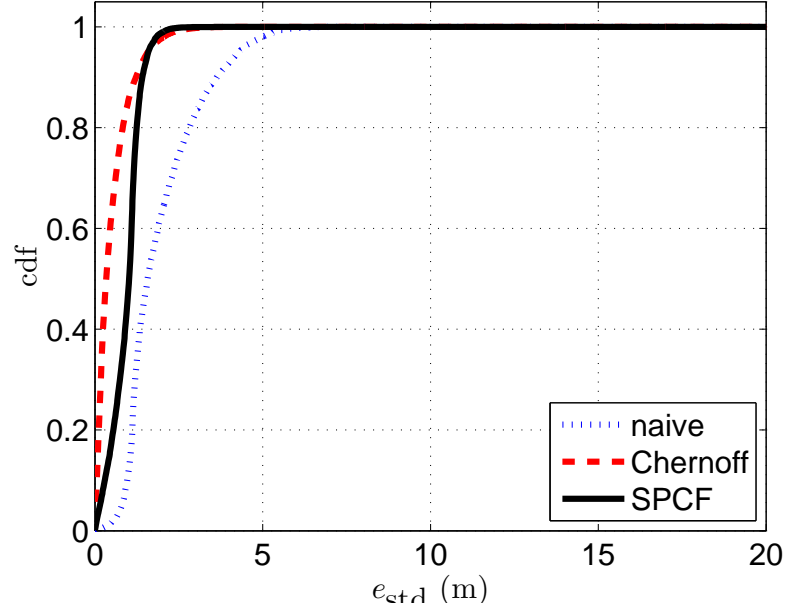


Figure 2.7: The cdfs for e_{std} for parameter selection II.

2.5 Comparison of Different Fusion Techniques with Numeric Chernoff Fusion Based on Simulations

This part analyzes the performance of SPCF for a problem that is used for this purpose in [26] which we take as a benchmark scenario. Results obtained by applying SPCF are compared with that of existing techniques like Pairwise Component Covariance Intersection (PCCI), Pseudo Chernoff-1 and Pseudo Chernoff-2. Performance of the fused densities is evaluated by comparing their contour plots with that of numerical Chernoff fusion and by utilizing a metric proposed by Comaniciu [17]. The metric provides the distance between two distributions and is given by (2.44).

$$d = \sqrt{1 - \rho[p(x), \hat{p}(x)]} \quad (2.44)$$

where

$$\rho[p(x), \hat{p}(x)] = \int \sqrt{p(x)\hat{p}(x)} dx \quad (2.45)$$

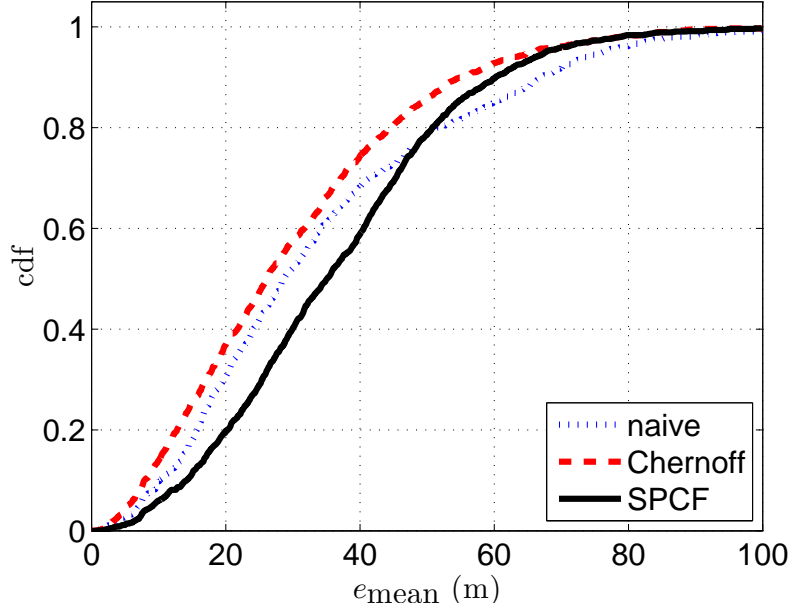


Figure 2.8: The cdfs for e_{mean} for parameter selection for 2D.

is the Bhattacharyya coefficient.

PCCI method stated in [26] relies on the application of CI technique to each pair of Gaussians in the Gaussian Mixture densities. Resultant individual solutions are combined into the global Gaussian mixture which is certainly a suboptimal solution. Other approximations called Pseudo Chernoff-1 and Pseudo Chernoff-2 are based on the first order approximation of w^{th} and $(1 - w)^{\text{th}}$ power of the two Gaussian mixtures and then applying Naive fusion on these expansions. Pseudo Chernoff-2 is an augmented version of Pseudo Chernoff-1.

Details of the fusion example in [26] are not provided hence we used the following parameters regarding the input estimate densities 1 and 2. Contour plots of the input densities using these parameters are obtained as in Figure 2.10.

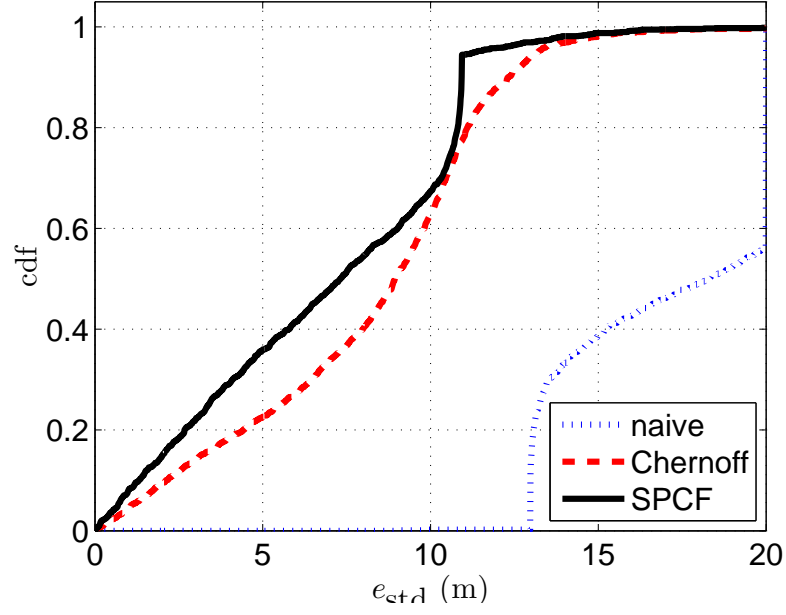


Figure 2.9: The cdfs for e_{std} for parameter selection for 2D.

$$p_1(x) = \sum_{i=1}^3 \beta_i \mathcal{N}(m_{1,i}, P) \quad (2.46)$$

$$p_2(x) = \sum_{i=1}^3 \alpha_i \mathcal{N}(m_{2,i}, P) \quad (2.47)$$

where $\{\beta_i\}_{i=1}^3 = \{0.35, 0.3, 0.35\}$, $\{m_{1,i}\}_{i=1}^3 = \{[-5 \ -3], [0 \ 0], [7 \ 7]\}$, $\{\alpha_i\}_{i=1}^3 = \{0.38, 0.5, 0.12\}$, $\{m_{2,i}\}_{i=1}^3 = \{[7 \ -7], [2 \ -2], [5 \ 2]\}$ and $P = 1.6 * I_2$.

Fused densities obtained by the stated techniques together with SPCF are given in Figure 2.11. It is obvious that SPCF performs much better than the other proposed techniques if the contour plots of numerically evaluated Chernoff fusion is taken as “best fusion” for the experimentation. This result also indicates that SPCF is a good approximation to Chernoff fusion.

Quantitative performance analysis based on (2.44) demonstrates again the outstanding performance of SPCF against other approximations in Table 2.1. SPCF is almost three times better than the Pseudo Chernoff-2 which is the best approach according to that study.

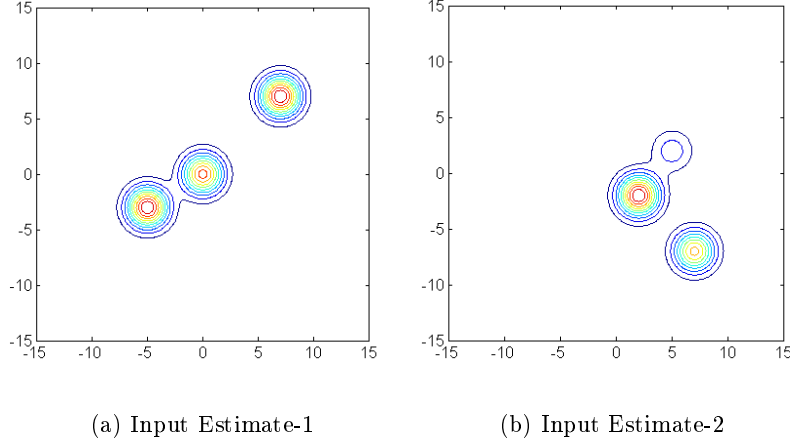


Figure 2.10: Input estimates for the benchmark scenario.

Table 2.1: Cost of different approximations. Results of PCCI and Pseudo Chernoff-1 techniques are adopted from [26].

Algorithm	Cost
PCCI	0.7286
Pseudo Chernoff-1	0.6608
Pseudo Chernoff-2	0.4523
SPCF	0.0700

Approximate computation times for each method are given in Table 2.2 for this example. Note that these results are dependent on the processor that we run the algorithms though they give intuition about the relative complexity of each approach.

SPCF significantly decreases the computation time of the Chernoff operation when compared to the numeric method. Also note that SPCF is 15 times slower than the Pseudo Chernoff-2 method. This is an expected result since SPCF technique includes a complex algorithm to find the exponent of the input densities.

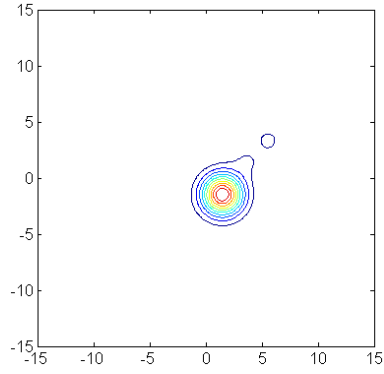
Table 2.2: Approximate computation times for numeric Chernoff, Pseudo Chernoff and SPCF techniques.

Algorithm	Computation Time
Numeric Chernoff	62.9 sec.
Pseudo Chernoff-2	0.13 sec.
SPCF	1.87 sec.

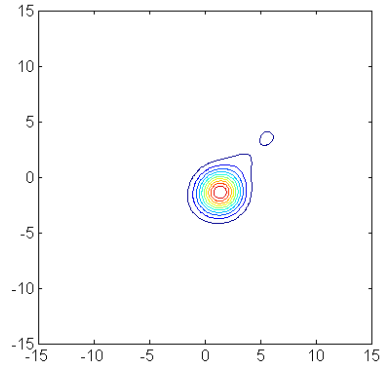
2.6 Discussions

In this chapter, we propose a solution to the problem of Chernoff fusion of Gaussian mixtures by approximating the exponent of the input Gaussian mixture densities with sigma points and then performing the Chernoff technique. This technique is explained in detailed in this chapter and the effectiveness of the technique is demonstrated by comparing it with the optimal solution, numeric Chernoff fusion and naive fusion. The results of the proposed approach are comparable to those obtained by Chernoff fusion and persistently more consistent than naive fusion. SPCF is an approximation to Chernoff fusion. So, to compare it with some other approximations proposed in the literature, the method is applied to the benchmark problem of [26]. The clear superiority of SPCF is demonstrated in Table 2.1.

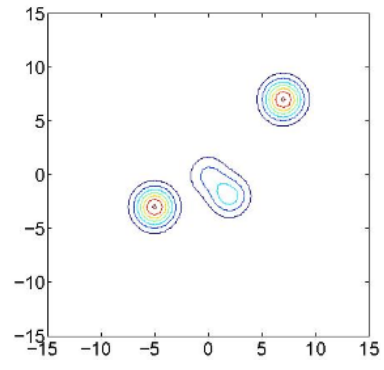
Track fusion problems is one of the interesting fusion area which requires the elimination of unknown correlations obtained from different sensors. They are generally defined in high dimensional state spaces and elimination of unknown correlation requires numerical approaches for exponentiation of the mixtures which is impossible in general. So, the proposed technique in this chapter will give way to the fusion of target density and intensity functions in track fusion problems. Specifically in this study, we use SPCF method in various fusion architectures for fusion of IMM and PHD filters.



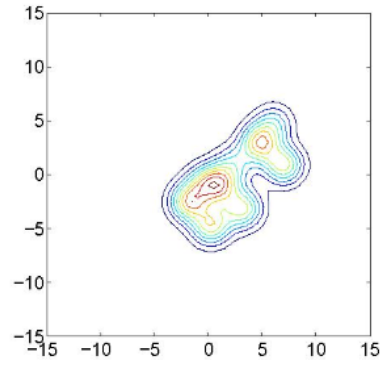
(a) Numeric Chernoff



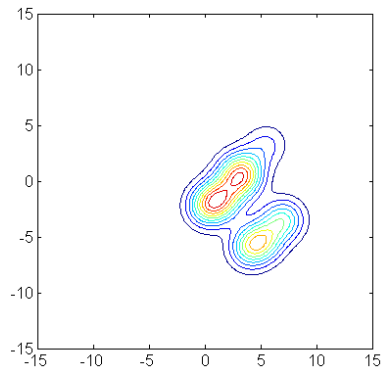
(b) SPCF



(c) PCCI



(d) Pseudo Chernoff-1



(e) Pseudo Chernoff-2

Figure 2.11: Fusion results for the benchmark scenario. Results of PCCI and Pseudo Chernoff-1 techniques are adopted from [26].

CHAPTER 3

FUSION OF IMM'S IN A DECENTRALIZED RADAR SYSTEM

3.1 Introduction

Interacting Multiple Model (IMM) filter is often preferred by the tracking community because of its flexibility to adapt different target motion models and it is quite natural to face with the problem of fusion of IMM filters in a multisensor environment. So, the application that we introduce in this chapter covers the fusion strategies for two sensors having IMM trackers which produce Gaussian mixture densities. We assume that the two radar systems produce state probability densities that can be exchanged and fusion can be performed to combine the information of the local and remote Gaussian mixtures. As previously stated, the information exchange architecture taken as a baseline for these strategies is provided in Figure 1.5. Even in this simple scenario, a few fusion architectures and methods can be proposed to yield good state estimates. Prior to further discussions on these fusion strategies, some information for the classic IMM filter and necessary equations for its implementation will be provided for the completeness of the subject. Fusion derivations related to the Naive and SPCF methods in the related fusion architectures will be discussed next. Lastly, performance evaluations for the different fusion approaches will be provided using simulated and realistic target scenarios.

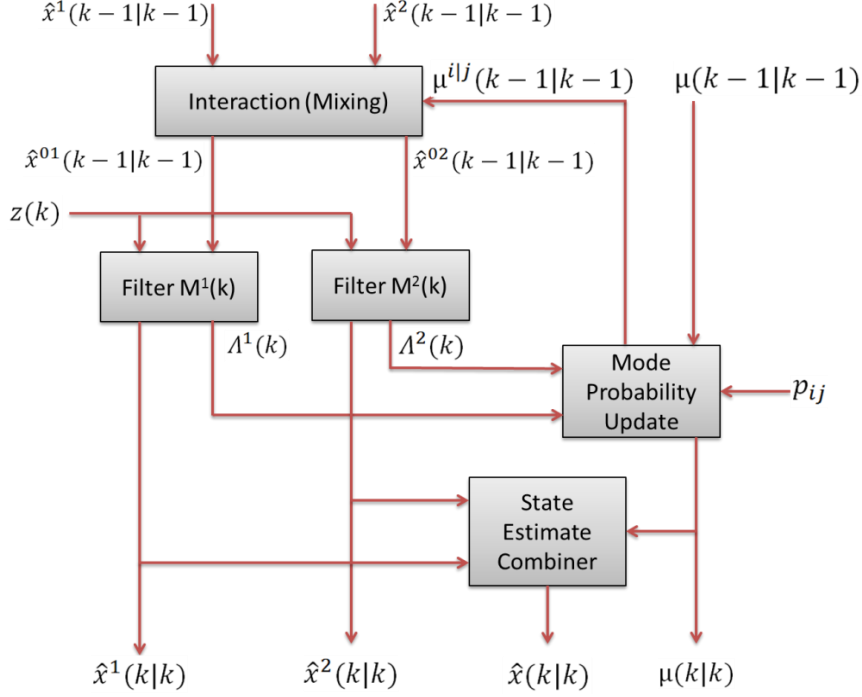


Figure 3.1: Block diagram of the IMM for two models.

3.2 Short Description of IMM (Adopted from [5])

A block diagram for a single step of the IMM filter for two models is given in Figure 3.1. For the time k , the inputs are the previous model conditioned estimates; $\hat{x}^1(k-1|k-1)$ and $\hat{x}^2(k-1|k-1)$, the associated covariances $P^1(k-1|k-1)$ and $P^2(k-1|k-1)$ (the covariances are not shown in the figure) and the previous model probabilities $\mu(k-1|k-1) = [\mu^1(k-1|k-1) \ \mu^2(k-1|k-1)]'$ from the time $k-1$. Here, $\mu^j(k-1|k-1)$ is the probability that model j is the correct model at the previous time instant. Each of the filters uses a different combination (mixture) of $x^1(k-1|k-1)$ and $x^2(k-1|k-1)$ as the initial state.

In the figure, the four conditional model probabilities $\mu^{i|j}(k-1|k-1)$, $(i, j = 1, 2)$ are used in the mixing procedure, which produces the two mixed estimates $\hat{x}^{01}(k-1|k-1)$ and $\hat{x}^{02}(k-1|k-1)$. The mixed estimates along with the current measurement $z(k)$, are then used in the filters to compute the updated state estimates $\hat{x}^1(k|k)$ and $\hat{x}^2(k|k)$ for the current time. The filters also com-

pute the likelihoods $\Lambda^1(k)$ and $\Lambda^2(k)$ that each estimate is from the correct filter. The likelihoods, the previous model probabilities, and the model switching probabilities p_{ij} are then used to compute the updated model probabilities $\mu(k|k) = [\mu^1(k|k) \ \mu^2(k|k)]'$. Finally, the state estimate combiner computes the overall state estimate $\hat{x}(k|k)$ as a weighted combination of $\hat{x}^1(k|k)$ and $\hat{x}^2(k|k)$, where the weights are $\mu^1(k|k)$ and $\mu^2(k|k)$.

The IMM estimator is outlined below (See [4] for a derivation). For the current update cycle, the IMM estimator starts with the r -model-conditioned state estimates $\hat{x}^i(k-1|k-1)$, state error covariances $P^i(k-1|k-1)$, and the model probabilities $\mu^i(k-1|k-1) = Pr\{M^i(k-1)|Z_1^{k-1}\}$ from the previous time instant. Here, $Z_1^{k-1} = \{z(1), \dots, z(k-1)\}$ denotes the set of past measurements, and $Z_1^k = \{Z_1^{k-1}, z(k)\}$ denotes all measurements, including the current measurement $z(k)$. $M^i(k-1)$ stands for the state of target's motion matching with the i^{th} model. When the current measurement $z(k)$ is received, the IMM is implemented using the following steps:

1. **Mixing of the State Estimates (Interaction):** For the filter matched to $M^j(k)$, the mixed estimate $\hat{x}^{0j}(k-1|k-1)$ and covariance $P^{0j}(k-1|k-1)$ are computed by

$$\hat{x}^{0j}(k-1|k-1) = \sum_{i=1}^r \mu^{ij}(k-1|k-1) \hat{x}^i(k-1|k-1) \quad (3.1)$$

$$\begin{aligned} P^{0j}(k-1|k-1) = & \sum_{i=1}^r \mu^{ij}(k-1|k-1) \{P^i(k-1|k-1) + \\ & [\hat{x}^i(k-1|k-1) - \hat{x}^{0j}(k-1|k-1)] [\hat{x}^i(k-1|k-1) - \hat{x}^{0j}(k-1|k-1)]'\} \end{aligned} \quad (3.2)$$

where the conditional model probabilities $\mu^{ij}(k-1|k-1)$ are given by

$$\mu^{ij}(k-1|k-1) = Pr\{M^i(k-1)|M^j(k), Z_1^{k-1}\} \quad (3.3)$$

$$= \frac{1}{\mu^j(k|k-1)} p_{ij} \mu^i(k-1|k-1) \quad (3.4)$$

and the predicted model probability $\mu^j(k|k-1)$ is computed by

$$\mu^j(k|k-1) = Pr \{M^j(k)|Z_1^{k-1}\} \quad (3.5)$$

$$= \sum_{i=1}^r p_{ij} \mu^i(k-1|k-1) \quad (3.6)$$

2. Model Conditioned Updates. For the filter matched to $M^j(k)$, the update is given by the Kalman filtering equations:

$$\hat{x}^j(k|k-1) = \Phi^j(k, k-1) \hat{x}^{0j}(k|k-1) \quad (3.7)$$

$$P^j(k|k-1) = \Phi^j(k, k-1) P^{0j}(k|k-1) [\Phi^j(k, k-1)]' + G^j(k, k-1) Q^i(k-1) [G^j(k, k-1)]' \quad (3.8)$$

$$v^j(k) = z(k) - H^j(k) \hat{x}^j(k|k-1) \quad (3.9)$$

$$S^j(k) = H^j(k) P^j(k|k-1) [H^j(k)]' + R^j(k) \quad (3.10)$$

$$K^j(k) = P^j(k|k-1) [H^j(k)]' [S^j(k)]^{-1} \quad (3.11)$$

$$\hat{x}^j(k|k) = \hat{x}^j(k|k-1) + K^j(k) v^j(k) \quad (3.12)$$

$$P^j(k|k) = [I - K^j(k) H^j(k)] P^j(k|k-1) \quad (3.13)$$

where $\hat{x}^j(k|k-1)$ is the predicted state estimate under $M^j(k)$, corresponding prediction covariance is $P^j(k|k-1)$, $v^j(k)$ is the residual, $S^j(k)$ is the residual covariances, $K^j(k)$ is the Kalman gain, $\hat{x}^j(k|k)$ is the updated state estimate under $M^j(k)$, $P^j(k|k)$ is the updated covariance matrix, and I is the identity matrix.

3. Model Likelihood Computations. The likelihood of the filter matched to $M^j(k)$ is defined by $\Lambda^j(k) = f[z(k)|M^j(k), Z_1^{k-1}]$, where $f[.]$ denotes a conditional density. The likelihood is computed using the filter residual, the residual covariances, and the assumption of Gaussian statistics.

$$\Lambda^j(k) = \frac{1}{\sqrt{\det[2\pi S^j(k)]}} \exp \left\{ \frac{-1}{2} [v^j(k)]' [S^j(k)]^{-1} v^j(k) \right\} \quad (3.14)$$

4. **Model Probability Updates.** The probability $\mu^j(k|k)$ for $M^j(k)$ is

$$\mu^j(k|k) = Pr \{ M^j(k) | Z_1^k \} \quad (3.15)$$

$$= \frac{1}{c} \mu^j(k|k-1) \Lambda^j(k) \quad (3.16)$$

where the normalization factor c is

$$c = \sum_{i=1}^r \mu^i(k|k-1) \Lambda^i(k) \quad (3.17)$$

5. **Combination of the State Estimates.** The overall or combined state estimate $\hat{x}(k|k)$ and $P(k|k)$ for the IMM are given by

$$\hat{x}(k|k) = \sum_{i=1}^r \mu^i(k|k) \hat{x}^i(k|k) \quad (3.18)$$

$$P(k|k) = \sum_{i=1}^r \mu^i(k|k) \left(P^i(k|k) + [\hat{x}^i(k|k) - \hat{x}(k|k)][\hat{x}^i(k|k) - \hat{x}(k|k)]' \right) \quad (3.19)$$

3.3 Fusion Strategies Regarding the Fusion of Information Produced by Local and Remote IMM's

Inclusion of the fusion strategies into the traditional IMM filter might require some modifications and calculations on the flow of the standard filter. The problem here is to fuse the local information obtained from “interaction, filtering and mode probability update” blocks with that obtained from the remote radar system. Note that the type of the local and remote densities may be the estimate

pdf of each sensor which is a single Gaussian or a Gaussian Mixture which may lead to different architectures including aforementioned fusion techniques. In this section, not all of the architectures or techniques are analyzed but those which are suitable to the flow of an IMM filter are selected and detailed inspection of the SPCF technique with resort to other techniques is made. For this aim, four different fusion strategies are chosen as the framework for the fusion of IMM's and their fusion expressions are analytically found. The expressions below are derived for the general case for which number of the models in both IMM 's are identical and taken as a variable r while the experiments will rely on two models which will be explained in detail, later on.

- **Strategy-1:** Both local and remote information are Gaussian Mixture densities. Naive and SPCF fusion methods are both applicable. Feedback to the tracker is provided.
- **Strategy-2:** Both local and remote information are Gaussian Mixture densities. SPCF fusion method is chosen. No feedback to the tracker is provided.
- **Strategy-3:** Both local and remote information are Gaussian densities. CI technique is chosen for this case. Feedback exists.
- **Strategy-4:** Both local and remote information are Gaussian densities, CI technique is chosen for this case. No feedback exists.

3.3.1 Fusion Strategy-1

This strategy is proposed for fusing two Gaussian mixtures while not violating the rules of a standard IMM filter. Figure 3.2 shows the internal structure of the local fusion system adapted to fuse local information and remote Gaussian mixture in the most appropriate way.

Notice that in this case, while remote information is in the form of a Gaussian mixture density, the local one is the information function matched to $M^j(k)$ with

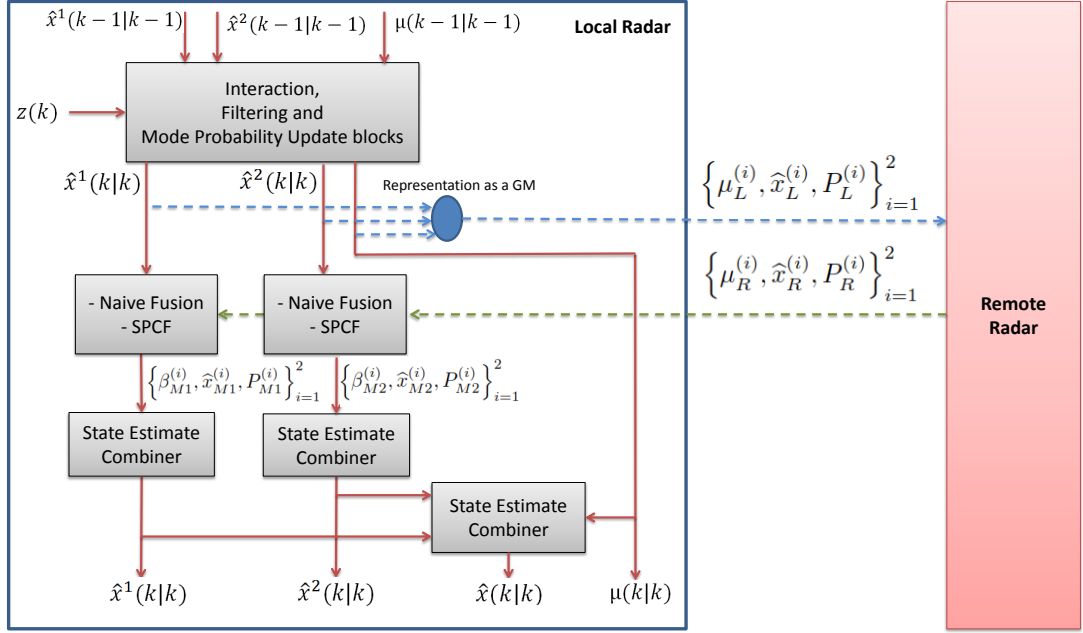


Figure 3.2: IMM fusion structure in which Gaussian mixtures are exchanged and Naive/SPCF methods are applicable.

model probability $\mu_L^j(k|k)$ which is in the form of a scaled Gaussian. Equation for the former is given in (3.20) and that of the latter is in (3.21).

$$f_R(x) = \sum_{i=1}^r \mu_R^i(k|k) \mathcal{N}(x; \hat{x}_R^i(k|k), P_R^i(k|k)) \quad (3.20)$$

$$f_L^j(x) = \mu_L^j(k|k) \mathcal{N}(x; \hat{x}_L^j(k|k), P_L^j(k|k)) \quad (3.21)$$

where the letters “R”, “L” and “F” denote “Remote”, “Local” and “Fused”, respectively, throughout the chapter. Only Naive and SPCF fusion techniques can be applicable to fuse a Gaussian function with a Gaussian mixture.

3.3.1.1 Implementation of Naive Fusion Technique

The implementation is explained by referring to Figure 3.2.

Step 1 IMM Interaction, Filtering and Mode Probability Update

Block This step is the same as that of a classic IMM filter and are followed in the same way without any modification.

Step 2 Fusion of Local and Remote Information Utilizing the idea beneath the Naive Fusion approach to produce the fused information from the functions obtained, multiplication of $f_R(x)$ and $f_L^j(x)$ gives out the desired function carrying the fused information as stated in the equation (3.25):

$$f_F^j(x) = f_L^j(x)f_R(x) \quad (3.22)$$

$$= \mu_L^j \mathcal{N}(x; \hat{x}_L^j, P_L^j) \sum_{i=1}^r \mu_R^i \mathcal{N}(x; \hat{x}_R^i, P_R^i) \quad (3.23)$$

$$= \mu_L^j \sum_{i=1}^r \mu_R^i \mathcal{N}(x; \hat{x}_R^i, P_R^i) \mathcal{N}(x; \hat{x}_L^j, P_L^j) \quad (3.24)$$

Then the multiplication of the Gaussians results in another Gaussian multiplied by a scalar.

$$f_F^j(x) = \mu_L^j \sum_{i=1}^r \mu_R^i \mathcal{N}(\hat{x}_L^j; \hat{x}_R^i, P_R^i + P_L^j) \mathcal{N}(x; \hat{x}^{i|j}, P^{i|j}) \quad (3.25)$$

where $\hat{x}^{i|j} = ((P_R^i)^{-1} + (P_L^j)^{-1})^{-1}((P_R^i)^{-1}\hat{x}_R^i + (P_L^j)^{-1}\hat{x}_L^j)$ and $P^{i|j} = ((P_R^i)^{-1} + (P_L^j)^{-1})^{-1}$.

Rearranging the multiplication gives out the resultant equation in (3.26).

$$f_F^j(x) = \mu_L^j C(j) \frac{1}{C(j)} \sum_{i=1}^r \mu_R^i \mathcal{N}(\hat{x}_L^j; \hat{x}_R^i, P_R^i + P_L^j) \mathcal{N}(x; \hat{x}^{i|j}, P^{i|j}) \quad (3.26)$$

where

$$C(j) = \int \sum_{i=1}^r \mu_R^i \mathcal{N}(\hat{x}_L^j; \hat{x}_R^i, P_R^i + P_L^j) \mathcal{N}(x; \hat{x}^{i|j}, P^{i|j}) dx \quad (3.27)$$

$$= \sum_{i=1}^r \mu_R^i \mathcal{N}(\hat{x}_L^j; \hat{x}_R^i, P_R^i + P_L^j) \quad (3.28)$$

is the normalizing constant for the Gaussian mixture. If we denote

$$p_F^j(x) \triangleq \frac{1}{C(j)} \sum_{i=1}^r \mu_R^i \mathcal{N}(\hat{x}_L^j; \hat{x}_R^i, P_R^i + P_L^j) \mathcal{N}(x; \hat{x}^{i|j}, P^{i|j}) \quad (3.29)$$

as the new density function, $\mu_L^j C(j)$ corresponds to the updated model probability for the filter matched to $M^j(k)$:

$$\mu_{L,upd}^j \triangleq \mu_L^j C(j) \quad (3.30)$$

Note that the sum of mode probabilities must be equal to unity. To guarantee this, normalization is applied and the updated information function becomes:

$$\mu_{L,upd,nor}^j = \frac{\mu_{L,upd}^j}{\sum_{j=1}^r \mu_{L,upd}^j} \quad (3.31)$$

$$f_F^j(x) = \mu_{L,upd,nor}^j \mathcal{P}_F^j(x) \quad (3.32)$$

Combination of the Gaussians in $f_F^j(x)$ is required since $\hat{x}_{final}^j(k|k)$ must be the mean of a single Gaussian at the end to run the procedure same as that of the classic IMM filter.

$$\hat{x}_{final}^j(k|k) = \frac{1}{C(j)} \sum_{i=1}^r \mu_R^i \mathcal{N}(\hat{x}_L^j; \hat{x}_R^i, P_R^i + P_L^j) \hat{x}^{i|j} \quad (3.33)$$

$$P_{final}^j(k|k) = \frac{1}{C(j)} \sum_{i=1}^r \mu_R^i \mathcal{N}(\hat{x}_L^j; \hat{x}_R^i, P_R^i + P_L^j) (P^{ij} + [\hat{x}^{i|j} - \hat{x}_{final}^j][\hat{x}^{i|j} - \hat{x}_{final}^j]') \quad (3.34)$$

Step-3 Combination of the State Estimates The overall or combined state estimate $\hat{x}(k|k)$ and $P(k|k)$ for the IMM are given by

$$\hat{x}(k|k) = \sum_{j=1}^r \mu_{L,upd,nor}^j(k|k) \hat{x}_{final}^j(k|k) \quad (3.35)$$

$$P(k|k) = \sum_{j=1}^r \mu_{L,upd,nor}^j(k|k) (P_{final}^j(k|k) + [\hat{x}_{final}^j(k|k) - \hat{x}(k|k)][\hat{x}_{final}^j(k|k) - \hat{x}(k|k)]') \quad (3.36)$$

3.3.1.2 Implementation of SPCF Technique

Steps 1 IMM Interaction, Filtering and Mode Probability Update

Block This step is the same as that of a classic IMM filter and are followed in the same way without any modification.

Step 2 Fusion of Local and Remote Information Utilizing the idea beneath the Chernoff Fusion approach to produce the fused information from the functions obtained, multiplication of $f_R(x)$ and $f_L^j(x)$ gives out the desired fused function as stated in the equations (3.37) and (3.38):

$$f_F^j(x) = (f_L^j(x))^w (f_R(x))^{1-w} \quad (3.37)$$

$$= (\mu_L^j)^w \mathcal{N}(x; \hat{x}_L^j, P_L^j) \left[\sum_{i=1}^r \mu_R^i \mathcal{N}(x; \hat{x}_R^i, P_R^i) \right]^{1-w} \quad (3.38)$$

For the calculation of $(1-w)^{\text{th}}$ power of the Gaussian Mixture obtained from remote radar system SPCF technique can be exploited and (3.38) is approximated as (3.40).

$$f_F^j(x) \cong (\mu_L^j)^w \frac{(2\pi |w^{-1}P_L^j|)^{0.5}}{(2\pi |P_L^j|)^{w/2}} \mathcal{N}(x; \hat{x}_L^j, w^{-1}P_L^j) \sum_{i=1}^r \beta_R^i \mathcal{N}(x; \hat{x}_R^i, (1-w)^{-1}P_R^i) \quad (3.39)$$

$$= (\mu_L^j)^w \frac{(2\pi |w^{-1}P_L^j|)^{0.5}}{(2\pi |P_L^j|)^{w/2}} \sum_{i=1}^r \beta_R^i \mathcal{N}(x; \hat{x}_L^j, w^{-1}P_L^j) \mathcal{N}(x; \hat{x}_R^i, (1-w)^{-1}P_R^i) \quad (3.40)$$

then the multiplication of the Gaussians results in another Gaussian multiplied by a scalar.

$$f_F^j(x) = (\mu_L^j)^w \frac{(2\pi |w^{-1}P_L^j|)^{0.5}}{(2\pi |P_L^j|)^{w/2}} \sum_{i=1}^r \beta_R^i \mathcal{N}(\hat{x}_L^j; \hat{x}_R^i, (1-w)^{-1}P_R^i + w^{-1}P_L^j) \mathcal{N}(x; \hat{x}_{i|j}, P_{i|j}) \quad (3.41)$$

where

$$\hat{x}^{i|j} = ((1-w)(P_R^i)^{-1} + w(P_L^j)^{-1})^{-1}((1-w)(P_R^i)^{-1}\hat{x}_R^i + w(P_L^j)^{-1}\hat{x}_L^j) \quad (3.42)$$

$$P^{i|j} = ((1-w)(P_R^i)^{-1} + w(P_L^j)^{-1})^{-1} \quad (3.43)$$

Rearranging the multiplication in (3.41) gives (3.44).

$$f_F^j(x) = (\mu_L^j)^w \frac{(2\pi |w^{-1}P_L^j|)^{0.5}}{(2\pi |P_L^j|)^{w/2}} C(j) \frac{1}{C(j)} \sum_{i=1}^r \beta_R^i \mathcal{N}(\hat{x}_L^j; \hat{x}_R^i, (1-w)^{-1}P_R^i + w^{-1}P_L^j) \mathcal{N}(x; \hat{x}_{i|j}, P_{i|j}) \quad (3.44)$$

where

$$C(j) = \int \sum_{i=1}^r \beta_R^i \mathcal{N}(\hat{x}_L^j; \hat{x}_R^i, (1-w)^{-1}P_R^i + w^{-1}P_L^j) \mathcal{N}(x; \hat{x}_{i|j}, P_{i|j}) \quad (3.45)$$

$$= \sum_{i=1}^r \beta_R^i \mathcal{N}(\hat{x}_L^j; \hat{x}_R^i, (1-w)^{-1}P_R^i + w^{-1}P_L^j) \quad (3.46)$$

is the normalizing constant for the Gaussian Mixture.

If we donate $\frac{1}{C(j)} \sum_{i=1}^r \beta_R^i \mathcal{N}(\hat{x}_L^j; \hat{x}_R^i, (1-w)^{-1}P_R^i + w^{-1}P_L^j) \mathcal{N}(x; \hat{x}_{i|j}, P_{i|j})$ as the new density function, remaining terms correspond to the updated model probability for the filter matched to $M^j(k)$:

$$\mu_{L,upd}^j \triangleq (\mu_L^j)^w \frac{(2\pi |w^{-1}P_L^j|)^{0.5}}{(2\pi |P_L^j|)^{w/2}} C(j) \quad (3.47)$$

$$p_F^j(x) \triangleq \frac{1}{C(j)} \sum_{i=1}^r \beta_R^i \mathcal{N}(\hat{x}_L^j; \hat{x}_R^i, (1-w)^{-1}P_R^i + w^{-1}P_L^j) \mathcal{N}(x; \hat{x}_{i|j}, P_{i|j}) \quad (3.48)$$

Optimal w selection is made by variance minimizing criteria, i.e.,

$$w^* \triangleq \arg \min_{w \in [0,1]} \mathcal{L}(p_F^j(x)) \quad (3.49)$$

where the function $\mathcal{L}(\cdot)$ is selected as the trace of the pdf covariance in this study.

Note that the sum of mode probabilities must be equal to unity. To guarantee this, normalization is applied to the resultant model probabilities. So,

$$\mu_{L,upd,nor}^j = \frac{\mu_{L,upd}^j}{\sum_{j=1}^r \mu_{L,upd}^j} \quad (3.50)$$

$$f_F^j(x) = \mu_{L,upd,nor} p_F^j(x) \quad (3.51)$$

Combination of the Gaussians in $p_F^j(x)$ is required since $\hat{x}_{final}^j(k|k)$ must be the mean of a single Gaussian at the end so as to run the procedure same as that of the classic IMM filter.

$$\hat{x}_{final}^j(k|k) = \frac{1}{C(j)} \sum_{i=1}^r \mu_R^i \mathcal{N}(\hat{x}_L^j; \hat{x}_R^i, (1-w)^{-1}P_R^i + w^{-1}P_L^j) \hat{x}^{i|j} \quad (3.52)$$

$$P_{final}^j(k|k) = \frac{1}{C(j)} \sum_{i=1}^r \mu_R^i \mathcal{N}(\hat{x}_L^j; \hat{x}_R^i, (1-w)^{-1}P_R^i + w^{-1}P_L^j) (P^{ij} + [\hat{x}^{i|j} - \hat{x}_{final}^j][\hat{x}^{i|j} - \hat{x}_{final}^j]') \quad (3.53)$$

Step-3 Combination of the State Estimates The overall or combined state estimate $\hat{x}(k|k)$ and $P(k|k)$ for the IMM are given by

$$\hat{x}(k|k) = \sum_{j=1}^r \mu_{L,upd,nor}^j(k|k) \hat{x}_{final}^j(k|k) \quad (3.54)$$

$$P(k|k) = \sum_{j=1}^r \mu_{L,upd,nor}^j(k|k) (P_{final}^j(k|k) + [\hat{x}_{final}^j(k|k) - \hat{x}(k|k)][\hat{x}_{final}^j(k|k) - \hat{x}(k|k)]') \quad (3.55)$$

3.3.2 Fusion Strategy-2

In this strategy, output state Gaussian mixture densities are exchanged in between remote and local radar systems. Fusion, based on SPCF technique, is performed outside the information loop of each IMM filter and does not provide any feedback to the local tracking structure (Figure 3.3). Final state estimate is found by combining the Gaussians in the resultant Gaussian mixture. Notice that both radar yield the same state estimates at the end.

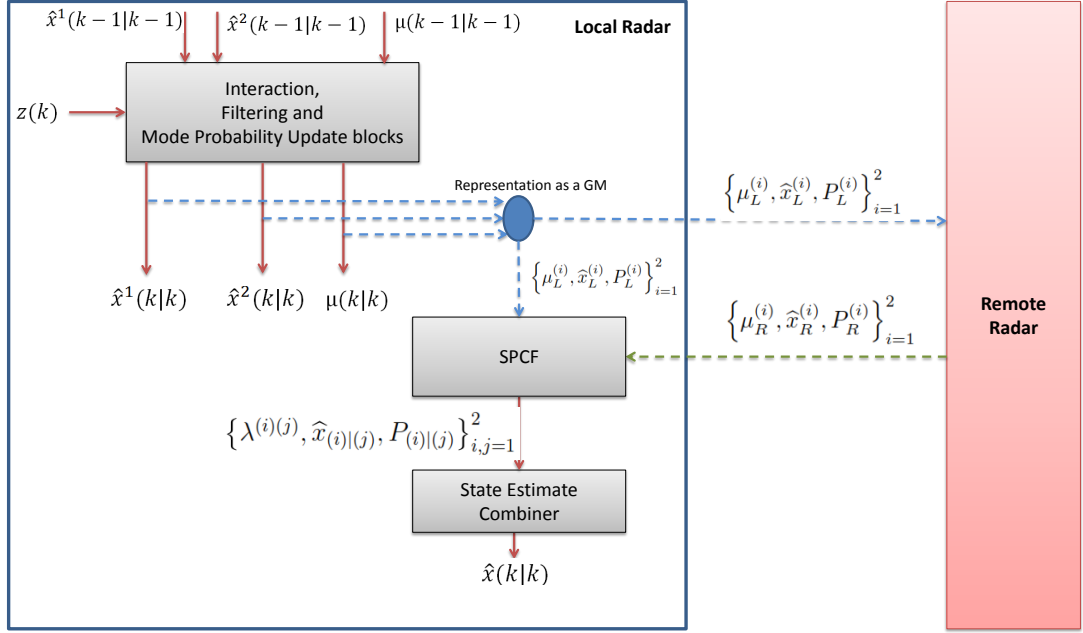


Figure 3.3: IMM fusion structure in which Gaussian mixtures are exchanged and SPCF method is used.

Equation for the remote radar density is given in (3.56) and that of the local is in (3.57).

$$f_R(x) = \sum_{i=1}^r \mu_R^i(k|k) \mathcal{N}(x; \hat{x}_R^i(k|k), P_R^i(k|k)) \quad (3.56)$$

$$f_L(x) = \sum_{j=1}^r \mu_L^j(k|k) \mathcal{N}(x; \hat{x}_L^j(k|k), P_L^j(k|k)) \quad (3.57)$$

SPCF fusion technique is selected as the fusion approach of this method. Referring to Figure 3.3, its implementation is explained next.

Steps 1 IMM Interaction, Filtering and Mode Probability Update Block This step is the same as that of a classic IMM filter and are followed in the same way without any modification.

Step 2 Fusion of Local and Remote Information If Chernoff Fusion formulae is applied to $f_R(x)$ and $f_L(x)$, the desired fused function is found by the

equations (3.58) and (3.59):

$$f_F(x) = \frac{1}{C} f_L^w(x) f_R^{1-w}(x) \quad (3.58)$$

$$= \left[\sum_{j=1}^r (\mu_L^j) \mathcal{N}(x; \hat{x}_L^j, P_L^j) \right]^w \left[\sum_{i=1}^r \mu_R^i \mathcal{N}(x; \hat{x}_R^i, P_R^i) \right]^{1-w} \quad (3.59)$$

where C is the normalization constant. For the calculation of w^{th} and $(1-w)^{\text{th}}$ power of the Gaussian Mixtures, SPCF technique can be exploited and (3.59) is approximated as (3.61).

$$f_F(x) \cong \frac{1}{C} \sum_{j=1}^r \alpha_L^j \mathcal{N}(x; \hat{x}_L^j, w^{-1} P_L^j) \sum_{i=1}^r \beta_R^i \mathcal{N}(x; \hat{x}_R^i, (1-w)^{-1} P_R^i) \quad (3.60)$$

$$= \frac{1}{C} \sum_{j=1}^r \sum_{i=1}^r \alpha_L^j \beta_R^i \mathcal{N}(x; \hat{x}_L^j, w^{-1} P_L^j) \mathcal{N}(x; \hat{x}_R^i, (1-w)^{-1} P_R^i) \quad (3.61)$$

Then the multiplication of the Gaussians results in another Gaussian multiplied by a scalar.

$$f_F(x) = \frac{1}{C} \sum_{j=1}^r \sum_{i=1}^r \alpha_L^j \beta_R^i \mathcal{N}(\hat{x}_L^j; \hat{x}_R^i, (1-w)^{-1} P_R^i + w^{-1} P_L^j) \mathcal{N}(x; \hat{x}_{i|j}, P_{i|j}) \quad (3.62)$$

where

$$\hat{x}^{i|j} = ((1-w)(P_R^i)^{-1} + w(P_L^j)^{-1})^{-1} ((1-w)(P_R^i)^{-1} \hat{x}_R^i + w(P_L^j)^{-1} \hat{x}_L^j) \quad (3.63)$$

$$P^{i|j} = ((1-w)(P_R^i)^{-1} + w(P_L^j)^{-1})^{-1} \quad (3.64)$$

If we denote the weights of the new Gaussian mixture density as $\lambda^{ij}(w)$ as given below,

$$\lambda^{ij}(w) \triangleq \frac{1}{C} \alpha_L^j \beta_R^i \mathcal{N}(\hat{x}_L^j; \hat{x}_R^i, (1-w)^{-1} P_R^i + w^{-1} P_L^j) \quad (3.65)$$

$$C = \sum_{j=1}^r \sum_{i=1}^r \alpha_L^j \beta_R^i \mathcal{N}(\hat{x}_L^j; \hat{x}_R^i, (1-w)^{-1} P_R^i + w^{-1} P_L^j) \quad (3.66)$$

fused density is represented as (3.67).

$$f_F(x) = \sum_{j=1}^r \sum_{i=1}^r \lambda^{ij}(w) \mathcal{N}(x; \hat{x}_{i|j}, P_{i|j}) \quad (3.67)$$

Optimal w selection is made by variance minimizing criteria, i.e.,

$$w^* \triangleq \arg \min_{w \in [0,1]} \mathcal{L}(f_F(x)) \quad (3.68)$$

where the function $\mathcal{L}(\cdot)$ is selected as the trace of the covariance of the pdf in this study.

Step-3 Combination of the State Estimates The overall or combined state estimate $\hat{x}(k|k)$ and $P(k|k)$ for the fusion structure are given by

$$\hat{x}(k|k) = \sum_{j=1}^r \sum_{i=1}^r \lambda^{ij}(w^*) \hat{x}_{i|j} \quad (3.69)$$

$$P(k|k) = \sum_{j=1}^r \sum_{i=1}^r \lambda^{ij}(w) (P_{i|j} + [\hat{x}_{i|j} - \hat{x}(k|k)][\hat{x}_{i|j} - \hat{x}(k|k)]') \quad (3.70)$$

3.3.3 Fusion Strategy-3

This strategy is proposed for fusing two Gaussian densities in a feedback mechanism while not violating the rules of a standard IMM filter. Figure 3.4 demonstrates the internal structure of the local fusion system adapted to fuse local information and remote Gaussian density in the most appropriate way.

In this type of strategy, while remote information is a Gaussian density, the local one is a scaled Gaussian density which is the information function matched to $M^j(k)$ with model probability $\mu_L^j(k|k)$. Equation for the former is given in (3.71) and that of the latter is in (3.72).

$$f_R(x) = \mathcal{N}(x; \hat{x}_R(k|k), P_R(k|k)) \quad (3.71)$$

$$f_L^j(x) = \mu_L^j(k|k) \mathcal{N}(x; \hat{x}_L^j(k|k), P_L^j(k|k)) \quad (3.72)$$

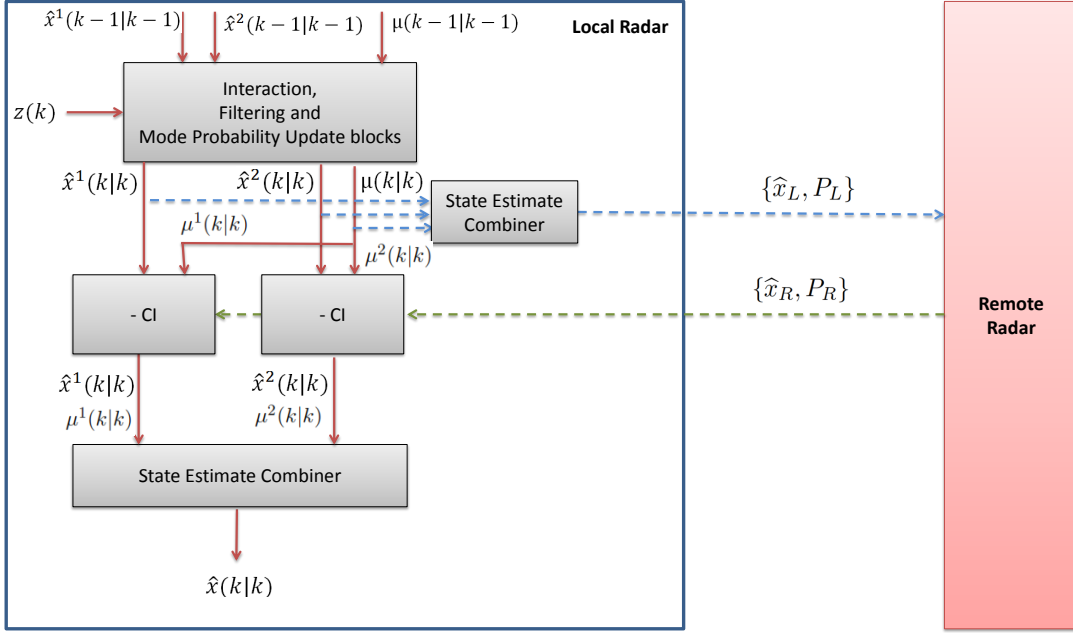


Figure 3.4: IMM fusion structure in which Gaussian densities are exchanged and CI method is applied in a feedback mechanism.

where the letters “R”, “L” and “F” denote “Remote”, “Local” and “Fused”, respectively, throughout the chapter. CI technique is chosen to fuse two Gaussian functions for this case. Implementation steps for this approach are provided as below:

Steps 1 IMM Interaction, Filtering and Mode Probability Update Block This step is the same as that of a classic IMM filter and are followed in the same way without any modification.

Step 2 Fusion of Local and Remote Information Utilizing the idea beneath the Chernoff Fusion approach to produce the fused information from the functions obtained, multiplication of $f_R(x)$ and $f_L^j(x)$ gives out the desired fused function as stated in the equations (3.73) and (3.74):

$$f_F^j(x) = (f_L^j(x))^w (f_R(x))^{1-w} \quad (3.73)$$

$$= (\mu_L^j)^w \mathcal{N}^w(x; \hat{x}_L^j, P_L^j) \mathcal{N}^{1-w}(x; \hat{x}_R, P_R) \quad (3.74)$$

Taking the exponent of the Gaussians in (3.74) results in the Equation (3.75)

for the fused density.

$$f_F^j(x) = (\mu_L^j)^w \frac{(2\pi |w^{-1}P_L^j|)^{0.5}}{(2\pi |P_L^j|)^{w/2}} \frac{(2\pi |(1-w)^{-1}P_R|)^{0.5}}{(2\pi |P_R|)^{(1-w)/2}} \mathcal{N}(x; \hat{x}_L^j, w^{-1}P_L^j) \mathcal{N}(x; \hat{x}_R, (1-w)^{-1}P_R) \quad (3.75)$$

then the multiplication of the Gaussians results in another Gaussian multiplied by a scalar.

$$f_F^j(x) = (\mu_L^j)^w (2\pi w^{-n} (1-w)^{-n})^{0.5} |P_L^j|^{0.5} \left(\frac{|P_R|}{|P_L^j|} \right)^{w/2} \mathcal{N}(\hat{x}_L^j; \hat{x}_R, (1-w)^{-1}P_R + w^{-1}P_L^j) \mathcal{N}(x; \hat{x}_{j|R}, P_{j|R}) \quad (3.76)$$

where n is the dimension of the state and

$$\hat{x}^{j|R} = ((1-w)(P_R)^{-1} + w(P_L^j)^{-1})^{-1} ((1-w)(P_R)^{-1} \hat{x}_R + w(P_L^j)^{-1} \hat{x}_L^j) \quad (3.77)$$

$$P^{j|R} = ((1-w)(P_R)^{-1} + w(P_L^j)^{-1})^{-1} \quad (3.78)$$

If we donate the Gaussian density in (3.75) as the new density function, remaining terms correspond to the updated model probability for the filter matched to $M^j(k)$:

$$\mu_{L,upd}^j \triangleq (\mu_L^j)^w (2\pi w^{-n} (1-w)^{-n})^{0.5} |P_L^j|^{0.5} \left(\frac{|P_R|}{|P_L^j|} \right)^{w/2} \quad (3.79)$$

$$p_F^j(x) \triangleq \mathcal{N}(x; \hat{x}_{j|R}, P_{j|R}) \quad (3.80)$$

Optimal w selection is made by variance minimizing criteria, i.e.,

$$w^* \triangleq \arg \min_{w \in [0,1]} \mathcal{L}(p_F^j(x)) \quad (3.81)$$

where the function $\mathcal{L}(\cdot)$ is selected as the trace of the pdf covariance in this study.

Note that the sum of mode probabilities must be equal to unity. To guarantee this, normalization is applied to the resultant model probabilities. So,

$$\mu_{L,upd,nor}^j = \frac{\mu_{L,upd}^j}{\sum_{j=1}^r \mu_{L,upd}^j} \quad (3.82)$$

$$f_F^j(x) = \mu_{L,upd,nor}^j p_F^j(x) \quad (3.83)$$

Step-3 Combination of the State Estimates The overall or combined state estimate $\hat{x}(k|k)$ and $P(k|k)$ for the IMM are given by

$$\hat{x}(k|k) = \sum_{j=1}^r \mu_{L,upd,nor}^j(k|k) \hat{x}^{j|R}(k|k) \quad (3.84)$$

$$P(k|k) = \sum_{j=1}^r \mu_{L,upd,nor}^j(k|k) (P^{j|R}(k|k) + [\hat{x}^{j|R}(k|k) - \hat{x}(k|k)][\hat{x}^{j|R} - \hat{x}(k|k)]') \quad (3.85)$$

3.3.4 Fusion Strategy-4

In this strategy, only output state estimates are exchanged in between remote and local radar systems. Information fusion, based on CI technique, is performed outside the information loop of each IMM filter and does not provide any feedback to the local tracking structure (Figure 3.5). Notice that both local and remote information is in the form of a Gaussian density. Density for the former is given in (3.86) and that of the latter is in (3.87).

$$f_L(x) = \mathcal{N}(x; \hat{x}_L(k|k), P_L(k|k)) \quad (3.86)$$

$$f_R(x) = \mathcal{N}(x; \hat{x}_R(k|k), P_R(k|k)) \quad (3.87)$$

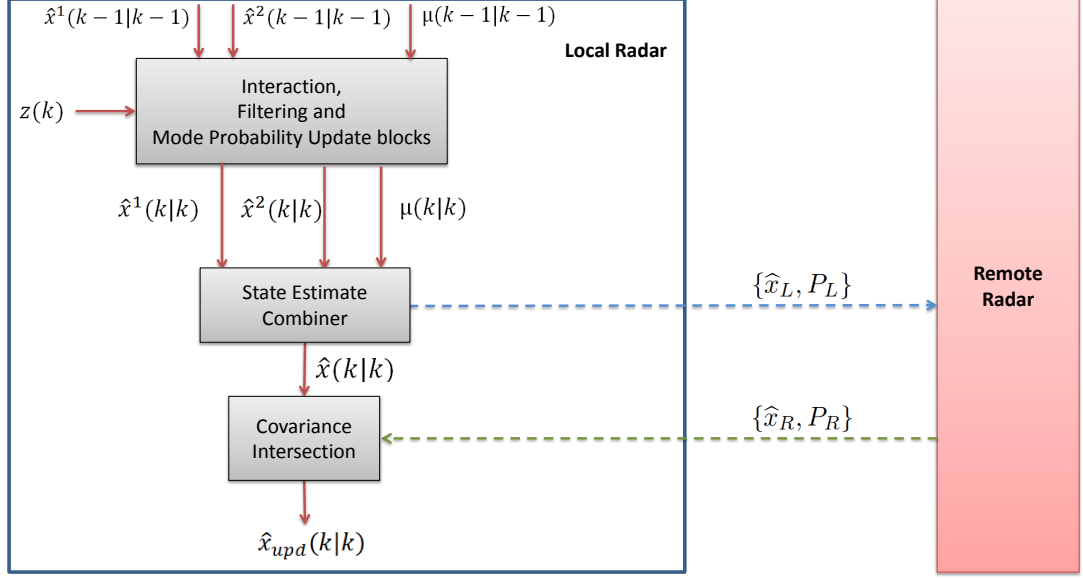


Figure 3.5: IMM fusion structure in which only state estimates are exchanged and CI method is applicable.

Application of Chernoff fusion technique on the Gaussian densities boils down to nothing but the CI technique:

$$P_{upd}^{-1} \hat{x}_{upd} = w^* P_L^{-1} \hat{x}_L + (1 - w^*) P_R^{-1} \hat{x}_R \quad (3.88)$$

$$P_{upd}^{-1} = w^* P_L^{-1} + (1 - w^*) P_R^{-1} \quad (3.89)$$

where $w^* \in [0, 1]$ is calculated using the following optimization

$$w^* \triangleq \arg \min_{w \in [0, 1]} \mathcal{L}(w P_L^{-1} + (1 - w) P_R^{-1}) \quad (3.90)$$

and where the function \mathcal{L} is selected as the trace of the covariance matrix.

3.4 Performance Evaluation

To test the performances of the strategies and the fusion methods explained in the previous section, a set of experiments is planned. The experiments are based

on 2D air platform scenarios in which the correlated track information obtained from different radar systems have to be fused. The scenarios are selected so as to understand the performance characteristics of the fusion methods in ideal and in more realistic situations. Ideal scenarios are based on the generation of the target trajectory for the predefined motion models and production of the related noisy radar measurements generated by adding white Gaussian noise to the true trajectory. On the other hand, the realistic case includes trajectories of two possible targets and randomly generated realistic radar measurements.

The performance of the methods, SPCF, Naive and CI are compared with each other and with the performance of the centralized measurement fusion. The centralized measurement fusion relies on fusing the unprocessed measurement information generated by the radars and will be considered as a benchmark for the experimental outputs. Individual performances are obtained by the difference of their outputs from the target ground truth trajectory by using L2-norm. The result is used as a measure for the accuracy of the state estimates.

The experiments use 50 randomly generated tracks with a length of 100 seconds which are produced by constant velocity models with large and small process noises corresponding to Model-1 and Model-2, respectively. Based on the ground truth generated, radar measurements are produced and fed to both local and remote radar IMM filters. The measurements are also fed to a centralized IMM, which is expected to perform the best fusion amongst all for comparison purposes. All the fusion results are compared with the ground truth trajectory of the target in the L2 norm sense. Then ensemble average of the resultant estimates of the 50 targets are taken at each time instant. A rough overview of the experiment set-up is provided in Figure 3.6.

The assessment methodology stated here will be a basis for both ideal and realistic target scenarios for which detailed information will be given in the upcoming sections.

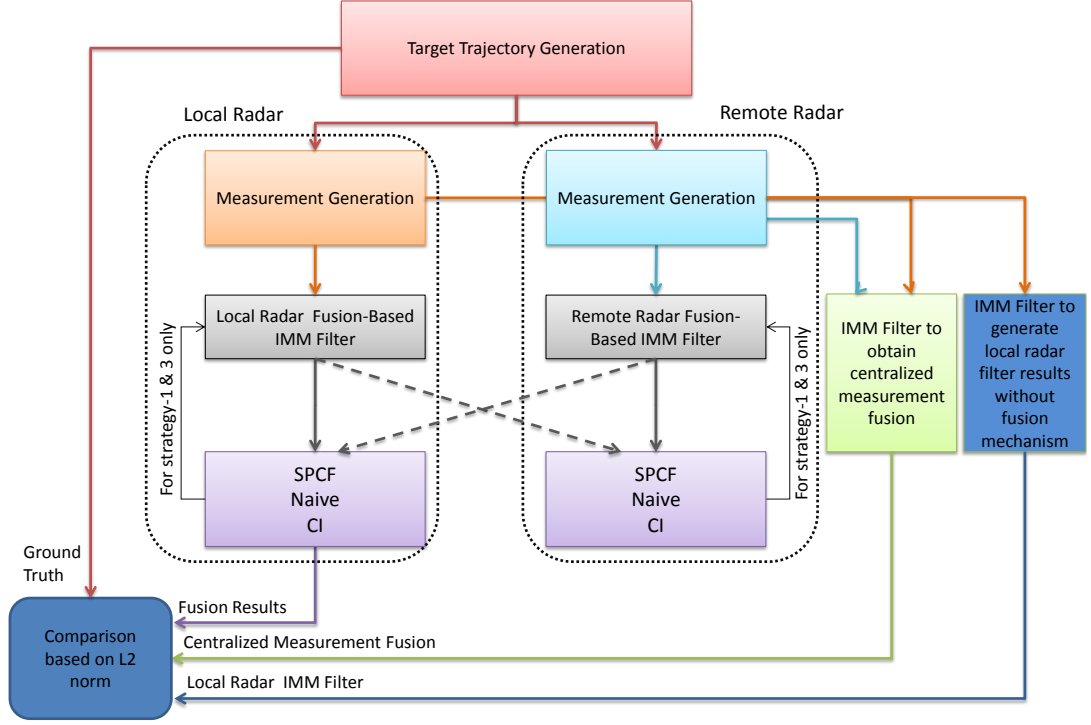


Figure 3.6: Experimental set-up to analyze different fusion approaches.

3.4.1 Ideal System Scenarios

3.4.1.1 Selection of the Target and the Radar Characteristics

The ideal scenarios are proposed to understand the performance boundaries of the approaches based on the process and measurement noise standard deviations. During the simulation phase of the thesis, it is observed that the level of correlation of the information obtained from the radars can certainly be different for different process and measurement noise selections. Specifically, relative value of the measurement noise with respect to process noise certainly effects the correlation of the output densities of the Kalman-based IMM filters and details of this observation will be emphasized in this section.

For the ideal case, motion / measurement models of IMM filters are perfectly fitted to those of the ground truth and all the parameters in the filter are compatible with those of target and radar models. With this choice, model mismatch

errors are avoided which may prevent objective comparison of the fusion strategies.

Another issue is the relative positions of the target with respect to the radars which is an important parameter. It is likely to affect the overall system performance in the sense that contribution of the azimuth and range measurement noises to the results is a function of the deployment. Since the contribution of the deployment to the performance is quite difficult to analyze, radar measurement noises are simply selected as white Gaussian noises in x and y dimensions. Measurement models for the radar are given in (3.91) and (3.92).

$$y_1(x_k) = Hx_k + v_k(r_1) \quad (3.91)$$

$$y_2(x_k) = Hx_k + v_k(r_2) \quad (3.92)$$

where $v(r_1) \sim \mathcal{N}(\tilde{v}, 0, r_1)$, $v(r_2) \sim \mathcal{N}(\tilde{v}, 0, r_2)$ and $H = [1 \ 0 \ 0 \ 0; 0 \ 1 \ 0 \ 0]$. In this work, $r_1 = r_2$ is taken and they represent uncorrelated measurement noise variances of the radars.

Selected target motion model is based on two models including low and high process noise models:

$$x_{k+1} = Fx_k + Bw_k(q_i), \quad i = 1, 2 \quad (3.93)$$

where

$$F = \begin{bmatrix} 1 & 0 & \Delta t & 0 \\ 0 & 1 & 0 & \Delta t \\ 0 & 0 & 1 & 0 \\ 0 & 0 & 0 & 1 \end{bmatrix} \quad (3.94)$$

and

$$B = \begin{bmatrix} \frac{\Delta t^2}{2} & 0 \\ 0 & \frac{\Delta t^2}{2} \\ \Delta t & 0 \\ 0 & \Delta t \end{bmatrix} \quad (3.95)$$

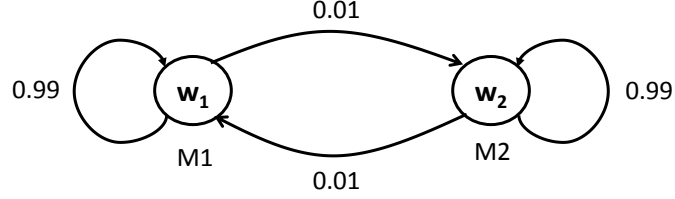


Figure 3.7: Markov chain for the selection of the process noise model.

and $w_k(\cdot)$ is selected by using the Markov process stated in Figure 3.7 where $w_k(q_1) \sim \mathcal{N}(w, 0, q_1)$ and $w_k(q_2) \sim \mathcal{N}(w, 0, q_2)$ correspond to the low and high process noise covariances, respectively.

3.4.1.2 Analysis of the IMM Filter to be Used

As stated before, IMM filter parameters are chosen as exactly the same as that of the target models in order to avoid the model mismatch errors during the simulations. Although mismatch is avoided, we investigate further the IMM filter and its coherency with the measurements and the target model before going towards the fusion experiments. For this aim, 50 tracks have been generated randomly for consistency check analysis. An example trajectory together with the corresponding radar measurements is given in Figure 3.8. IMM tracker outputs and the IMM weights belonging to this track are provided in Figure 3.9 and Figure 3.10, respectively.

Consistency check of the filter is performed by analyzing Normalized Innovations Squared (NIS) and Normalized Estimate Error Squared (NEES) values generated within the filter. These parameters are used for statistical testing of Kalman and IMM filters [4] and are measures of the model match. Ensemble averages of these values and upper and lower allowable limits are computed and displayed in Figures 3.11 and 3.12. Results show that, in most of the times, the NIS and NEES values lie in the boundaries, which indicate that the model mismatch errors are small.

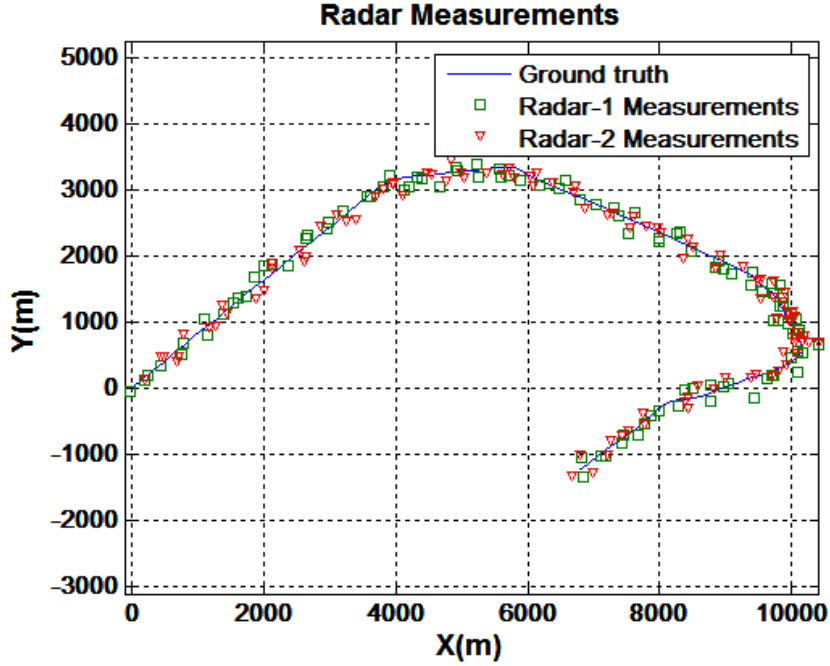


Figure 3.8: One of the generated targets and related radar measurements.

3.4.1.3 Fusion Experiments

In track fusion problems, the most important parameters seem to be the measurement noise variances, i.e., r_1 and r_2 , and process noise variances, i.e., q_1 and q_2 , since these certainly effect the level of correlation between the local and remote radars and the level of the rumor propagation in the radar trackers. Based on this fact, the experiments are performed for a variety of the variance parameters to understand the performance boundaries of the strategies and the fusion methods. Proposed experiments are given in Table 3.1 and the summary for the fusion techniques that will be analyzed is provided in Table 3.2.

Note that remote radar's fusion performance is not analyzed since we did not see significant difference between the results of the remote radar and that of the local one for the experiments and the strategies.

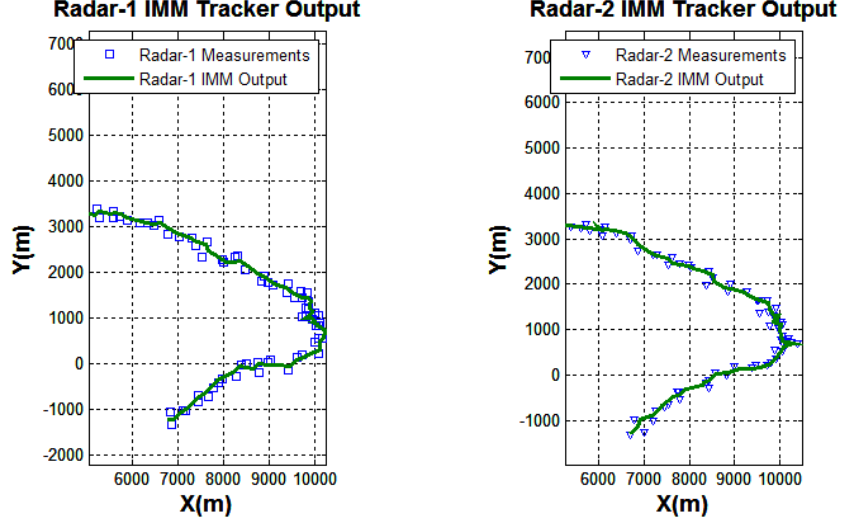


Figure 3.9: Radar measurements and IMM tracker outputs on the zoomed version of Figure 3.8.

Table 3.1: Experiments designed to understand performance boundaries of the strategies.

Experiment No	Aim	Parameter selection
1	To understand the effect of measurement noises in the fusion.	$\sigma_{p1} = 1$, $\sigma_{p2} = 35$ and $\sigma_r = \sigma_{r1} = \sigma_{r2} = \{10, 25, 50, 75, 100, 150, 200, 300, 400\}$
2	To understand the effect of process noises in the fusion.	$\sigma_r = \sigma_{r1} = \sigma_{r2} = 100$ and $(\sigma_{p1}, \sigma_{p2}) = \alpha x(1, 35)$ where α is a constant and selected from the set $\{1, 1.5, 2, 2.5, 3, 4, 8\}$

Ensemble averaged fusion results belonging to the parameters $\sigma_{p1} = 1$, $\sigma_{p2} = 35$ and $\sigma_r = 50$ are displayed in Figures 3.13 and 3.14. Notice that Naive fusion yielded divergent state estimates, and it does not seem to be a consistent fusion approach for the problem as expected. Divergence of the Naive fusion is caused by the fact that fusion results is fed back to the filtering algorithm and the correlated information accumulates in the estimates. When the other techniques are analyzed in detail, SPCF seems to yield the first two best results in the sense that the closest averaged norm to that of centralized fusion belongs to SPCF in

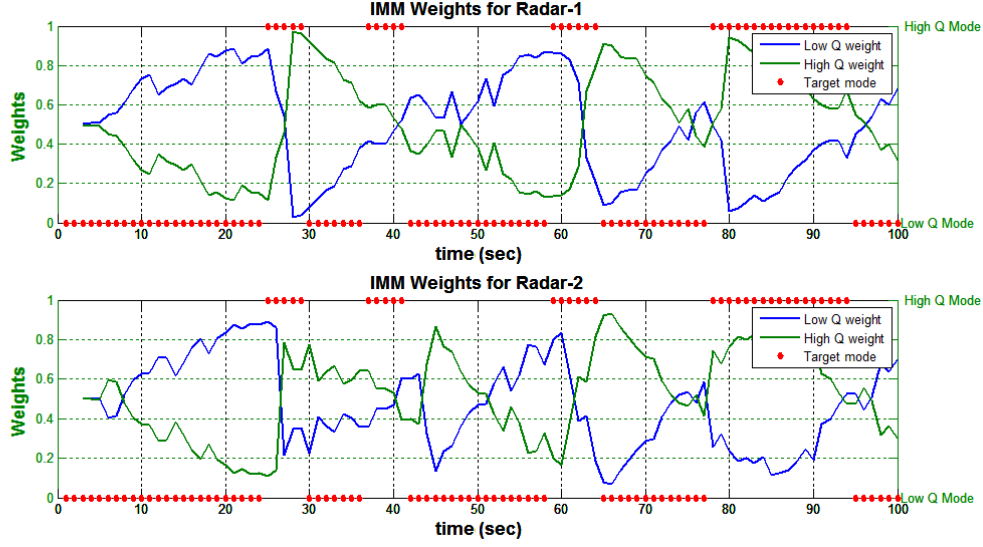


Figure 3.10: IMM weights for different models (belonging to the IMM example in Figure 3.9).

Table 3.2: Summary of the fusion techniques to be analyzed.

Fusion Technique	Strategy	Architecture	Implementation
Naive	Strategy-1, see Section 3.3.1 for details.	see Figure 3.2	see Section 3.3.1.1 for details.
SPCF	Strategy-1, see Section 3.3.1 for details.	see Figure 3.2	see Section 3.3.1.2 for details.
SPCF	Strategy-2, see Section 3.3.2 for details.	see Figure 3.3	see Section 3.3.2 for details.
CI	Strategy-3, see Section 3.3.3 for details.	see Figure 3.4	see Section 3.3.3 for details.
CI	Strategy-4, see Section 3.3.4 for details.	see Figure 3.5	see Section 3.3.4 for details.

Strategy-1 and 2.

This experiment belonging to a single parameter set does not prove that SPCF

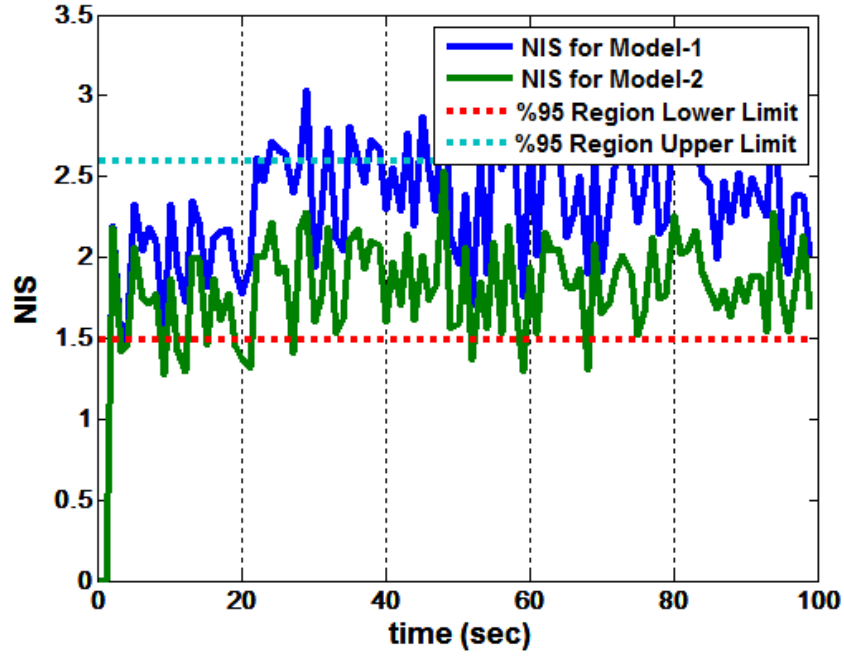


Figure 3.11: Ensemble average of NIS values and required boundaries.

is always better than the other fusion techniques. To understand the effectiveness and weaknesses of the proposed method, same experiment is performed for different parameter selections as stated in Table 3.1. Mean errors for the ensembles are found with respect to time for the defined experiments in the table.

Experiment-1 (Experiments to Analyze the Effect of Measurement Noise):

Experiment-1 is proposed to analyze the effect of measurement noises in the fusion results under model-match condition while keeping the other parameters fixed. Mean L2 error is obtained for each parameter and the plots related to the performance of the techniques against different measurement noises are computed and are given in Figure 3.15.

As it is seen in Figure 3.15, Naive fusion is the worst strategy amongst all. It can hardly reach an acceptable performance for very low measurement noise levels yet it has a divergent characteristics as the measurement noise increases.

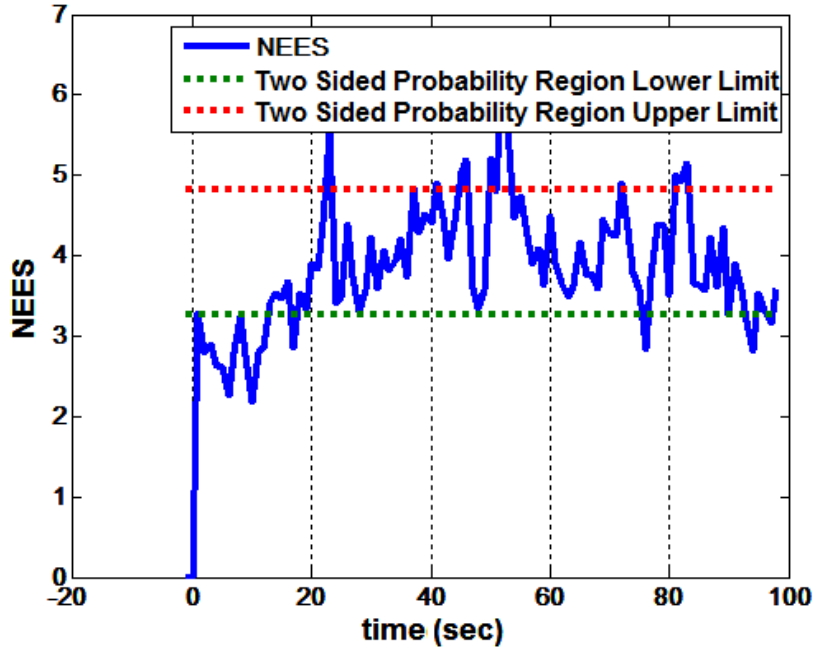


Figure 3.12: Ensemble average of NEES values and required boundaries.

Increase in the error with increasing measurement noise implies that the correlation level of the information in the fusion system cannot be removed as expected.

When the figure is zoomed to analyze the performances of the other approaches, as shown in Figure 3.16, SPCF technique in Strategy-1 and 2 seems to be more robust and effective than the other methods under the increase in the measurement noise. Note that as the measurement noise increases, the system relies on the process more, so the information that comes from the two radar systems become more correlated. This fact shows us that in case of high correlation between the tracker outputs of the local radar and the remote one, SPCF performs better which indicates that it is a conservative fusion method. On the other hand, SPCF technique in Strategy-1 seems to be slightly worse than SPCF in Strategy-2. This is because of the effect of the feedback mechanism in the structure, which contributes to the correlation level of the information loop and this results in a highly correlated data within the system.

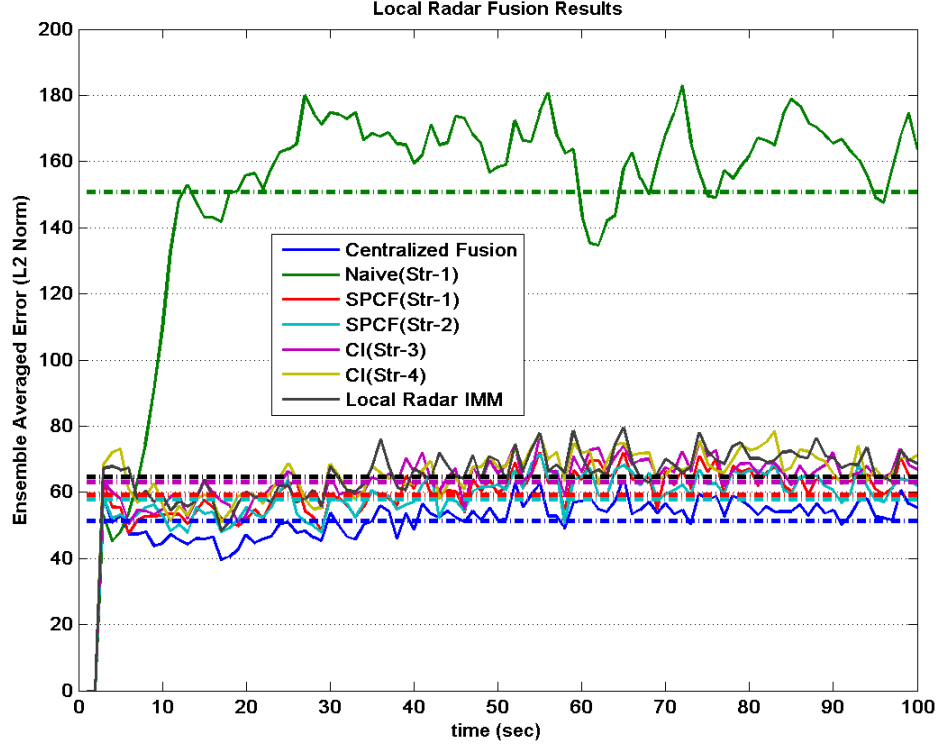


Figure 3.13: Ensemble average of the fusion results for the parameters $\sigma_{p1} = 1$, $\sigma_{p2} = 35$ and $\sigma_r = 50$. Dashed lines represent the mean lines for each result.

This fact shows us that in case of high correlation between the tracker outputs of the local radar and the remote one, SPCF in can eliminate this correlation in the way better than the other approaches can.

Figure 3.17 which is a zoomed version of 3.15 for the low measurement noise levels, (i.e., low correlation level). Figure shows that SPCF in both strategies is good in the whole range of measurement noise standard deviations. That is an indication of adaptability of SPCF to different noise values.

We have already mentioned that as observation noise of the two systems increase, then states become more correlated. This fact can be explained by the Kalman filter structure used in the IMM filter. It is well known that as measurement noise gets smaller, Kalman gain increases and the measurement contributes to the output estimates more compared to that provided by the process. Since the measurements are uncorrelated, the output densities tend to be uncorrelated, as

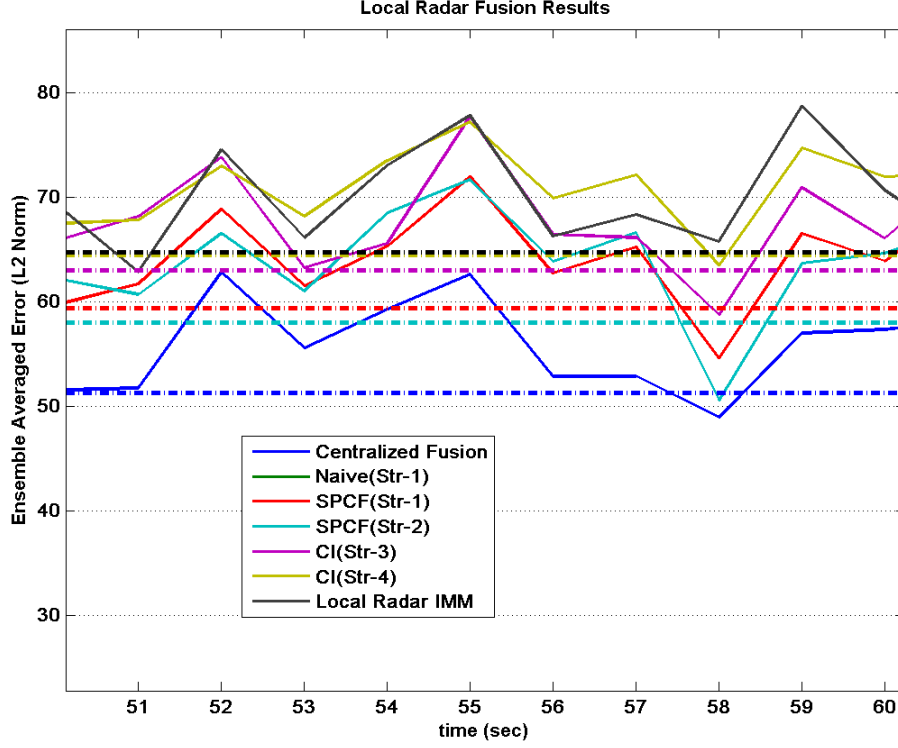


Figure 3.14: Zoomed version of Figure 3.13.

well. In the other way, when the measurement noise increases, the contribution of the measurements to the output gets smaller, and the process model which actually causes the correlation in the data becomes dominant and the input densities become more correlated.

Experiment-2 (Experiments to Analyze the Effect of Process Noise):

The basic idea of the next experiment is similar to that of Experiment-1 and the effect of process noises in the fusion results under model-match condition is investigated while keeping the other parameters fixed. Mean L2 norm is obtained for each parameter selection. The plots related to the performance of the techniques against different process noise standard deviations are shown in Figure 3.18. The parameter α is a scaling factor for both process noise standard deviations of Model-1 and Model-2, i.e., q_1 and q_2 , and increase in this parameter implies increase in both deviations in the same rate.

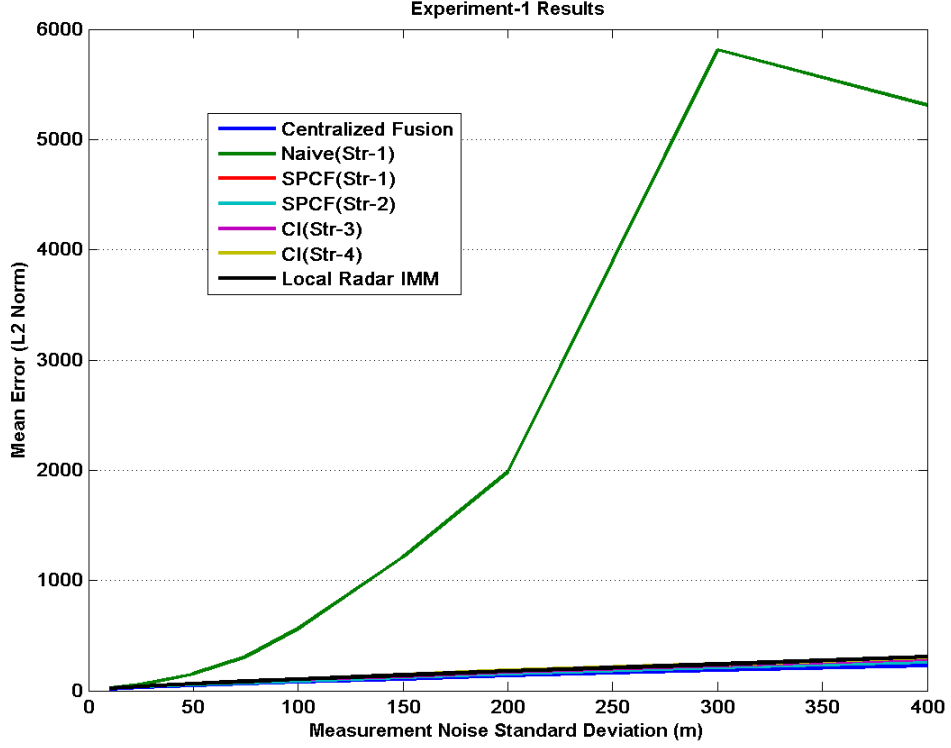


Figure 3.15: Mean of L2 Norm error of the ensemble averages vs different measurement noise standard deviations for $\sigma_{p1} = 1$ and $\sigma_{p2} = 35$.

Figure 3.18 shows that selection of low process noises degrades the performance of the Naive fusion, as expected. On the other hand, its performance gets better as the process noise levels increase. This is an expected result since for high process noises, measurement noise becomes more dominant which decreases the correlation between the estimated states of the two sources. Notice that after the alpha parameter exceeds 3, it even produces better results than the centralized approach. This demonstrates that centralized fusion technique cannot produce small enough covariance so its performance gets worse than the Naive technique for process noises greater than $(q_1, q_2) > (3, 105)$.

The performances of other fusion techniques are shown in Figure 3.19. This fact shows that SPCF technique in Strategy-1 and 2 is more robust and effective than the other methods.

The results of the two sets of experiments are consistent and they reveal that

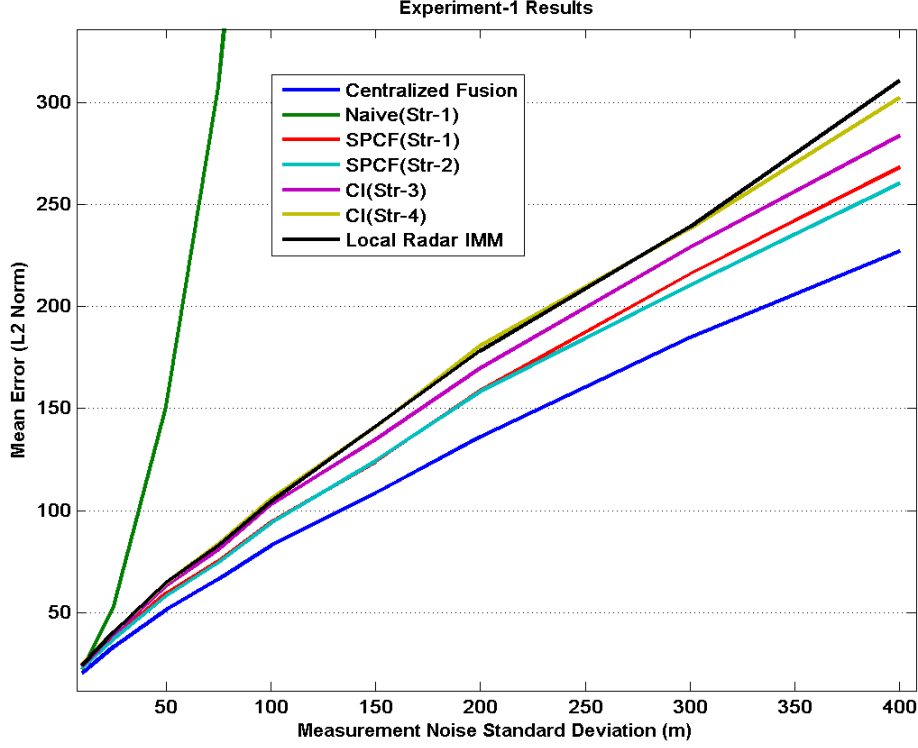


Figure 3.16: Zoomed version of Figure 3.15 to exclude Naive fusion.

SPCF performs better compared to the other decentralized fusion techniques for the overall spectrum of the process noise selections, which indicates its adaptability.

3.4.2 Realistic System Scenarios

Previous scenarios are based on simulation of perfect match of IMM filter parameters with those of target models and radar measurement models, and they are proposed in the way that the models are independent of the deployment. These experiments are done to investigate the performance boundaries of the fusion strategies under ideal conditions while keeping the deployment effect outside of the results. On the other hand, inspection of the performance of the fusion approaches for more realistic targets and radar cases is another point that has to be clarified. For this aim, some benchmark target scenarios existing in the

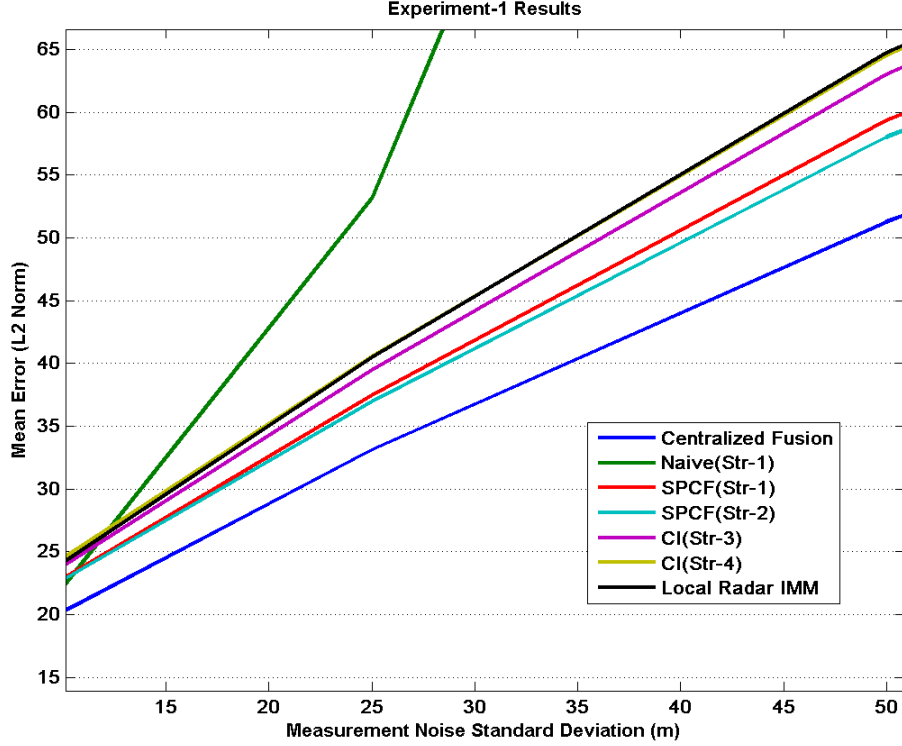


Figure 3.17: Zoomed version of Figure 3.15 focusing in the measurement noise standard deviation margin [10-50].

literature are selected and realistic radar simulation algorithms generating the azimuth and range measurements are used.

3.4.2.1 Selection of Targets

A remarkable target library belonging to several type of air targets exists in [7]. This library includes a variety of air targets which are preferred by some authors for their own work [42]. For this thesis, we choose two extreme scenarios which represent low and high maneuverable targets. These targets correspond to Target-2 and Target-6 in [7].

- **Target-2 (Low maneuverable target):** The trajectory of this target is shown in Figure 3.20 and represents a trajectory which would be expected from a small, maneuverable aircraft, such as a Learjet or other similar high

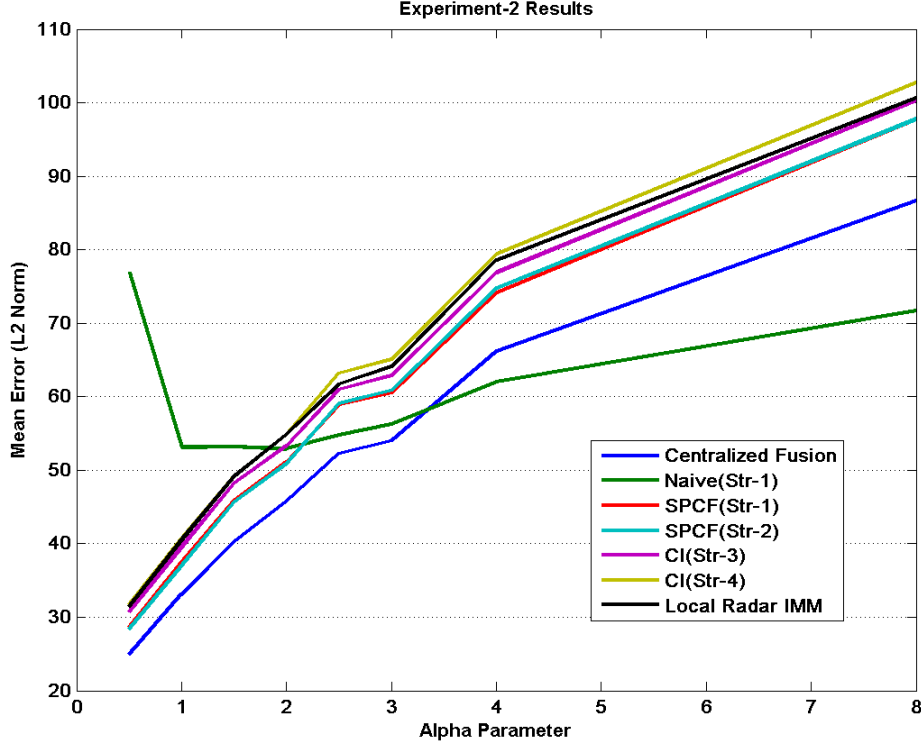


Figure 3.18: Mean of L2 Norm error of the ensemble averages vs. alpha parameter ($\sigma_{p1} = 1 \times \text{alpha}$, $\sigma_{p2} = 35 \times \text{alpha}$ and $\sigma_r = 25$).

performance commercial aircraft. It initializes at a speed of 305m/s and altitude of 4.57km. The target performs a 2.5g turn through 90° of course change. After the turn, the target descends gradually to an altitude of approximately 3.05km. A 4g turn rolling out to straight and level flight is performed at a constant speed of 305m/s and then the trajectory ends. The RCS of the target is 2m².

- **Target-6 (Highly maneuverable target):** This target starts at a speed of 426m/s and an altitude of 1.55km. Constant speed and course are maintained for a period of 30s upon which a 7 turn is performed. The new course is maintained for another 30s. A 6g turn is performed while the throttle is reduced and the aircraft is nosed over in order to decrease the altitude. After that a final altitude of 0.79km is obtained and a time span of 30s, another 6g turn is made and full throttle is commanded.

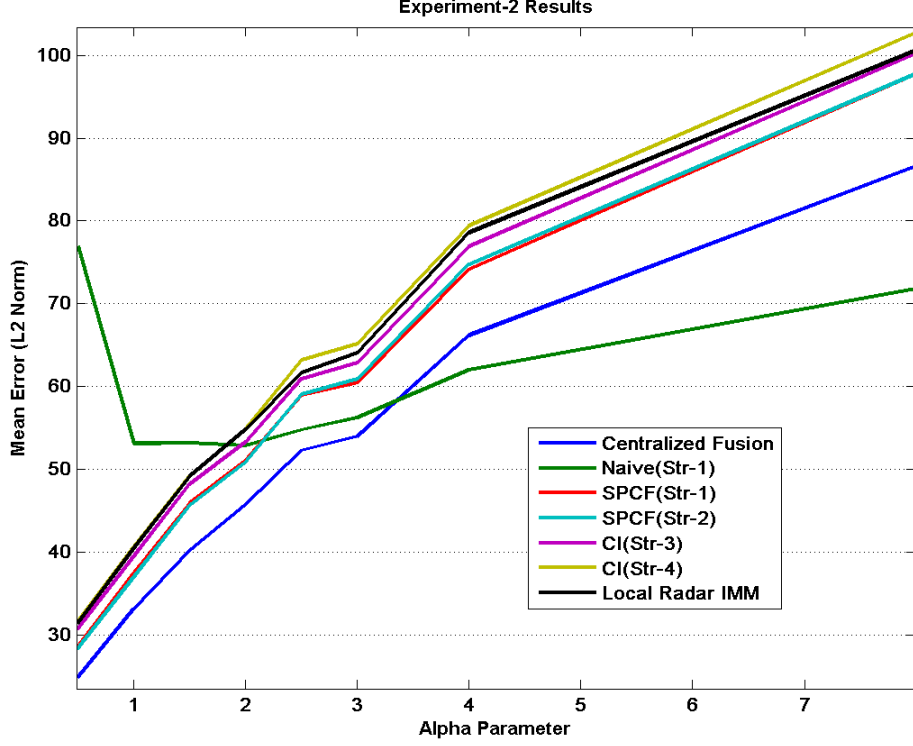


Figure 3.19: Zoomed version of Figure 3.18 to exclude Naive fusion.

After approximately 30s, a 7g turn is performed, and upon completion of the turn, straight and level, non-accelerating flight is maintained for the completion of the trajectory. The average RCS is 1.9m².

3.4.2.2 Radar Model

One of the main aims of this experiment is providing realistic radar measurements to the fusion system. In this study, we used a simplified radar simulator to generate measurements for a given trajectory (See [19] for the details.). The simple simulator first generates an SNR for given target and radar position, and using SNR value it calculates the probability of detection, $P_{\text{detection}}$ as follows:

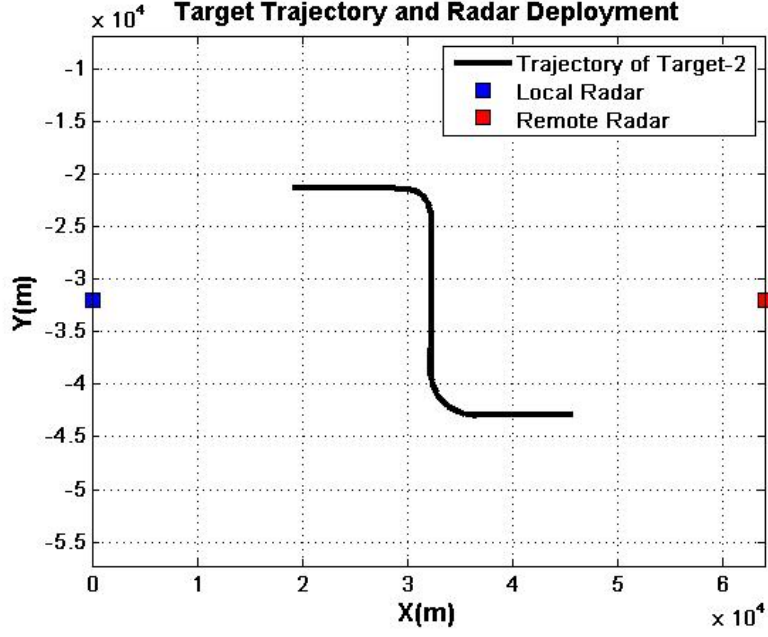


Figure 3.20: Trajectory of Target-2 and deployment of radars.

$$SNR = \frac{(SNR_{\text{ref}} \cdot d_{\text{ref}}^4)}{d^4} \quad (3.96)$$

$$P_{\text{detection}} = p_{\text{fa}}^{\frac{1}{1+SNR}} \quad (3.97)$$

In the above expression SNR_{ref} is the reference SNR , d_{ref} is the maximum range of the radar for SNR_{ref} , d is the distance between the radar and the target and p_{fa} is the corresponding false alarm.

Radar measurements are the range and the bearing angles. Measurement noise is another parameter of the radar model. In this study, range noise is assumed to be uniformly distributed along the range ambiguity. Bearing angle noises are modeled as Gaussian noises independent of each other.

Bias is another important cause of degradation in the radar measurements. Bias is generated by mislocating the radar and its north axis. However, in this study effects of the bias on fusion are not analyzed, so no bias is assumed. Table 3.3 gives the parameters used in this study to generate the radar measurements.

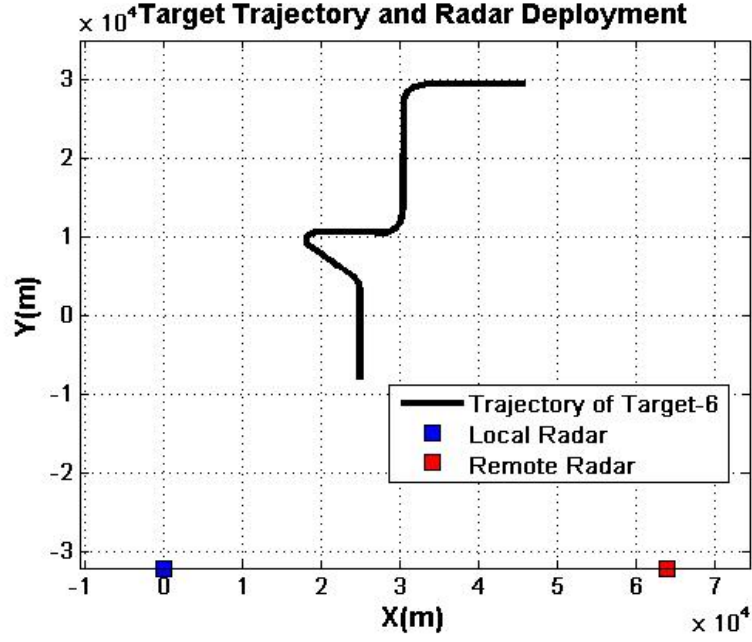


Figure 3.21: Trajectory of Target-6 and deployment of radars.

Table 3.3: Radar parameters selected for the experiments.

Radar Parameter	Value
Azimuth measurement error(rms)	0.3 deg.
Azimuth bias	0 deg.
Range measurement error(rms)	10 m.
Range bias	0 m.
Probability of detection	given in (3.97)
p_{fa}	10^{-14}
SNR_{ref}	10
d_{ref}	100 km.
Sampling period	1 sec.

The problem here is that track set obtained from the simulator may also contain false tracks due to the clutter and the relevant track/measurements must be picked up at the output of the radar simulator. To overcome this difficulty, adaptation process defined in Figure 3.22 is used to generate target related measurements which is required for the follow-on fusion mechanisms.

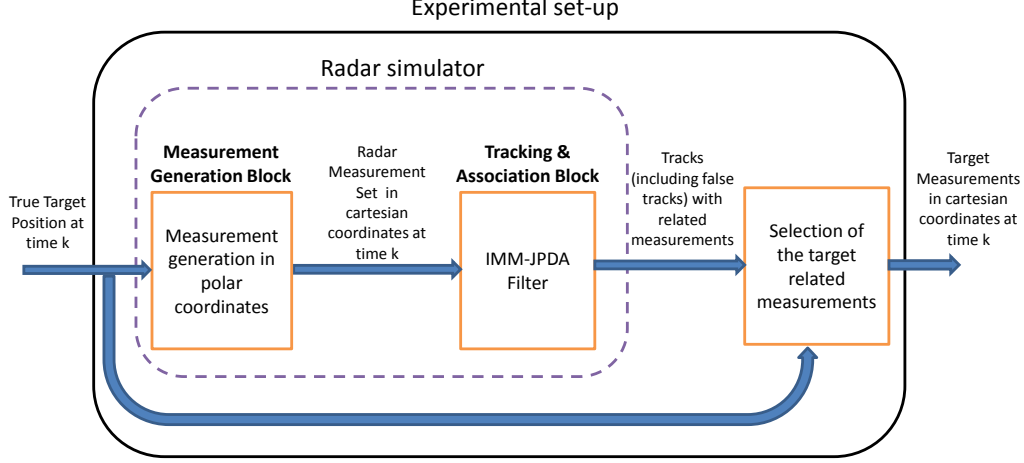


Figure 3.22: Experimental set-up adapted to radar simulator to pick-up the target related measurements.

3.4.2.3 Filter Parameters

Target motion model is selected as the same with that of the previous experiment given in (3.93). Standard deviation of low and high process noise models are selected as $q_1 = 1$ and $q_2 = 30$, respectively.

Measurement model of the filter is selected as in

$$y(x_k) = Hx_k + v(\tilde{x}_k) \quad (3.98)$$

where \tilde{x}_k is relative estimated position of the target with respect to the radar, $H = [1 \ 0 \ 0 \ 0; 0 \ 1 \ 0 \ 0]$ and $v(\tilde{x}_k) \sim \mathcal{N}(\tilde{v}, 0, R(\tilde{x}_k))$. Note that since the measurement noises are defined in azimuth and range and the filter runs in cartesian coordinate system, unbiased coordinate conversion operation is required to obtain the measurement noise covariance matrix, $R(\tilde{x}_k)$. Details of this operation are provided in [33].

3.4.2.4 Fusion Experiments

Evaluation of the performance of the fusion techniques are based on the predefined target scenarios, i.e., Target-2 and Target-6 scenarios. The experiments are based on the same fusion strategies with ideal case experiments and SPCF is compared with the other techniques: centralized fusion, Naive, CI and Local radar's IMM filter. Ensemble average of the L2 state error norms with respect to time is computed over and plotted for 50 Monte Carlo runs. In all of the figures, target acceleration values in g unit are provided to build up the relationship between the performances and the maneuvering state of the target.

Deployment of the radars and relative target positions are important factors on the performance of the fusion systems. The results may be varied depending on the radar system of interest. So, the results are displayed for both local and remote radar fusion systems to assess the robustness of the fusion system against target's relative position to the fusion site.

Experiments on low maneuverable target

Experimental results for Target-2 and Target-6 scenarios are given in Figures 3.23 and 3.24. When we look at the performance of the Target-2 scenario given in the related figures, the effect of fusion process in the performance seems quite remarkable. Both SPCF and CI provided almost 50 percent increase in the performance when compared with the individual radar trackers. Both methods provide slightly better results than those of the optimal one. The reason why centralized fusion is worse than the other two techniques relies on the model mismatch errors between the target model and the filter parameters.

In this scenario, target does not make significant maneuvers and, SPCF in Strategy-1 seems to be the best and there is not much difference between SPCF in Strategy-2 and CI in Strategy-3 and 4 for this case.

Experiments on High Maneuverable Target

The Target-6 experiments are analyzed in Figures 3.25 and 3.27. Zoomed versions of these figures are also provided as Figures 3.26 and 3.28, respectively. These last two figures focus on the fusion techniques by excluding the results of

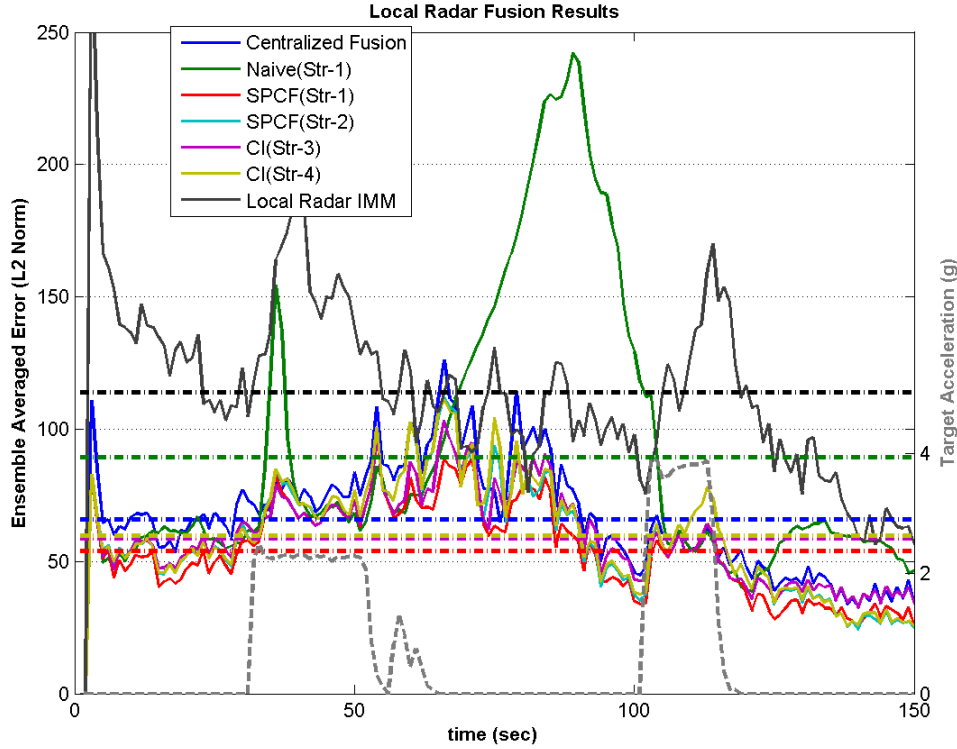


Figure 3.23: Fusion performances of the techniques at the “local radar” for target-2. Dashed gray line corresponds to the maneuver of the target and other dashed lines represent the mean lines for each result.

the local IMM.

Fusion process again significantly increases the over-all performance when compared with the radar IMM trackers. It can also be observed that acceleration of the target receive almost 7g which seems to affect all the performances.

SPCF in Strategy-1 again produces the best results in average and CI in Strategy-3 follows it. Note that these strategies have feedback mechanisms and this shows that the feedback enhances the performances for high maneuverable targets.

As stated before, the target acceleration corresponds to the process noise which is the main actor in the correlation of the data to be fused. The presence of the correlation can be seen by evaluating the results of Naive, SPCF and CI techniques during the maneuvering time intervals. During these intervals, Naive

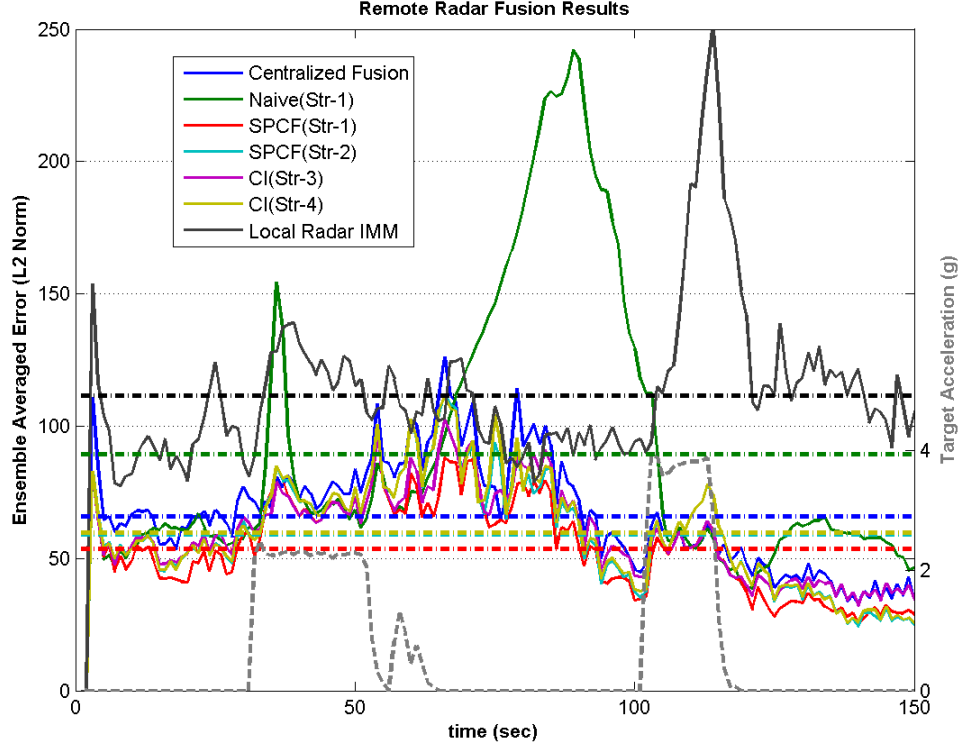


Figure 3.24: Fusion performances of the techniques at the “remote radar” for target-2. Dashed gray line corresponds to the maneuver of the target and other dashed lines represent the mean lines for each result.

generally produces less errors than the other methods by elimination of the unwanted correlation more effectively. This is an expected observation since high process noise model in IMM gets more dominant during these time frames and this results in increase in the effect of the measurements to the final state estimates. This causes the output estimates less correlated. In lower correlation cases, i.e., target’s low maneuvering state, SPCF and CI yield better performances since the low process model becomes dominant and output densities become more correlated.

Experiments on Hybrid Fusion Structures

The relationship between the performances of the proposed strategies and the maneuvering state of the target raises the idea of proposing adaptive hybrid fusion structures which includes more than one fusion strategy. In such a pro-

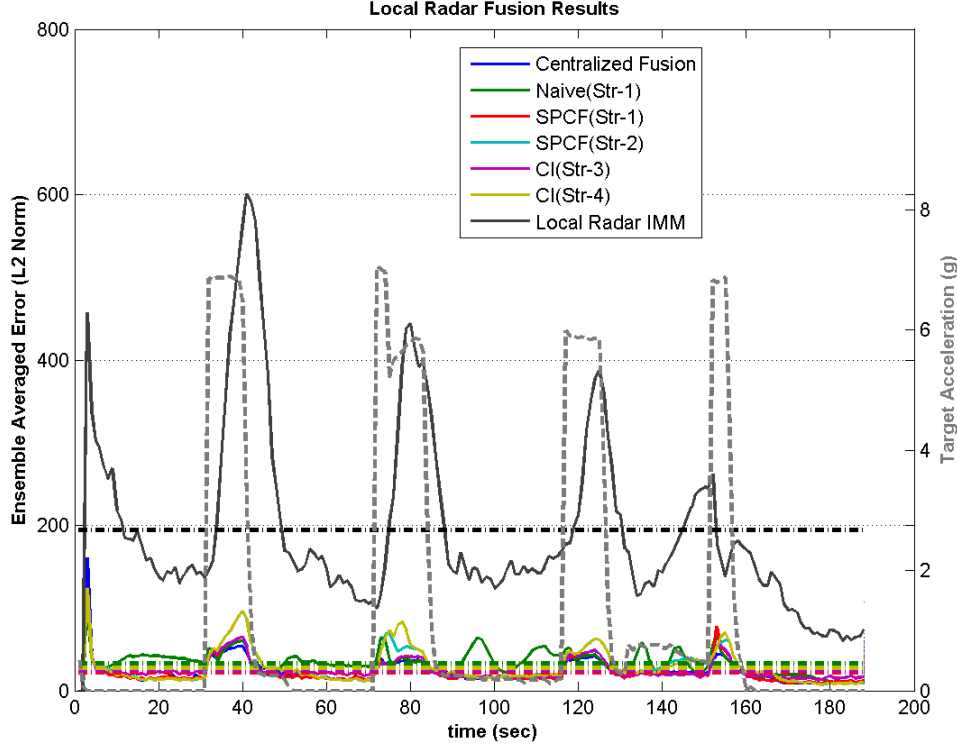


Figure 3.25: Fusion performances of the techniques at the “local radar” for Target-6. Dashed gray line corresponds to the maneuver of the target and other dashed lines represent the mean lines for each result.

positional, the system adaptively selects the fusion strategy depending on the mode probability of the target, which is actually a measure of a maneuver. Experiments on high maneuverable target demonstrates that Naive is a good choice if the target is maneuvering, and SPCF in Strategy-1 is in the opposite case. So, the strategy in Figure 3.29 is proposed as an adaptive fusion approach.

The resultant plots for the proposed hybrid strategy are given in Figure 3.30 where the threshold is selected as 0.85. According to the results, the hybrid structure, in the average, produces the best result which is slightly better than SPCF in Strategy-1. This experiment does not prove that this kind of fusion approach always provides improvements in the errors. Better parameter tuning is required to reach more reliable conclusions which is left as a future work.

Computational Perspectives

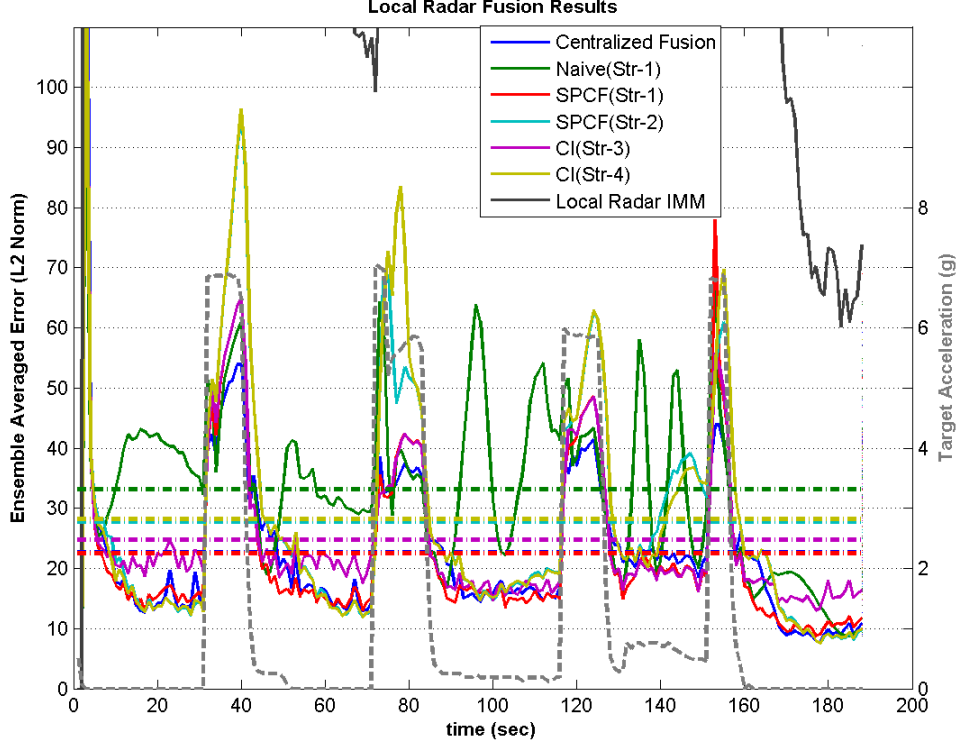


Figure 3.26: Zoomed version of Figure 3.25.

Average computation times obtained from Target-6 experiments for each fusion approach is provided in Table 3.4. The resultant times demonstrate that SPCF in Strategy-1 is computationally demanding when compared to other techniques, which is expected. SPCF solves three different optimization problems for each model in the IMM filter to find w^{th} and $(1-w)^{\text{th}}$ powers of the Gaussian mixtures and to find the optimum w in the Chernoff fusion operation. CI technique only solves for the optimum w so that it has quite low computation load in both Strategy-3 and 4. Note that no effort has been spent neither to simplify the algorithms nor to reduce the computation. We believe that the computational load can be reduced significantly with appropriate changes in the optimization algorithms. This part is left as future work.

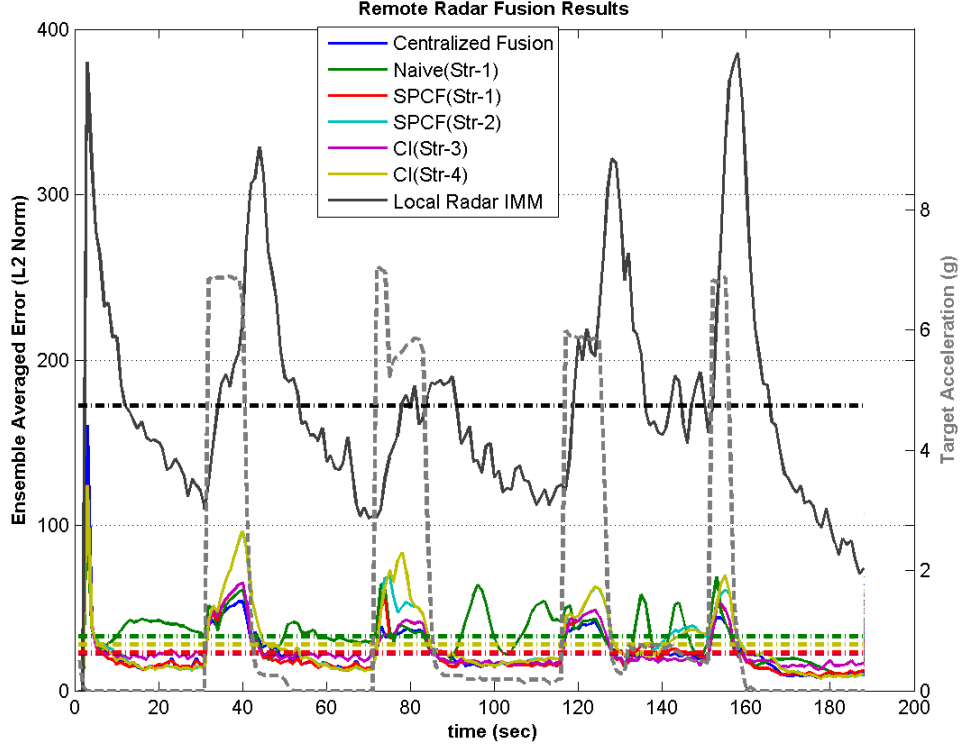


Figure 3.27: Fusion performances of the techniques at the “remote radar” for Target-6. Dashed gray line corresponds to the maneuver of the target and other dashed lines represent the mean lines for each result.

Table 3.4: Average computation times for each strategy.

Strategy	Computation Time
Centralized Fusion	0.0019 sec.
Naive (Strategy-1)	0.0034 sec.
SPCF (Strategy-1)	2.4318 sec.
SPCF (Strategy-2)	0.8460 sec.
CI (Strategy-3)	0.0360 sec.
CI (Strategy-4)	0.0080 sec.

3.5 Discussions

In this chapter, fusion strategies are analyzed for a two-radar fusion system based on IMM filters. Fusion systems send IMM output target density functions to

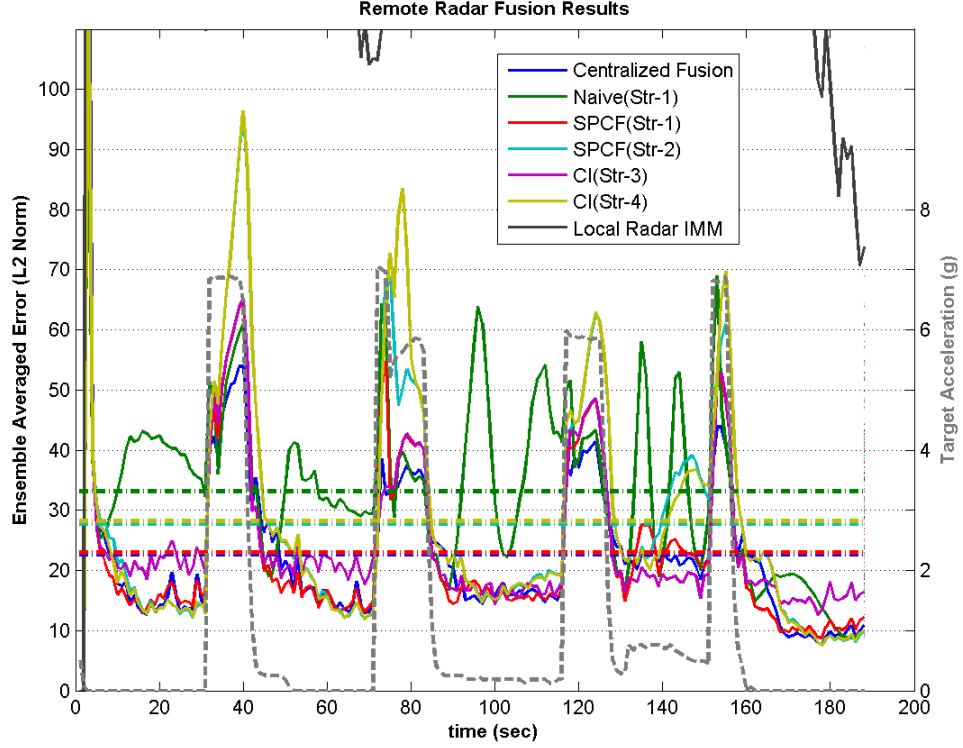


Figure 3.28: Zoomed version of Figure 3.27.

each other for fusion. The basic idea is to eliminate the correlation to obtain better state estimates. Four different strategies are proposed as solutions to this problem: Strategy-1, Strategy-2, Strategy-3 and Strategy-4. Strategy-1 relies on the fusion of remotely obtained Gaussian mixture density with a local Gaussian function by SPCF and Naive fusion techniques. Output of the fusion is provided back to the internal filter. Strategy-2 is proposed to fuse Gaussian mixture densities to find the state estimate. In this case, there exist no feedback to the IMM filter. Strategy-3 and 4 are simpler solutions in which Gaussian state estimates are exchanged for fusion with and without feedback mechanisms to the internal filter.

Assessment of the strategies are based on the computation of the error norms for ideal and more realistic target scenarios. Ideal scenarios are proposed to extract the performance boundaries for different parameter selections of process and measurement noise models. Average errors for each parameter selection

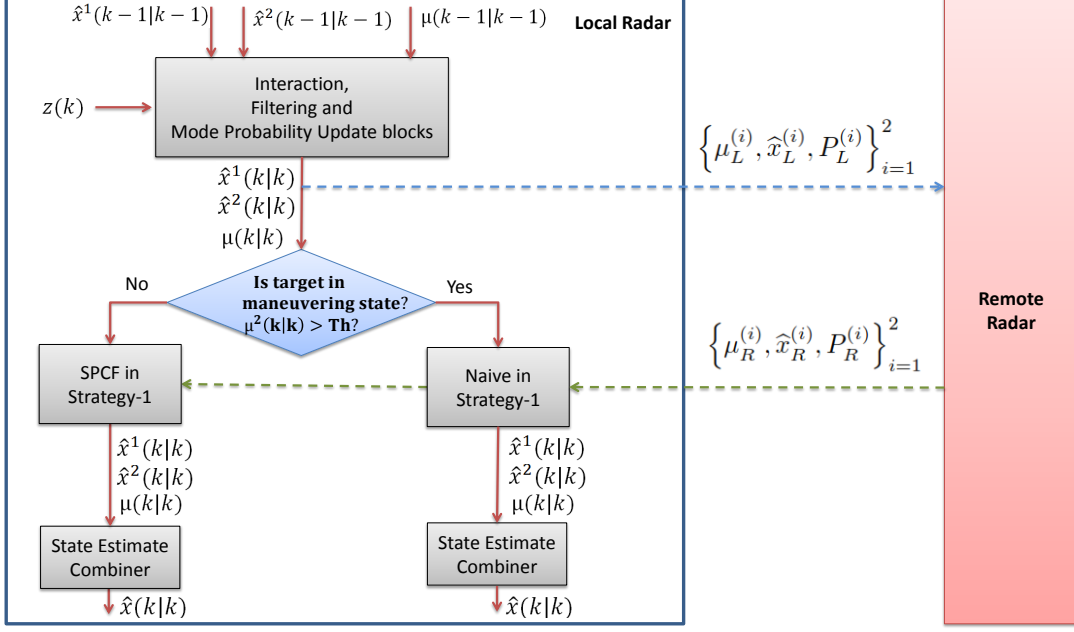


Figure 3.29: An adaptive hybrid fusion structure which includes SPCF and Naive techniques.

are found and explanations for the performance of the strategies are brought forward. According to the results, selection of measurement noise relative to the process noise seems to be important since this affects weight of the measurements in the state estimates. Results give clues about the selection of the fusion method for different tracking scenarios.

Experiments on realistic scenarios lead us to understand the applicability of the proposed technique for real environments including low and high maneuverable target trajectories and radar models generating azimuth and range measurements. The performance results build up the relationship between the target maneuvers and the correlation in the information to be fused. The results also reveal that elimination of the correlation by SPCF is satisfactory and SPCF can be a good choice for such kind of highly maneuverable targets. Similar results for both local and remote radar sites give us an indication of robustness of the proposed technique against different radar deployments and relative target positions. A hybrid solution including SPCF and Naive methods is also proposed depending on the target maneuvers and initial results are obtained. Deeper

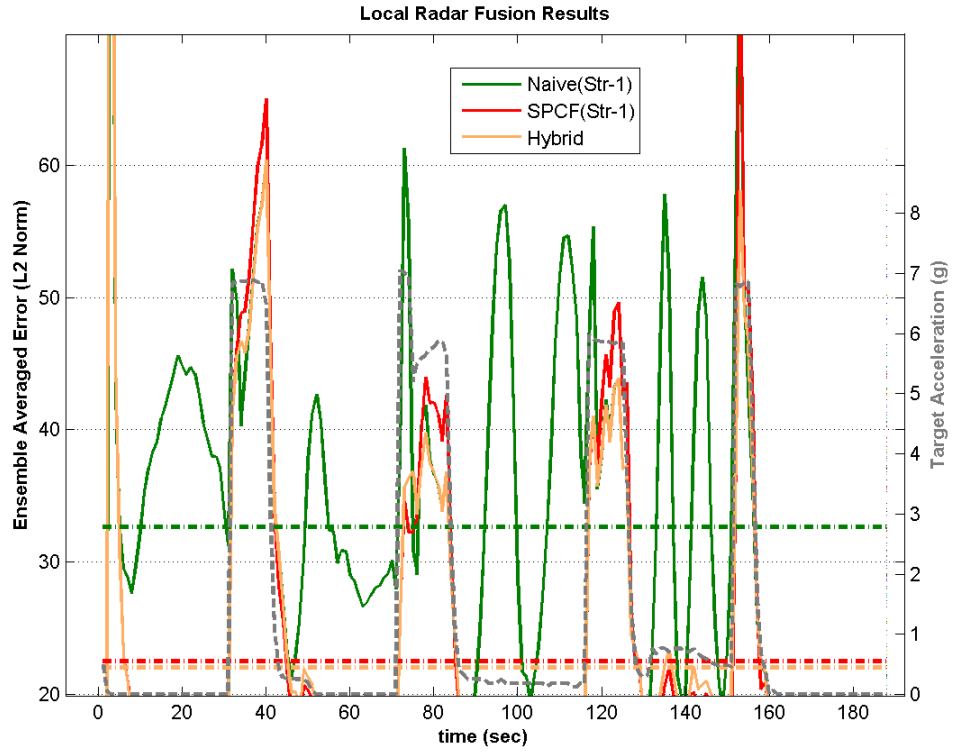


Figure 3.30: Target-6 results for the hybrid structure together with those of SPCF and Naive techniques. Dashed gray line corresponds to the maneuver of the target and other dashed lines represent the mean lines for each result.

analysis on hybrid fusion structures is a future work.

CHAPTER 4

FUSION OF PHD'S IN A DECENTRALIZED RADAR SYSTEM

4.1 Introduction

In recent years, the attention on Probability Hypothesis Density (PHD) filter, which is mainly based on tracking target intensity function, has significantly increased. The filter relies on the theory Finite Set Statistics (FISST) and its equations are derived according to the tools provided by FISST. Related equations, in fact, are not easy to realize so that some approaches have been brought forward which enables the implementation of this filter [48, 47]. Although there exist several applications of the PHD filter that use the proposed implementations, not many studies exist bringing multisensor PHD applications into life because of the difficulties in the implementation of the multisensor PHD fusion equations. Especially, in case of the correlation between the multiple PHD's is unknown, the problem turns out to be much more difficult to solve. Even though formulae for the equations related to the multisensor PHD fusion with unknown correlation is derived by utilizing the Chernoff fusion technique, which is one of the favorite methods used in the decentralized fusion systems, there does not exist any closed form problem formulation related to these derivations. SPCF technique is considered to be a good candidate to apply approximate Chernoff fusion for combining multiple PHD's in Gaussian Mixture PHD implementation. This study mainly focuses on the utilization of SPCF method for fusing GM-PHD filter outputs in a decentralized fusion system. Fusion equations of SPCF are obtained and performance of the technique is analyzed on some applicable

strategies.

The chapter starts with providing general information on PHD filter and then goes on with the literature survey related to multisensor PHD fusion methods. Later, some fusion strategies for multiple PHD filters and applicable decentralized fusion techniques based on SPCF method are discussed in Section 4.4.1. The performance assessment of the proposed fusion strategies and their comparison are given in Section 4.5. The chapter ends with the evaluation of the overall chapter and discusses the novelties regarding the proposed strategies.

4.2 The PHD Filter

As depicted in the introduction part, the main focus of this chapter is on PHD filtering and its possible multisensor fusion applications so that it is beneficial to provide basic and background information on PHD filtering. The idea of PHD filter is based on Finite Set Statistics (FISST) whose underlying key point is treating finite sets as random elements from probability theory point of view [34]. It provides the ability to unify the data obtained from various sources under a single Bayesian framework which gives us the opportunity to see all the detection, tracking and identification problems as a single problem.

Multitarget tracking challenges can be counted as random noises, missed and false detections (clutter), target dynamics (linear, nonlinear, maneuvering), imperfect and disparate observations, non-standard targets and scenarios (e.g. extended and unresolved targets), varying number of targets/sensors and data association problem. Conventional approaches for multitarget filtering problems follow the order of detection, association, tracking and finally identification. These approaches have some drawbacks because of their basic assumptions. Together with the measurements and the motion models, the means of solutions to the Bayes filtering and data association are approximations which are very likely to bring the system to a suboptimal point.

Extension of Bayes theorem to a Multi-target estimator is an even more challenging problem. Remembering the optimal Bayesian filtering, Bayes equation

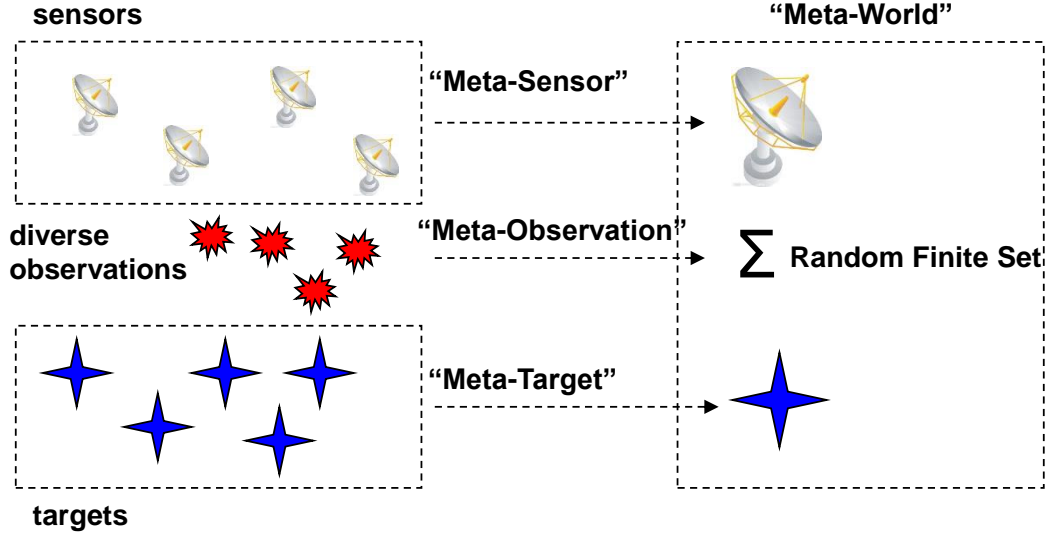


Figure 4.1: Transforming multitarget/sensor world into a meta world (adopted from the reference [2]).

contains integrals at the numerator and the denominator terms that can not generally be computed analytically even for single target case. Note that Kalman filtering is for a single target and it is optimal under the linearity and the Gaussianity assumptions and is considered as a closed form solution to the optimal Bayes filtering. For the multitarget case, the closed form analytic solution is almost impossible.

To overcome this challenge, FISST is considered as a remarkable tool that can be exploited to enable multitarget filtering [34]. It provides a natural yet rigorous mathematical tool enabling derivations and computations in multi-target estimation systems. The key idea of the utilization of FISST is to transform the multisource-multitarget problem into a mathematically equivalent single-sensor, single-target problem and to represent the multi-target state and observations as finite sets instead of the vectors (Figure 4.1).

Finite set representation has statistical attributes such as the set distance measure and other set operations like set derivative and integral (Table 4.1). This

representation has the power of indicating all possible occurrences of the multi-target scenario and there does not exist any inherent ordering of the measurements or targets. So, the nature of this representation allows explicit modeling of many challenging aspects of (multi) target estimation while solving the data association problem and formulating detection, tracking and identification as a unified problem.

Table 4.1: Some concepts in the single sensor/target domain and their correspondence in the multi one (adopted from the reference [39]).

Single-sensor/target domain	multi-sensor/target domain
sensor	meta-sensor
target	meta-target
vector observation, z	finite-set observation, Z
vector state, x	finite-set state, X
derivative	set-derivative
integral	set integral
probability-mass function	belief mass function
likelihood	multitarget likelihood
prior pdf	multitarget prior pdf
information theory	multitarget information theory
filtering theory	multitarget filtering theory

Although there exist several advantages of FISST for multitarget problems, there are some handicaps of the approach that needs to be dealt with. It is not a straightforward generalization of the single target case and the equations are mathematically complex. Furthermore the computational complexity of the approach is intractable and it brings no solution to the track continuity problem.

To overcome these disadvantages and to obtain an approximation to multitarget Bayesian filtering, Probability Hypothesis Density (PHD) filter has been proposed which propagates the first moment of the density function corresponding to the target intensity [38]. The PHD is characterized by the property that the integral of this intensity in a region equals to the expected number of targets in that hyper-volume. Integrating the intensity over the whole state space gives the expected number of targets present at any time. Besides, form of the intensity helps us to localize the targets whose number has already been found.

PHD filter provides solution to the multitarget Bayes rule which is given in (4.1). Solving this problem requires the Bayesian multitarget equations, the multisensor-multitarget measurement model in (4.2) and system dynamical model in (4.3).

$$p(X_k|Z^k) = \frac{p(Z_k|X_k)p(X_k|Z^{k-1})}{p(Z_k|Z^{k-1})} \quad (4.1)$$

where $X_k = \{x_1, \dots, x_n\}$, $Z_k = \{z_1, \dots, z_m\}$ and $Z^k = \{Z_i|i = 1, \dots, k\}$

$$Z = h(X) \cup \Delta Z \quad (4.2)$$

$h(X)$: set of target generated measurements

ΔZ : set of the measurements representing false alarms, clutter, etc.

$$X = g(X) \cup \Delta X \quad (4.3)$$

$g(X)$: set of states belonging to previously existing targets (including target disappearance)

ΔX : set of states belonging to newly appearing targets (target birth)

The models in (4.2) and (4.3) enable us to handle the following situations:

Measurement Model:

- Missed detection
- State dependent missed detection
- False alarms
- Extended targets (more than one measurement from a single target)
- Unresolved targets (targets moving so closely that they can not be distinguished)

System Dynamical Model:

- State dependent false alarms
- Target disappearance
- Target appearance
- Target spawning from an existing target (a target firing a missile)
- Coordinated Motion of a group of targets

When the literature is surveyed for recent developments on PHD filter, there exists several studies on various aspects of this filter like augmentation of PHD implementations ([49]), some novel techniques for solving PHD problems (track maintenance [51], extended targets [31] etc.), handling of sensor registration errors within PHD filters [29] and, of course, several PHD applications [50, 14, 21].

Further analytical derivations related to the PHD filtering is provided in Mahler's work [38] yet general structure of the filter and its main implementation types are given in the thesis for the completeness of the subject.

4.2.1 PHD Filter Stages

PHD filtering has two main stages: “prediction” and “measurement update”. Predicted target intensity at time $k + 1$ is found at the prediction step and the final intensity estimate is refined by the measurement update step (Figure 4.2).

Analytical expression of the predicted PHD at time $k + 1$ is found in terms of the PHD at time k as found in (4.4) which allows recursion.

$$\hat{D}_{\tilde{X}_{k+1}}(x) = D_{\tilde{B}_{k+1}}(x) + \int D_{\tilde{X}_k}(w)p_s(w)p_k(x|w)dw \quad (4.4)$$

where $D_{\tilde{B}_{k+1}}(x)$ is the target birth intensity at time $k + 1$, $D_{\tilde{X}_k}$ is the target intensity at time k , $p_s(w)$ is state dependent survival probability, and $p_k(x|w)$ is state transition density.

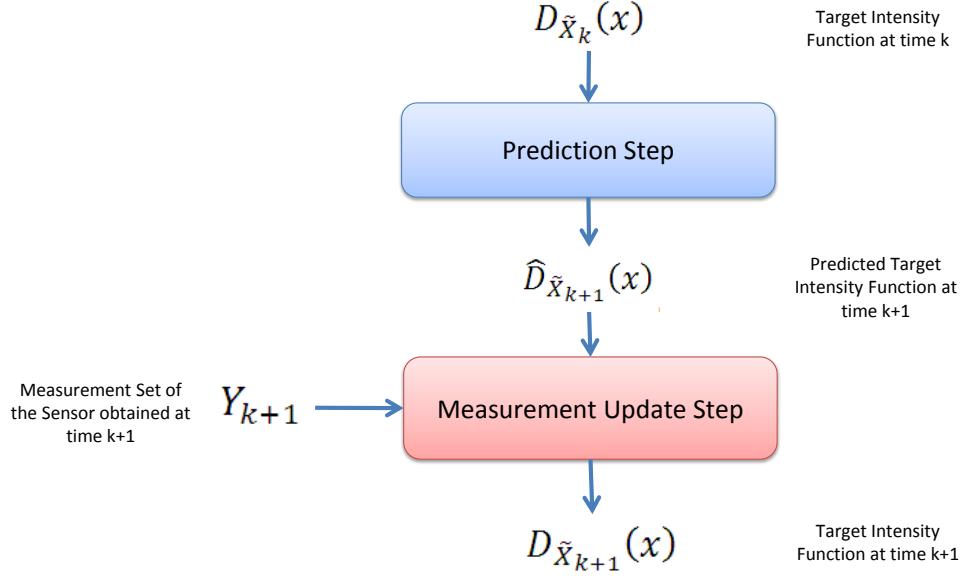


Figure 4.2: Basic steps in the PHD filtering process.

Measurement updated PHD obtained by using the measurement set and the predicted PHD is given in (4.5)

$$D_{\tilde{X}_{k+1}}(x) = \left(1 - p_D(x) + \sum_{y \in Y} \frac{p_D(x) p_{\tilde{y}|\tilde{x}}(y|x)}{D_{\tilde{C}}(y) + \hat{D}_{\tilde{X}_{k+1}}[p_D(x) p_{\tilde{y}|\tilde{x}}(y|x)]} \right) \hat{D}_{\tilde{X}_{k+1}}(x) \quad (4.5)$$

where $\hat{D}_{\tilde{X}_{k+1}}$ is the predicted intensity, $D_{\tilde{C}}(y)$ is the clutter intensity, $p_D(x)$ is the state dependent detection probability and $p_{\tilde{y}|\tilde{x}}(y|x)$ is the posterior density.

4.2.2 Basic PHD Implementations

4.2.2.1 Gaussian Mixture PHD Filter

Gaussian Mixture PHD (GMPHD), proposed by [47], is derived for linear Gaussian multi-target model and gives a closed form solution to the multitarget tracking problem. Detailed derivations, algorithms and pseudo-code of this method is provided in [47]. Here we give basic assumptions, prediction and measurement update stages of the method for the sake of completeness.

Assuming the target dynamical model and the sensor measurement model are linear Gaussian (given in (4.6) and (4.7), respectively) and assuming the target and birth intensities are in the form of Gaussian mixtures as in (4.8) and (4.9), predicted target intensity turns out to be a Gaussian mixture as in (4.10), as well. Measurement updated PHD also becomes a Gaussian Mixture which is given in (4.11).

For a single target set:

$$p_{k|k-1}(y|x) = \mathcal{N}(x; A_{k-1}w, Q_{k-1}) \quad (4.6)$$

$$p_{\tilde{y}|\tilde{x}}(y|x) = \mathcal{N}(y; C_k x, R_k) \quad (4.7)$$

$$D_{\tilde{B}_k}(x) = \sum_{i=1}^{J_{\tilde{B}_k}} w_{\tilde{B}_k}^{(i)} \mathcal{N}(x; m_{\tilde{B}_k}^{(i)}, P_{\tilde{B}_k}^{(i)}) \quad (4.8)$$

$$D_{\tilde{X}_k}(x) = \sum_{i=1}^{J_{\tilde{X}_k}} w_{\tilde{X}_k}^{(i)} \mathcal{N}(x; m_{\tilde{X}_k}^{(i)}, P_{\tilde{X}_k}^{(i)}) \quad (4.9)$$

$$\hat{D}_{\tilde{X}_{k+1}}(x) = \sum_{j=1}^{J_{\tilde{B}_{k+1}}} w_{\tilde{B}_{k+1}}^{(j)} \mathcal{N}(x; m_{\tilde{B}_{k+1}}^{(j)}, P_{\tilde{B}_{k+1}}^{(j)}) + p_s \sum_{i=1}^{J_{\tilde{X}_k}} w_{\tilde{X}_k}^{(i)} \mathcal{N}(x; \tilde{m}_{\tilde{X}_k}^{(i)}, \tilde{P}_{\tilde{X}_k}^{(i)}) \quad (4.10)$$

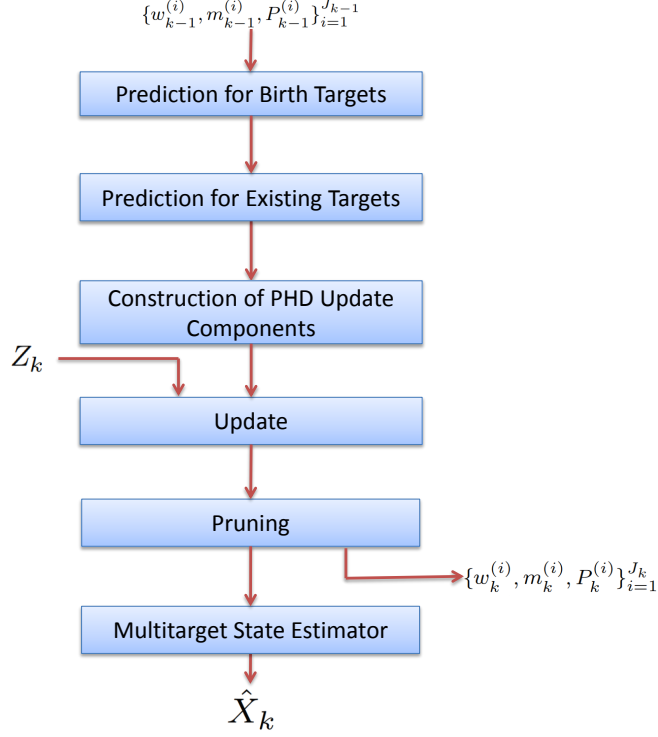


Figure 4.3: GMPHD Implementation.

$$\begin{aligned}
 D_{\tilde{X}_{k+1}}(x) = & (1 - p_D) \sum_{j=1}^{J_p} w_p^{(j)} \mathcal{N}(x; m_p^{(j)}, P_p^{(j)}) + \\
 & \sum_{j=1}^{J_p} \sum_{y \in Y} \frac{w_p^{(j)} q^{(j)}(y) p_D}{D_{\tilde{C}}(y) + p_D \sum_{i=1}^{J_p} w_p^{(i)} q^{(i)}(y)} \mathcal{N}(x; \tilde{m}^{(j)}, \tilde{P}^{(j)}) \quad (4.11)
 \end{aligned}$$

The complete flow of GMPHD filter algorithm is given in Figure 4.3. Note that other steps are added to classical PHD structure like pruning and state extraction. Pruning is required since the number of Gaussians after the update stage is proportional to the multiplication of the number of measurements and the number of Gaussians in the predicted target intensity. Pruning is required to reduce the total number of Gaussians and is done by thresholding the weights and/or clustering some Gaussians.

4.2.2.2 Particle PHD Filter

The main idea of the Particle PHD filters also known as Sequential Monte Carlo (SMC)-PHD filters, relies on the approximation of the integrals by random samples drawn from the density of interest. The PHD or intensity functions are represented by the weighted impulses at these random samples (or particles). The interesting thing about the resultant algorithm is that it is independent of the (time-varying) number of targets and computational complexity depends on the other parameters of the filter. This type of implementation is not the focus of this thesis. So, details regarding the particle PHD filter will not be provided. Readers who are interested may refer to [48].

4.3 Multisensor PHD Fusion

Recent evolution of PHD filters raised the problem of fusion of PHD's obtained from different information sources. The problem is defined as the fusion of unprocessed measurement sets obtained from the sensors and the fusion of target intensity functions obtained from sensor PHD filters. Based on the type of the fused information, multisensor PHD fusion is categorized into two: Centralized and Decentralized PHD fusion.

4.3.1 Centralized PHD Fusion

In centralized fusion systems, unprocessed sensor information is gathered at a central system node and fusion operation is performed there. Although this approach is optimal, it demands much from the communication infrastructure of the system so that it is not generally preferred for the fusion applications. Unfortunately, there does not exist exact formulation for this problem. [38] states that PHD and CPHD algorithms are single sensor filters and multisensor generalization of multitarget filtering is computationally intractable. Later, [34] proposes another approximation called as **“iterated – corrector approximation technique”**. This method is based on the idea of performing the mea-

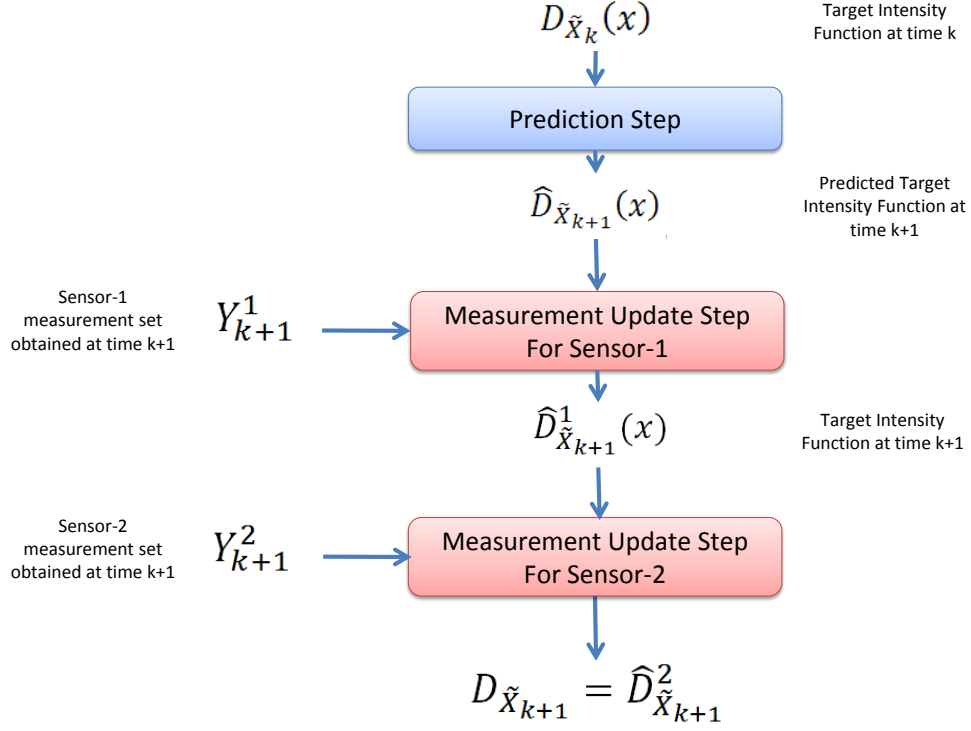


Figure 4.4: Iterated-corrector approximation technique for two sensor case.

surement update stage of PHD filtering for each sensor sequentially. In other words, output of measurement update of a sensor is used as the input of the measurement update stage of the next sensor (Figure 4.4). This technique has the drawback that changing the order of the sensors produces different updated PHDs. However, the simulations indicate that this does not result in noticeable differences in the performance [36].

The study [37] proposes an approximate fusion approach for PHD and CPHD (Cardinalized PHD) filters, which is sensor order invariant. This approach includes simplifying assumptions and is computationally tractable (for CPHD only). The author of the paper called these approximations product multisensor PHD (PM-PHD) and product multisensor CPHD (PM-CPHD), yet there does not exist any simulation results for them. Then, [41] extends the idea of [37] by solving the scale unbalance problem and revealing some multisensor simulation results which are based on the OSPA (Optimum SubPattern Assignment) metric [43]. Besides these generalization trials, [35] reduces the multisensor problem to

the specific two-sensor case and proposes a method to fuse the data.

A different approach has been suggested in [18], which is based on performing partitioning on the sensor measurements depending on the sensors' field of views (FOVs) to decrease the computational cost of the multisensor PHD filter.

4.3.2 Decentralized PHD Fusion

A decentralized PHD fusion system is based on the fusion of target intensity functions and the intensities are fused at the system fusion nodes. One of the main problems of a decentralized fusion system is the elimination of the common information in the data to be fused. Only [45, 46] propose a multisensor PHD tracker based on a Poisson Intensity approach and a general solution for the multisensor fusion problem is given based on the fusion of individual PHD intensities belonging to different sensors. This work does not consider the correlated information and claims that the fused intensity turns out to be the average intensities of the radar filters in the region of interest. As far as we understand, there is no indication of whether this approach is optimal or not. However, [36] states that this approach does not rely on a mathematical back-bone and, does not show acceptable performance on some predefined scenarios.

To the best of our knowledge, there do not seem to exist satisfactory studies that analyzes practical means of decentralized fusion of target intensity functions which are correlated. Next section will discuss this point in detail.

4.4 Fusion of Multiple PHD Filters with Unknown Correlation

As stated in Chapter 1, one of the most important problems in a decentralized sensor network is consistent and robust fusion. An analysis of decentralized fusion of densities is already performed in Chapter 3 and various aspects of it are analyzed in detail. The other recent problem is decentralized fusion of target intensities in case the sensor systems run PHD filters as the tracking subsystem. Unfortunately, to our knowledge, there does not exist any satisfactory practical

solution to overcome this problem yet. [16] derived the required fusion equations for Poisson multi-object intensities based on the Chernoff fusion technique yet there is not any further improvement on that work that proves the effectiveness of the approach.

This section discusses the application of SPCF method for fusing multi-object intensities and compares it with Naive fusion and iterated – corrector approximation fusion technique for the measurement fusion [34]. Note that there is not any applicable optimal solution to this problem and iterated – corrector approximation technique performance will be taken as a baseline for the analysis.

4.4.1 PHD Fusion Strategies

GMPHD filter implementation is chosen as the radar tracker in this work since generated intensity in the filter is a Gaussian mixture. Fusion strategies inserted into a traditional GMPHD filter might require some modifications and calculations in the flow of the standard filter. The problem here is to fuse the local information obtained from the measurement update block with that obtained from the remote radar system. Note that local and remote intensities are Gaussian Mixtures which may lead to different architectures in which SPCF and Pseudo Chernoff-2 ([26]) fusion methods can be applied. In this section, the proposed techniques are adapted into the GMPHD filter and the detailed inspection of the SPCF technique with resort to other approaches is made. For this aim, four different fusion strategies are chosen as the framework for fusion of PHD's and their fusion expressions are analytically provided. The fusion structure given in Figure 4.5 is proposed assuming the overall system is a two radar fusion system (Figure 1.6).

Notice that both local and remote information are Gaussian Mixture intensity so that only SPCF and Pseudo Chernoff-2 fusion methods are applicable while Numeric Chernoff fusion can not be applied because of the high state dimension of the track fusion problem. Equations for the local intensity is given in (4.13) and that of the remote intensity is in (4.16).

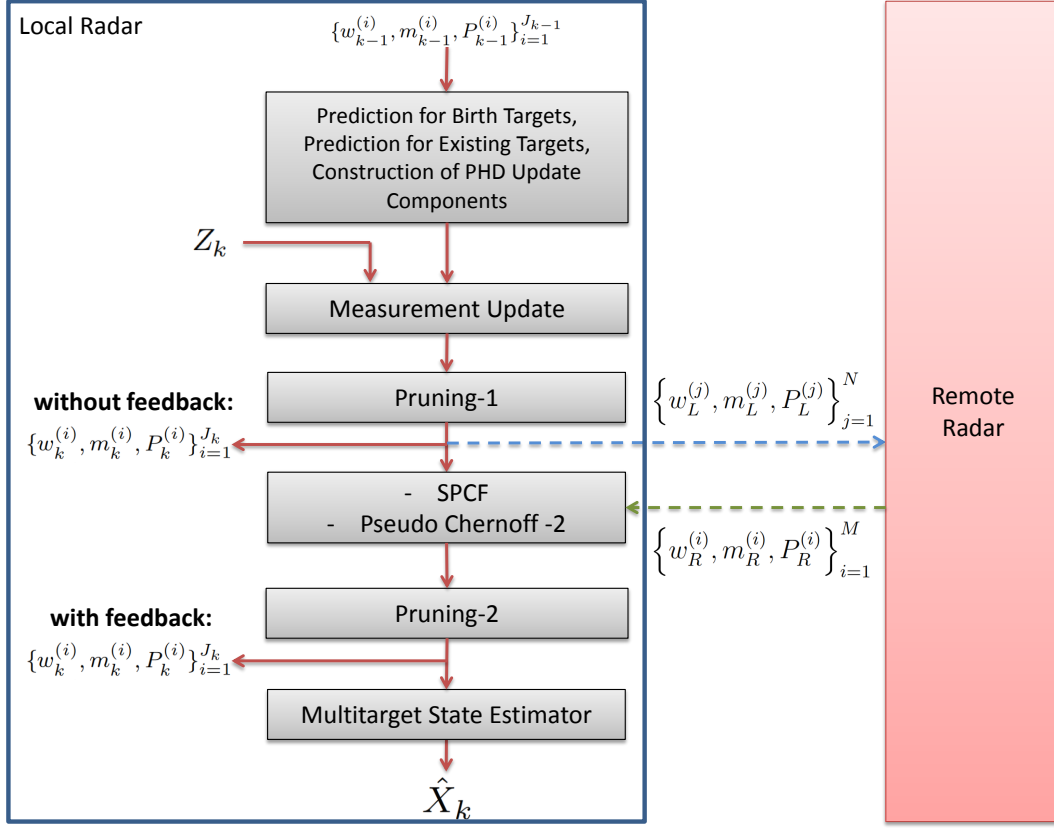


Figure 4.5: GMPHD fusion structure in which Gaussian mixtures are exchanged and SPCF/Pseudo Chernoff-2 methods are used.

$$D_L(x) = \sum_{j=1}^N w_L^j \mathcal{N}(x; m_L^j, P_L^j) \quad (4.12)$$

$$= \underbrace{\sum_{k=1}^N w_L^k}_{\mu_L} \sum_{j=1}^N \underbrace{\frac{w_L^j}{\sum_{k=1}^N w_L^k}}_{\tilde{w}_L^j} \mathcal{N}(x; m_L^j, P_L^j) \quad (4.13)$$

$$= \mu_L s_L(x) \quad (4.14)$$

$$D_R(x) = \sum_{i=1}^M w_R^i \mathcal{N}(x; m_R^i, P_R^i) \quad (4.15)$$

$$= \underbrace{\sum_{k=1}^M w_R^k}_{\mu_R} \sum_{i=1}^M \underbrace{\frac{w_R^i}{\sum_{k=1}^M w_R^k}}_{\tilde{w}_R^i} \mathcal{N}(x; m_R^i, P_R^i) \quad (4.16)$$

$$= \mu_R s_R(x) \quad (4.17)$$

where μ_L and μ_R are the average number of objects, each distributed according to the spatial single object density $s_L(x)$ and $s_R(x)$, respectively. μ_L and μ_R can be found as the sum of the weights and $s_L(x)$ and $s_R(x)$ are normalized versions of $D_L(x)$ and $D_R(x)$, respectively. The letters in the equations “R”, “L” and “F” denote “Remote”, “Local” and “Fused” throughout the chapter, respectively.

Note that the selection of the fusion strategies may be based on the type of the target intensity to be fused and the feedback mechanism in the fusion structure.

Fusion Strategies Based on the Type of the Intensity: Chernoff fusion formulae derived by [16] enables the formulation of the fusion problem. Based on the resultant fusion formulae, the fusion problem can be defined as below:

$$D_F(x) = \mu_R^{(1-w^*)} \mu_L^{w^*} s_R^{(1-w^*)}(x) s_L^{w^*}(x) \quad (4.18)$$

where w^* is selected as below

$$w^* = \arg \min_{w \in [0,1]} \mathcal{L} \left(\mu_R^{(1-w)} \mu_L^w s_R^{(1-w)}(x) s_L^w(x) \right). \quad (4.19)$$

Here, the function $\mathcal{L}(\dots)$ represents an uncertainty measure from the space of density functions into real numbers and is selected as the trace of the covariance matrix of the resultant density in this thesis.

The fusion equation in (4.18) is derived for the fusion of multitarget intensities. Additionally, another idea may be based on fusion of single-object densities as given below:

$$D_F(x) = \underbrace{\mu_R^{(1-w^*)} \mu_L^{w^*}}_{\mu_F(x)} \underbrace{\frac{s_R^{(1-w^*)}(x) s_L^{w^*}(x)}{\int s_R^{(1-w^*)}(x) s_L^{w^*}(x) dx}}_{s_F(x)} \quad (4.20)$$

where w^* is selected as below

$$w^* = \arg \min_{w \in [0,1]} \mathcal{L}(s_F(x)). \quad (4.21)$$

Here, the function $\mathcal{L}(\dots)$ is selected same as before.

Note that since the aim is the fusion of single-object densities, normalization operation is required to obtain the single-object fused density at the end.

The proposed fusion equations and assumptions above bring us to two types fusion methods:

- Method-1, Fusion of multi-target intensity
- Method-2, Fusion of single object density

Fusion Strategies Based on the Feedback Mechanism: According to whether fused output is fed back to the PHD filter, or not, two options can be taken into account as shown in Figure 4.5.

- **with feedback:** fused PHD is used for the next time step.
- **without feedback:** fusion output is not fed back to the PHD filter. Filter's own intensity estimate is used for the next step

Combination of these different perspectives results in four different fusion strategies at the end. Derivations related to SPCF are provided in the next section and evaluations and results for each combination are discussed at the end of this chapter.

4.4.2 Derivations for SPCF Fusion of Local and Remote PHD Filters

Chernoff fusion of two Gaussian mixtures can be performed by utilizing the proposed SPCF technique. The equation in (4.18) requires taking the exponent

of the densities to be fused. Inserting (4.13) and (4.16) into (4.18) yields the fusion function of Chernoff technique for Method-1.

$$D_{\text{SPCF,Method-1}}(x) = \mu_R^{(1-w)} \mu_L^w \left[\sum_{j=1}^N \tilde{w}_L^j \mathcal{N}(x; m_L^j, P_L^j) \right]^w \left[\sum_{i=1}^M \tilde{w}_R^i \mathcal{N}(x; m_R^i, P_R^i) \right]^{(1-w)} \quad (4.22)$$

At this point, w^{th} and $(1-w)^{\text{th}}$ of the Gaussian mixtures in (4.22) can be found by the SPCF approximation technique, and the fused PHD is found as in (4.23).

$$D_{\text{SPCF,Method-1}}(x) \cong \mu_R^{(1-w)} \mu_L^w \sum_{j=1}^N \alpha_L^j \mathcal{N}(x; m_L^j, w P_L^j) \sum_{i=1}^M \alpha_R^i \mathcal{N}(x; m_R^i, (1-w) P_R^i) \quad (4.23)$$

the variables $\{\alpha_L^{(j)}\}_{j=1}^N$ and $\{\alpha_R^{(i)}\}_{i=1}^M$ are found by the technique proposed in Chapter 2. Multiplication of the Gaussians results in another scaled Gaussian.

$$D_{\text{SPCF,Method-1}}(x) = \mu_R^{(1-w)} \mu_L^w \sum_{j=1}^N \sum_{i=1}^M \alpha_L^j \alpha_R^i \mathcal{N}(m_R^j; m_L^j, w P_L^j + (1-w) P_R^i) \mathcal{N}(x; m^{i|j}, P^{i|j}) \quad (4.24)$$

where,

$$m^{i|j} = ((1-w)(P_R^i)^{-1} + w(P_L^j)^{-1})^{-1} ((1-w)(P_R^i)^{-1} m_R^i + w(P_L^j)^{-1} m_L^j) \quad (4.25)$$

$$P^{i|j} = ((1-w)(P_R^i)^{-1} + w(P_L^j)^{-1})^{-1} \quad (4.26)$$

If we define $\gamma^{i,j} \triangleq \alpha_L^j \alpha_R^i \mathcal{N}(m_R^j; m_L^j, w P_L^j + (1-w) P_R^i)$ in (4.24), so fused density for the SPCF technique is obtained as in (4.27).

$$D_{\text{SPCF,Method-1}}(x) = \mu_R^{(1-w)} \mu_L^w \sum_{j=1}^N \sum_{i=1}^M \gamma^{i,j} \mathcal{N}(x; m^{i|j}, P^{i|j}) \quad (4.27)$$

$$= \mu_{\text{SPCF,Method-1}} s_{\text{SPCF,Method-1}} \quad (4.28)$$

where

$$\mu_{\text{SPCF,Method-1}} \triangleq \mu_R^{(1-w)} \mu_L^w \sum_{j=1}^N \sum_{i=1}^M \gamma^{i,j} \quad (4.29)$$

$$s_{\text{SPCF,Method-1}} \triangleq \sum_{j=1}^N \sum_{i=1}^M \tilde{\gamma}^{i,j} \mathcal{N}(x; m^{i|j}, P^{i|j}) \quad (4.30)$$

Equations for method-2 can be computed based by similar derivations as method-1 and fused intensity can be obtained as in (4.32).

$$D_{\text{SPCF,Method-2}}(x) = \mu_R^{(1-w)} \mu_L^w \sum_{j=1}^N \sum_{i=1}^M \tilde{\gamma}^{i,j} \mathcal{N}(x; m^{i|j}, P^{i|j}) \quad (4.31)$$

$$= \mu_{\text{SPCF,Method-2}} s_{\text{SPCF,Method-2}} \quad (4.32)$$

where

$$\mu_{\text{SPCF,Method-2}} \triangleq \mu_R^{(1-w)} \mu_L^w \quad (4.33)$$

$$s_{\text{SPCF,Method-2}} \triangleq \sum_{j=1}^N \sum_{i=1}^M \tilde{\gamma}^{i,j} \mathcal{N}(x; m^{i|j}, P^{i|j}) \quad (4.34)$$

4.5 Performance Evaluation

For understanding the performance of the proposed PHD fusion strategies and the fusion methods, again 2D air platform scenarios is selected for which the correlated target intensity information obtained from different radar systems have to be fused. Specifically, the scenario stated in [47] is selected as the benchmark scenario and a modified version of this scenario is also proposed for deeper understanding of the performance of the methods.

The performance of the methods, SPCF and Pseudo Chernoff-2 are compared with each other and are also compared with the iterated corrector approximation

technique. The iterated corrector approximation technique will rely on fusing the unprocessed measurement information set generated by the radars and will be considered as an optimal fusion method. Individual performances will be obtained by finding the OSPA distances between the resultant estimate set and the true target set.

4.5.1 OSPA(Optimal SubPattern Assignment) Metric

OSPA is a very well-known measure which reflects the difference between two target sets. It stands for “Optimum SubPattern Assignment” and is proposed by [43]. Its basic properties in [43] are provided as:

- being a metric on the space of finite sets,
- having a natural (meaningful) physical interpretation,
- capturing cardinality errors and state errors meaningfully,
- being easily computed.

The OSPA metric used here gives the distance between two finite sets $X = x_1, \dots, x_m$ and $Y = y_1, \dots, y_n$, where X is the target position extracted by the PHD fusion system, Y is the ground truth target set and $m, n \in \mathbb{N}_0 = \{0, 1, 2, \dots\}$. The metric is calculated for $m \leq n$ and $1 \leq p < \infty$ as in (4.35). $\bar{d}_p^{(c)}$ is called the OSPA metric of order p with cut-off c .

$$\bar{d}_p^{(c)}(X, Y) := \left(\frac{1}{n} \left(\min_{\pi \in \Pi_n} \sum_{i=1}^m d^{(c)}(x_i, y_{\pi(i)})^p + c^p(n - m) \right) \right) \quad (4.35)$$

where $d^c(x, y) := \min(c, d(x, y))$, $c > 0$ is defined as the cut off, Π_k is the set of permutations on $\{1, 2, \dots, k\}$ for any $k \in \mathbb{N} = \{1, 2, \dots\}$ and $d(x, y)$ is the L2 norm.

In case $m > n$, $\bar{d}_p^{(c)}(X, Y)$ is found as $\bar{d}_p^{(c)}(Y, X)$.

Notice that OSPA metric of order 2 with cut-off 100 is selected for the experiments in this thesis.

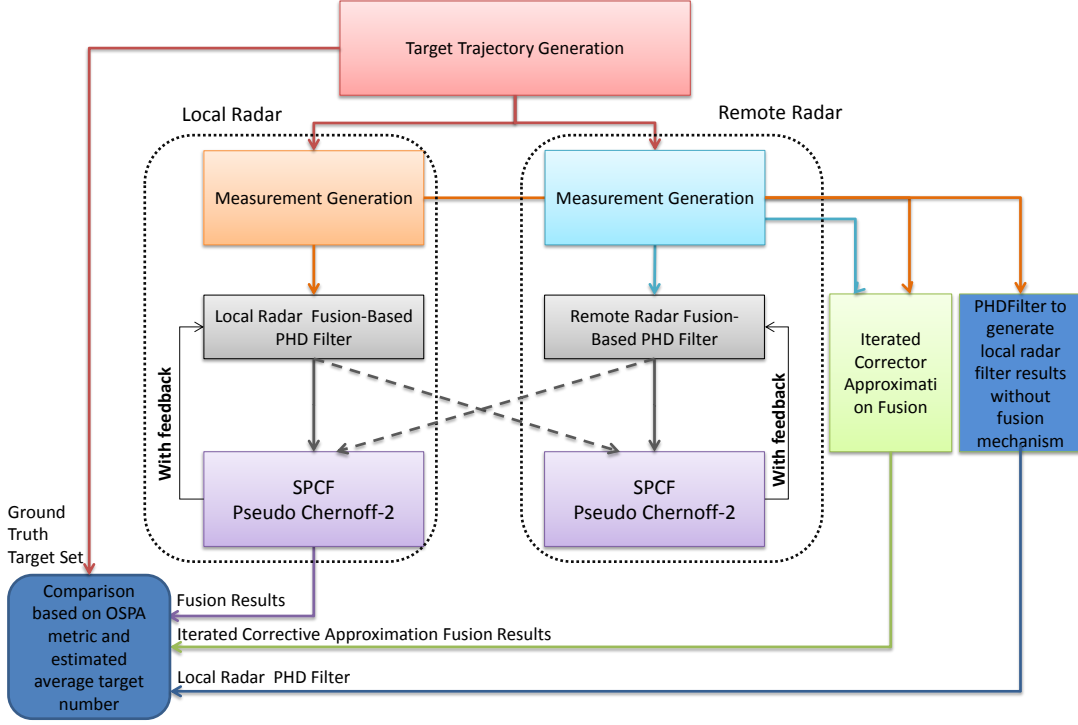


Figure 4.6: Experimental set-up to analyze different fusion approaches.

4.5.2 Experiment Set-up

The experiments are based on 250 randomly generated Monte Carlo runs. Radar measurements are generated according to the radar model given in Section 4.5.5 and fed to both the local and the remote radar PHD filters. The measurements are also fed to a centralized PHD, which is expected to perform the best fusion amongst all for comparison purposes. All of the fusion results are compared with the ground truth target set in terms of OSPA metric and expected number of targets. Ensemble average of the OSPA metric and average number of targets is computed with respect to time. A rough overview of the experimental set-up is provided in Figure 4.6.

Next sections will describe the target trajectories and radar models. Note that the trajectories in Scenario-1 are generated as similar as possible to those in [47]. Additionally, the parameters are selected exactly the same as those stated in [47], except the birth intensity.

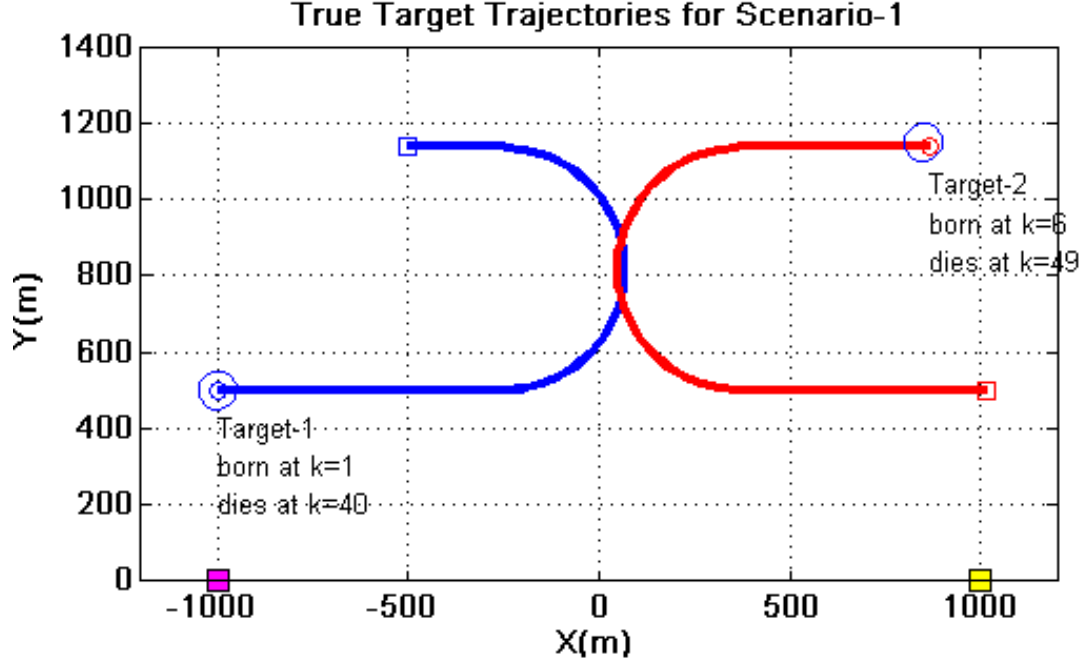


Figure 4.7: Trajectories of Scenario-1. Start points of the red and blue trajectories are marked by circles. Radar positions are denoted by magenta and yellow squares. Large circles at the starting point show the “birth” regions.

4.5.3 Target Scenarios

Multitarget scenarios are required to show and compare the performance of the proposed approaches since the aim is to fuse target intensities distributed throughout the entire state space. [47] gives a two-target scenario in which the distance between the targets decreases down up to a certain time and then increases again. This target scenario is called “Scenario-1” and its trajectories are provided in Figure 4.7. In the figure, magenta and yellow squares represent local and remote radar deployments, respectively.

Another scenario is defined to enrich the target scenario database and to examine the robustness of proposed fusion strategies in different scenarios. The second scenario is called “Scenario-2”. The trajectories of the targets in this scenario are given in Figure 4.8. Note that in this scenario the two targets get close to each other not only positionally but their velocities become similar. Both scenarios have target trajectories that can be considered as “coordinated turn”.

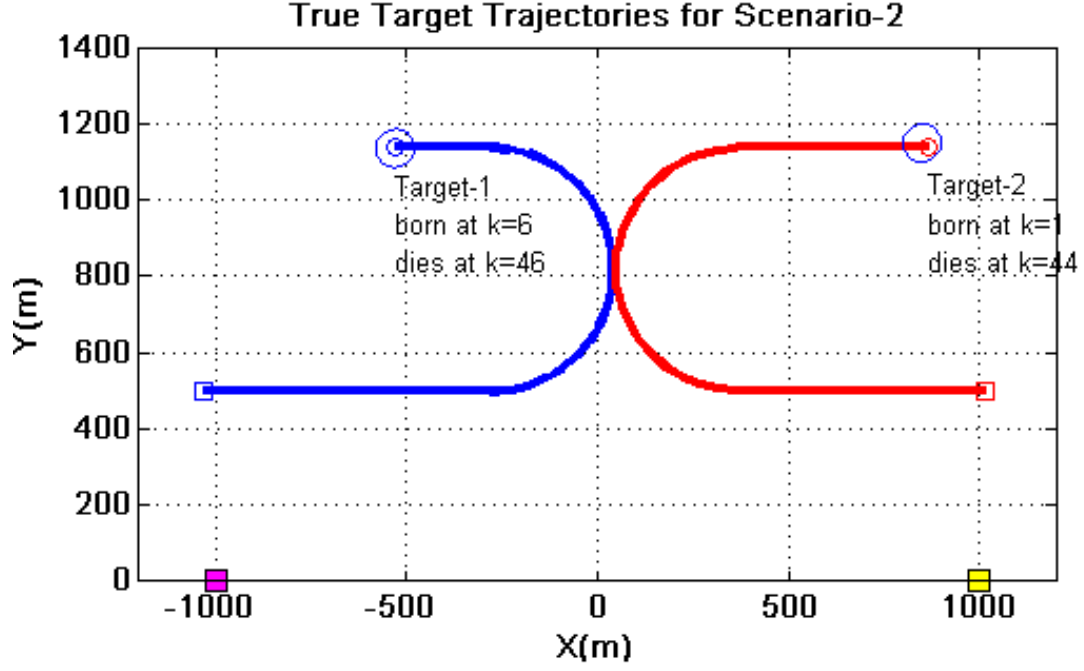


Figure 4.8: Trajectories of Scenario-2. Start points of the red and blue trajectories are marked by circles. Radar positions are denoted by magenta and yellow squares. Large circles at the starting point show the “birth” regions.

4.5.4 Target Model and Related Parameters

Survival probability of the target is taken as $p_{S,k} = 0.99$ and follows a nonlinearity nearly constant turn model [30]. The target state $x_k = [y_k, w_k]^T$ where $y_k = [p_{x,k}, p_{y,k}, v_{x,k}, v_{y,k}]^T$ and w_k is the turn rate. State dynamics are given in (4.36) and (4.37).

$$y_k = F(\omega_{k-1})y_{k-1} + Gw_{k-1} \quad (4.36)$$

$$\omega_k = \omega_{k-1} + \Delta u_{k-1} \quad (4.37)$$

where

$$F(\omega) = \begin{bmatrix} 1 & 1 & \frac{\sin \omega \Delta}{\omega} & -\frac{1 - \cos \omega \Delta}{\omega} \\ 0 & 1 & \frac{1 - \cos \omega \Delta}{\omega} & \frac{\sin \omega \Delta}{\omega} \\ 0 & 0 & \cos \omega \Delta & -\sin \omega \Delta \\ 0 & 0 & \sin \omega \Delta & \cos \omega \Delta \end{bmatrix} \quad (4.38)$$

and

$$G = \begin{bmatrix} \frac{\Delta^2}{2} & 0 \\ 0 & \frac{\Delta^2}{2} \\ \Delta & 0 \\ 0 & \Delta \end{bmatrix} \quad (4.39)$$

$\Delta = 1$ s, $w_k \sim \mathcal{N}(:, 0, \sigma_w^2 I_2)$, $\sigma_w = 15$ m/s², $u_k \sim \mathcal{N}(:, 0, \sigma_u^2 I_2)$, and $\sigma_u = (\pi/180)$ rad/s. No spawning is assumed and the spontaneous birth intensity is given as:

$$\gamma_k(x) = 0.1\mathcal{N}(x; m_\gamma^{(1)}, P_\gamma) + 0.1\mathcal{N}(x; m_\gamma^{(2)}, P_\gamma) \quad (4.40)$$

where

$$m_\gamma^{(1)} = [-1000, 500, 0, 0, 0]^T \quad (4.41)$$

$$m_\gamma^{(2)} = [850, 1150, 0, 0, 0]^T \quad (4.42)$$

$$P_\gamma = \text{diag}([2500, 2500, 2500, 2500, (6\pi/180)^2]^T) \quad (4.43)$$

4.5.5 Radar Model

The measurement model consisting of bearing and range measurements is provided as in (4.44).

$$z_k = \begin{bmatrix} \arctan\left(\frac{p_{x,k}}{p_{y,k}}\right) \\ \sqrt{p_{x,k}^2 + p_{y,k}^2} \end{bmatrix} + \epsilon_k \quad (4.44)$$

where $\epsilon_k \sim \mathcal{N}(:, 0, R_k)$ with $R_k = \text{diag}([\sigma_\theta^2, \sigma_r^2])$, $\sigma_\theta = 2(\pi/180)$ rad/s and $\sigma_r = 20$ m. The clutter random finite set follows the uniform Poisson model (4.45) over

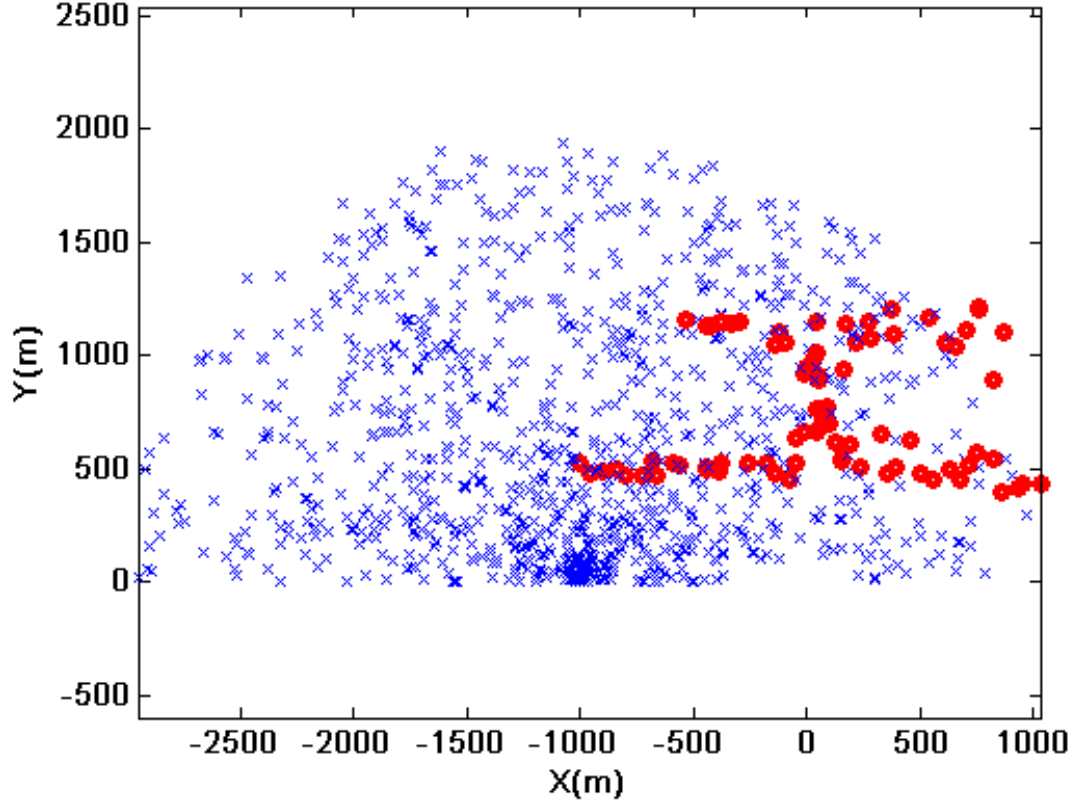


Figure 4.9: Measurements generated by the local radar for a single run. “x” and “o”s correspond to the measurements related to the clutter and the targets, respectively.

the surveillance region $[0, \pi]$ rad \times $[0, 2000]$ m, with $\lambda_c = 3.2 \times 10^{-3} (\text{rad m})^{-1}$ (i.e., an average of 20 clutter returns on the surveillance region).

$$\kappa_k(z) = \lambda_c V u(z) \quad (4.45)$$

where $u(\cdot)$ is the uniform density over the surveillance region, V is the volume of the surveillance region, and λ_c is the average number of clutter return per unit volume.

Note that the detection and survival probabilities of each target are taken as $p_{D,k} = 0.98$ and $p_{S,k} = 0.99$. Measurements generated by the local radar for a single run is provided in Figure 4.9 as an example.

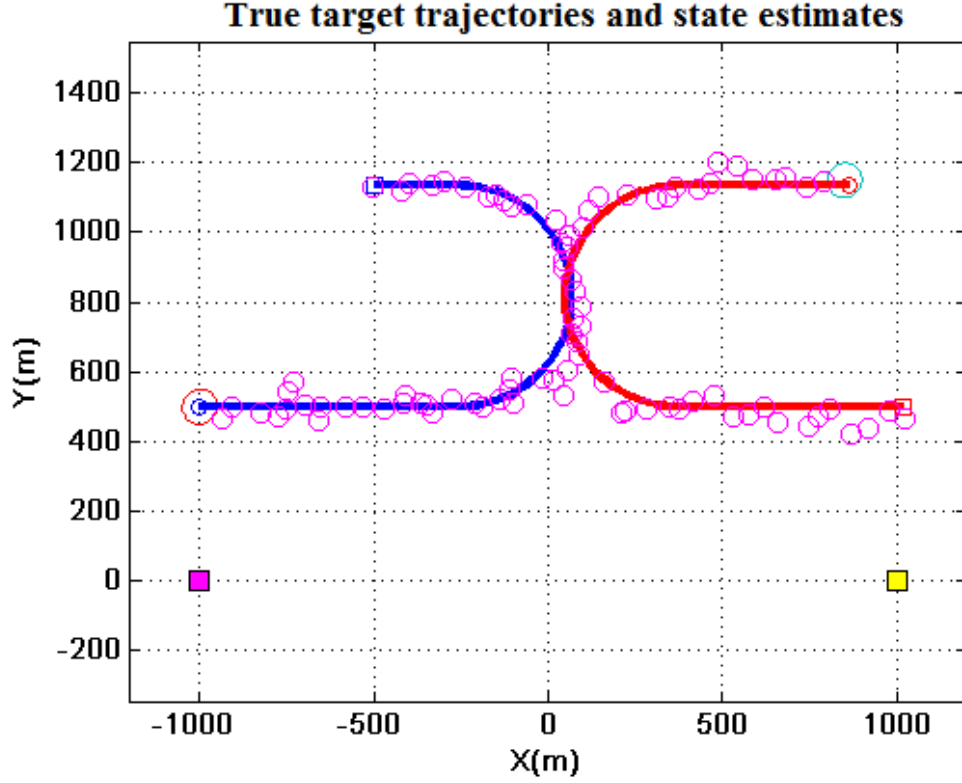


Figure 4.10: State estimates of the EK-GMPHD filter together with true target trajectories for Scenario-1. “o”s correspond to the filter state estimates.

4.5.6 PHD Filter

The filter type selected for the implementation is Extended Kalman GMPHD (EK-GMPHD), which is also selected in [47]. The implementation done here is a replica of the implementation of [47]. This provides the opportunity to compare the two implementations and the comparison shows almost same tracking results.

Pseudocode for the EK-GMPHD filter, the pruning and the state extraction steps in [47] are also given in Appendix A for the sake of completeness.

State estimate results of EK-GMPHD filter for a single run is also shown in the Figures 4.10 and 4.11. Additionally, Figure 4.12 represents the expected number of targets for the same run. Note that expected number of targets is simply the sum of the Gaussian mixture weights.

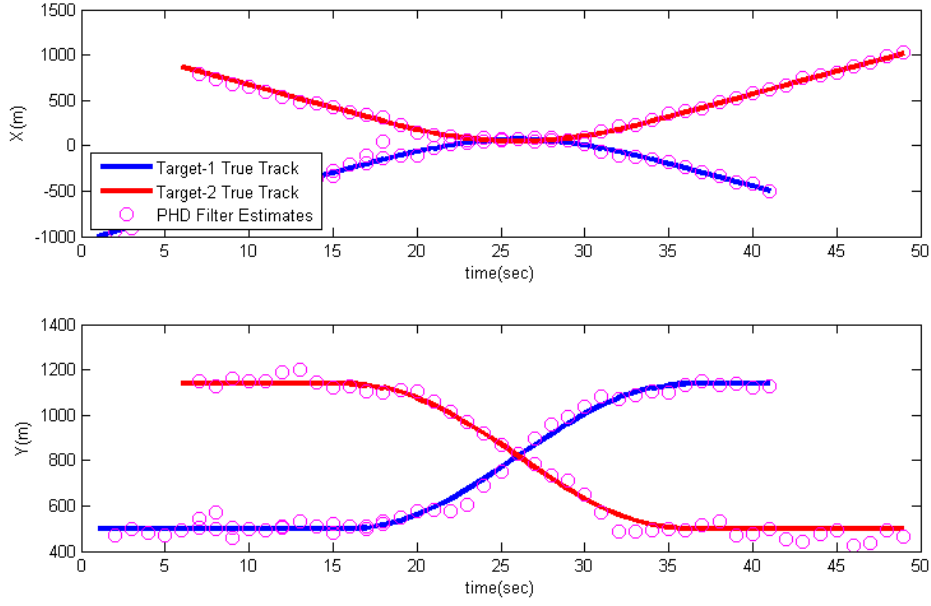


Figure 4.11: Representation of the state estimates of EK-GMPHD filter in terms of x and y coordinates. “o”s correspond to the filter state estimates.

4.5.7 Fusion Results

Evaluation of the fusion performance of the proposed techniques are based on the target scenarios defined in Section 4.5.3 and the radar models given in Section 4.5.5. Assuming there exist two radars communicating to each other and both radars have EK-GMPHD tracker, fusion operation is performed at each radar site for SPCF and Pseudo Chernoff-2 techniques. This operation relies on fusion of single target/multitarget intensities (method-1/method-2) and the feedback mechanism given in the fusion structure. Details of fusion strategies are already provided in Section 4.4.1. The evaluation of the proposed techniques is performed by providing the OSPA distance and expected number of targets. The ensemble average of these measures obtained in 250 Monte Carlo runs are taken for each time instance. The two strategies, SPCF and Pseudo Chernoff-2, are also compared with the iterated corrector approximation technique which takes all the measurements of both radars as input (Figure 4.4). Following sections illustrate the fusion performances for each target scenario based on four

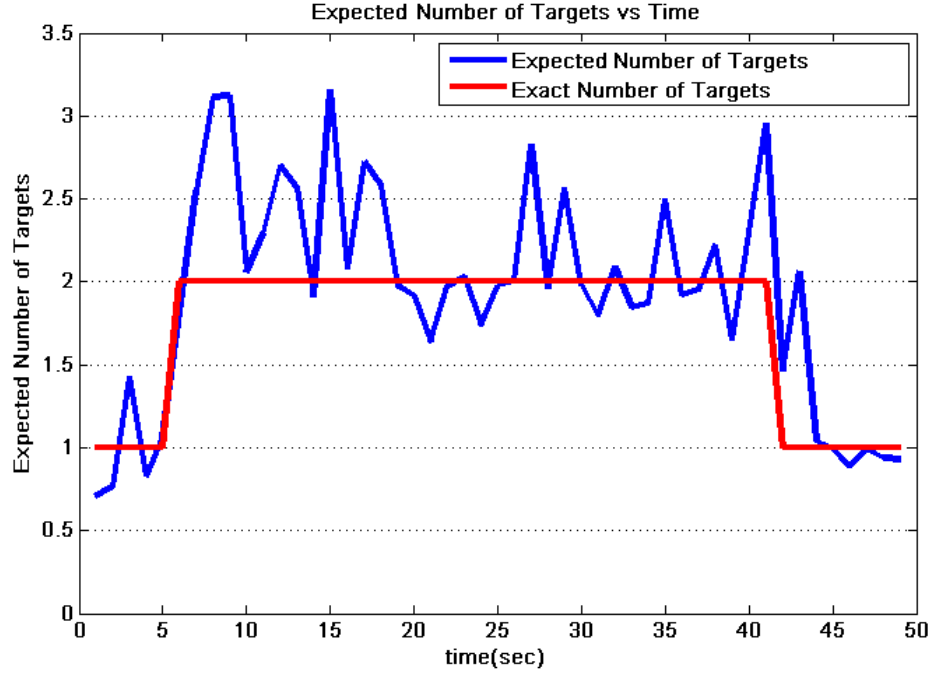


Figure 4.12: Estimated number of targets with respect to time for the same single run.

types of techniques stated in Section 4.4.1. A list of these techniques is also provided here for better understanding:

- Method-1, Fusion of multi-target intensity
 - with feedback
 - without feedback
- Method-2, Fusion of single object density
 - with feedback
 - without feedback

The feedback loop is shown in Figure 4.6. For the feedback case, the fused intensity is used in the next PHD iteration.

The resultant OSPA and average number of targets values of both scenarios are obtained for the following PHD trackers and PHD fusion techniques:

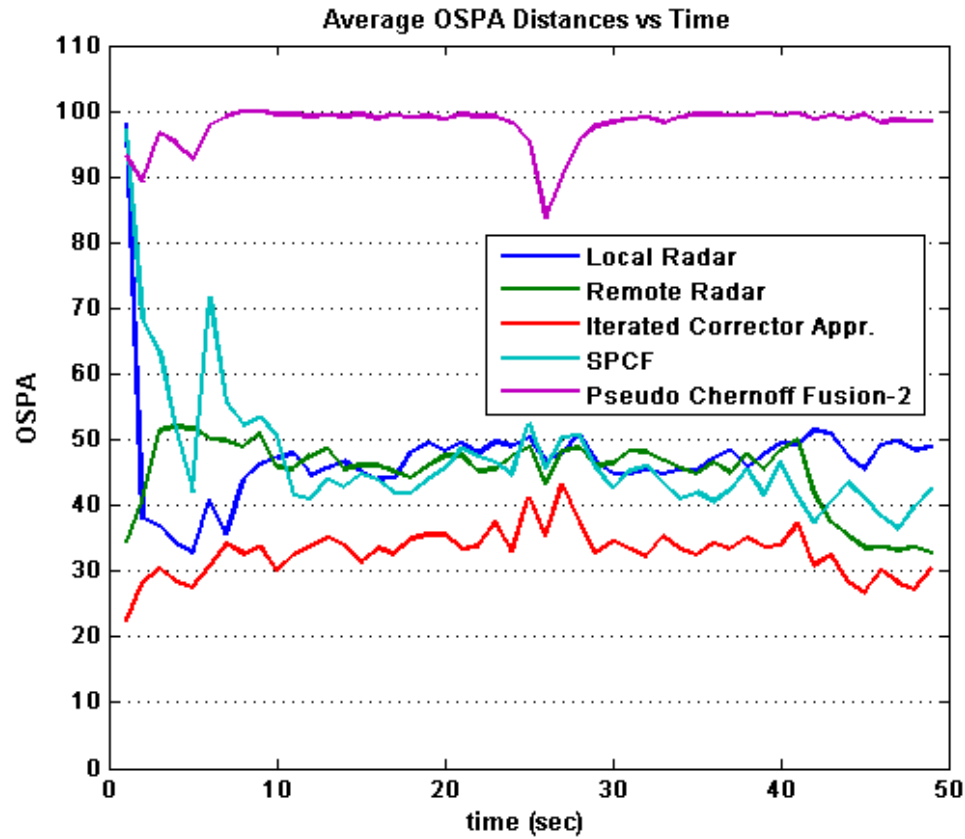


Figure 4.13: “Scenario-1”, “Method-1 with feedback”: Ensemble averaged OSPA distances of the trackers and the fusion techniques.

- Local Radar PHD Tracker
- Remote Radar PHD Tracker
- Iterated Corrector Approximation
- SPCF
- Pseudo Chernoff-2

When the results of each scenario are analyzed, following observations are made regarding the performances of the proposed fusion strategies:

- Pseudo Chernoff-2 fusion method yields worst results among all the techniques in terms of OSPA distance metric. If feedback is provided it even

gets worse which shows this technique is not robust when the feedback is provided.

- SPCF fusion technique based on Method-1 produces poor quality estimates for the number of targets . This observations is also projected into the OSPA distances and corresponding OSPA distances are worse than those of individual PHD filters when feedback is not provided. However, this approach is still much more better than the Pseudo Chernoff-2 method. Building up a feedback mechanism seems to improve the results of this method and makes it comparable with the individual filters.
- SPCF fusion technique based on Method-2 seems to be a consistent and robust fusion approach for both of the target scenarios and its performance is generally better than the performances of the individual PHD trackers. When compared with the results of iterated corrector approximation technique, SPCF produces the closest results to those of iterated corrective approximation technique compared to individual filters, in general. Feedback mechanism for this case slightly augments the OSPA distance and it even produces slightly better OSPA than the iterated corrector approximation.
- Providing a feedback from the fusion architecture to the tracker seems to improve the performance of the SPCF technique. Depending on the fusion architecture and communication demands of the system, any of the “with” or “without” feedback mechanisms can be chosen as a solution.
- Method-2 produces more accurate target set than Method-1 for both with and without feedback mechanisms. In terms of number of targets estimate, Method-2 is again much better than Method-1.
- Average computation times of Scenario-1 experiments for each fusion approach are obtained and given in Table 4.2. The results reveal that SPCF is computationally demanding in general when compared to the other techniques, which is an expected outcome. SPCF solves three different optimization problems to find w^{th} and $(1 - w)^{\text{th}}$ powers of the Gaussian mixtures and to find the optimum w in the Chernoff fusion operation. On

the other hand, Pseudo Chernoff technique only solves for the optimum w so that its computation time is lower.

Table 4.2: Average computation times in seconds for PHD fusion techniques.

Algorithm	Method-1		Method-2		Method-1		Method-2	
	with	feed-	with	feed-	without	without	without	without
	back	back	back	back	feedback	feedback	feedback	feedback
Iterated Corrector	0.03		0.03		0.03		0.03	
Approx.								
Pseudo Chernoff-2	2.96		2.83		0.29		0.28	
SPCF	2.73		3.26		5.26		5.30	

Also note that feedback mechanism decreases the computations for SPCF and increases that of Pseudo Chernoff-2 method. The cause of this observation is analyzed in detail and it is found that the number of Gaussians generated within each approach seriously effect the computation times. Figure 4.29 reveals that feedback mechanism decreases the number of Gaussians produced by the radar PHD filters which definitely decreases the computational load. On the other hand, when Pseudo Chernoff-2 technique is used with feedback, number of Gaussians yielded by the individual trackers increases which significantly results in more computations (Figure 4.30).

4.6 Discussions

In this chapter, fusion of multiple PHD filters with unknown correlation is investigated on a decentralized sensor network. SPCF fusion technique is analyzed in detail for two types of fusion approaches: single object density fusion and multitarget intensity fusion. Notice that although Chernoff fusion equations are proposed for multitarget intensity fusion in the literature, these proposals do not provide any applicable form of problem formulation for the fusion of Gaussian mixture intensity functions. One of the novelties of this thesis is to provide an applicable way to perform Chernoff fusion of Gaussian mixture intensities, which yields the fusion of PHD filter outputs. Apart from that, other novel idea

of fusing single object densities based on Chernoff fusion is raised during the thesis study period. This approach is actually inspired from the multitarget intensity Chernoff fusion formulae and necessary derivations for both fusion types are done analytically for the fusion of Gaussian mixture intensities. Together with SPCF, Pseudo Chernoff fusion results are also obtained so as to be able make a comparison of SPCF with an existing technique.

Performance of the stated techniques are assessed on a two radar PHD fusion problem in which EK-GMPHD filters exist. Some fusion strategies based on SPCF and Pseudo Chernoff fusion are brought forward in compatible with the internal structure of the PHD filter. The resultant intensities are compared with the exact trajectories by using OSPA distances and expected number of targets. Results are also assessed by using the results of the iterated corrector approximation technique, which is the best approach based on measurement fusion in the PHD filter. Effectiveness of single object density and multitarget intensity fusion based on SPCF technique is demonstrated in terms of consistency and accuracy.

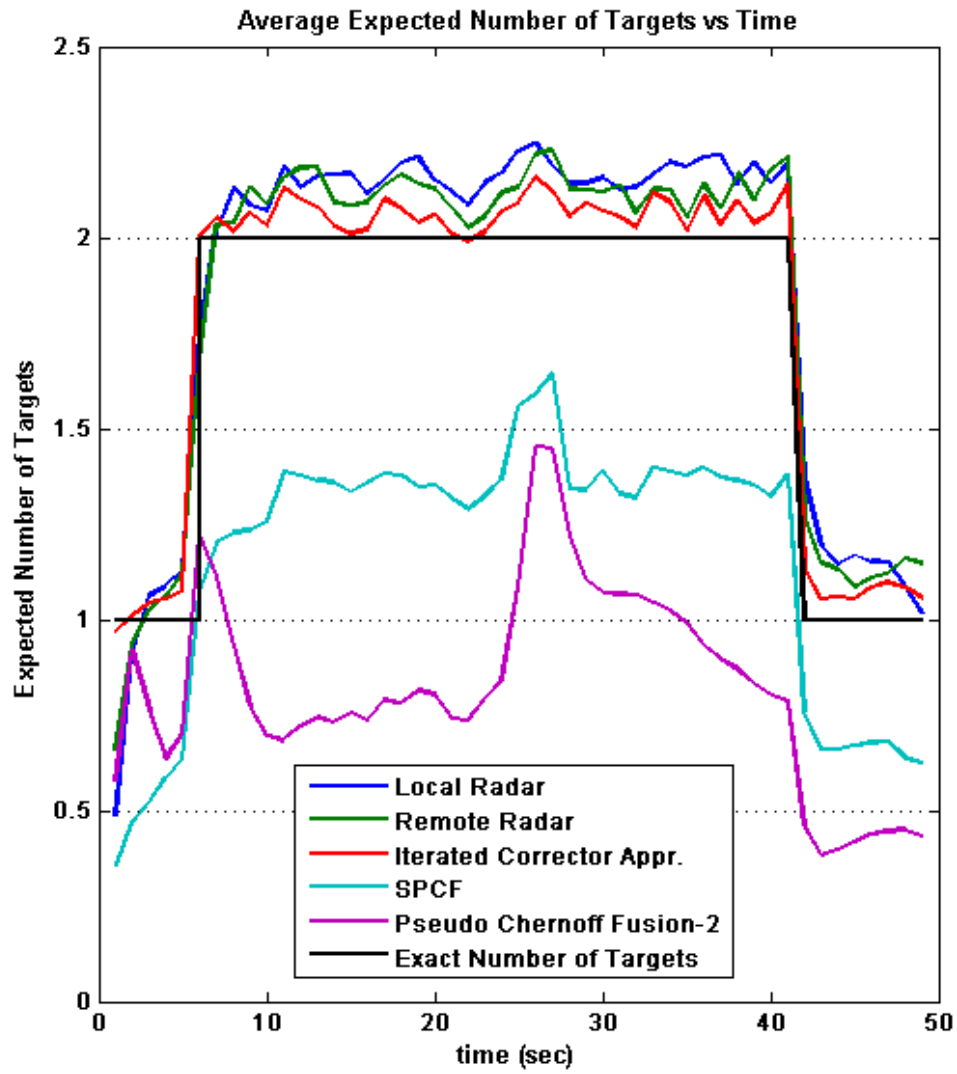


Figure 4.14: “Scenario-1”, “Method-1 with feedback”: Ensemble averaged expected number of targets of the trackers and the fusion techniques.

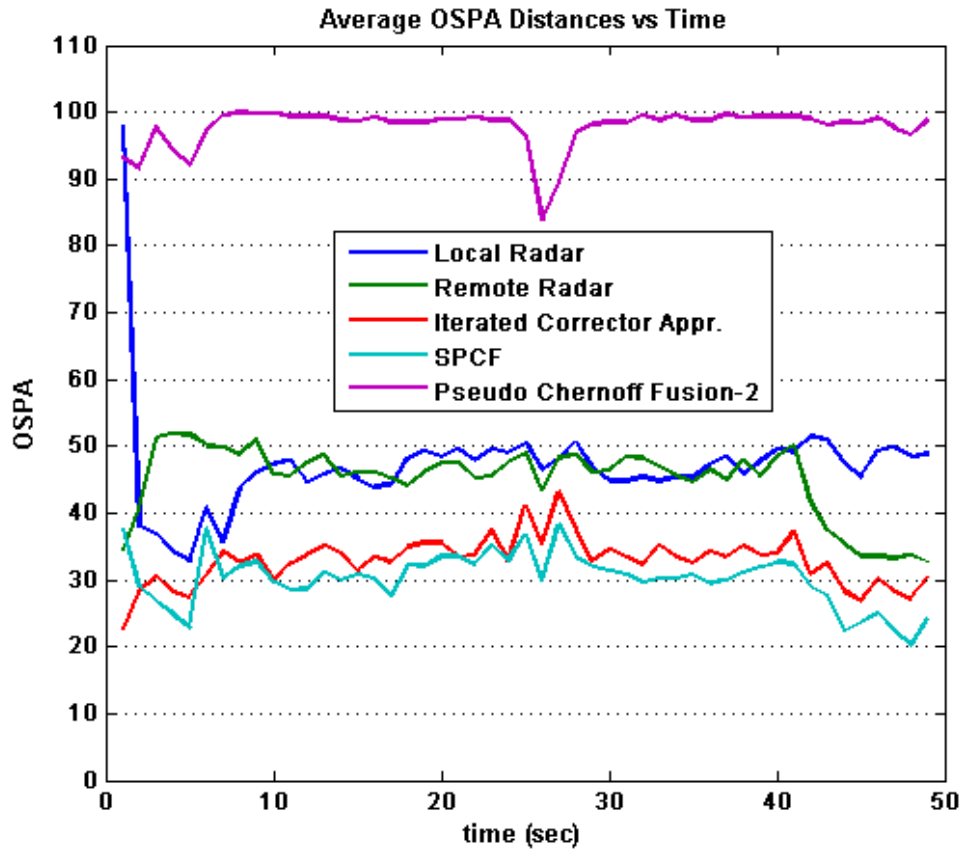


Figure 4.15: “Scenario-1”, “Method-2 with feedback”: Ensemble averaged OSPA distances of the trackers and the fusion techniques.

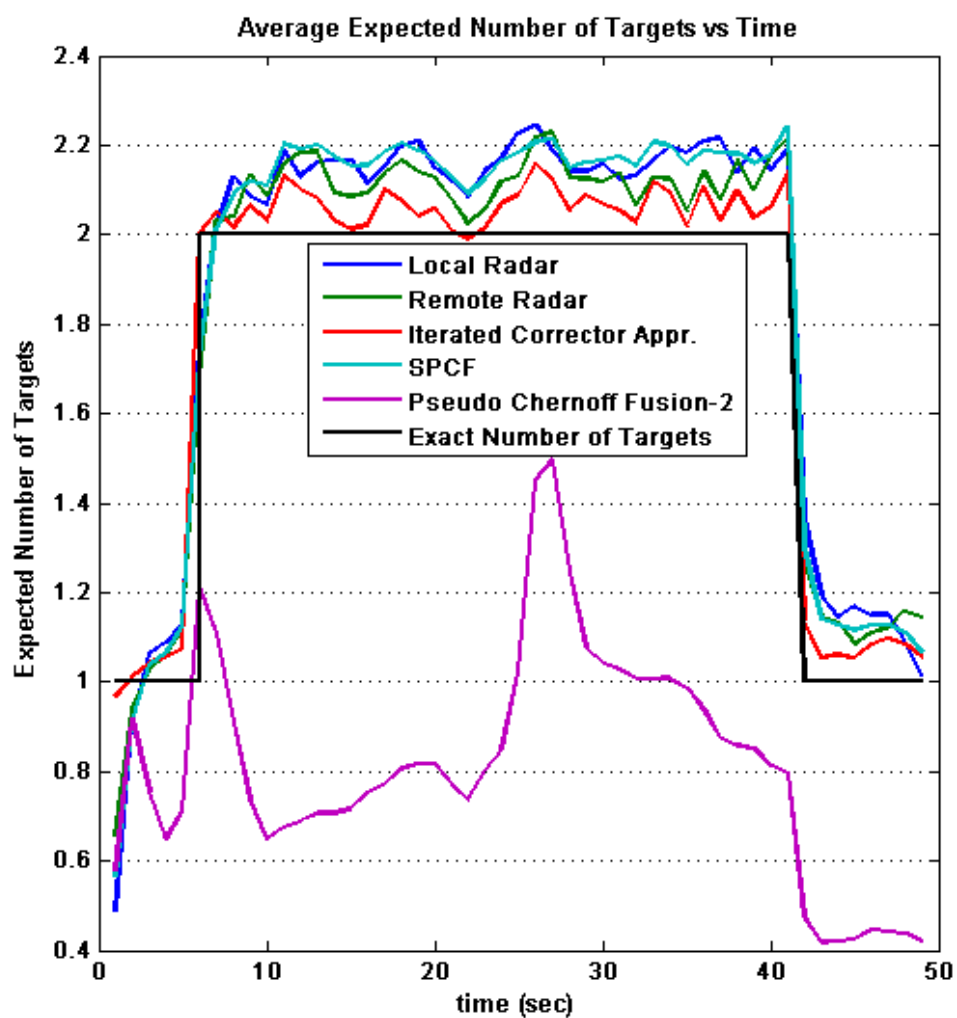


Figure 4.16: “Scenario-1”, “Method-2 with feedback”: Ensemble averaged expected number of targets of the trackers and the fusion techniques.

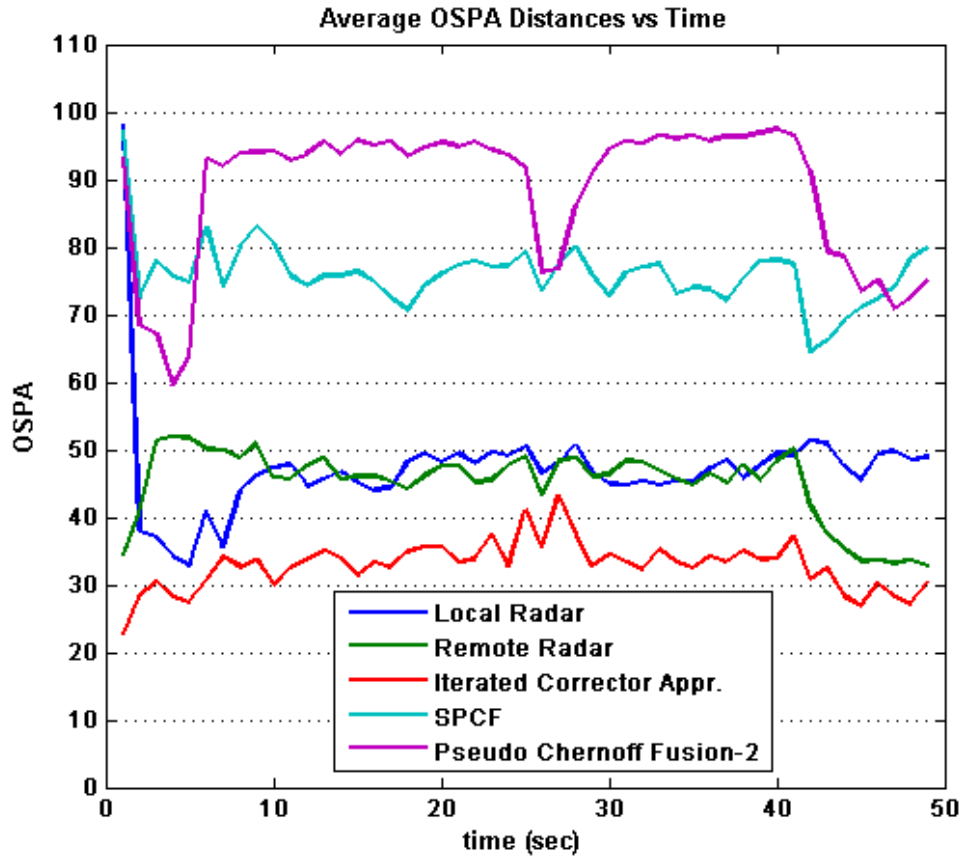


Figure 4.17: “Scenario-1”, “Method-1 without feedback”: Ensemble averaged OSPA distances of the trackers and the fusion techniques.

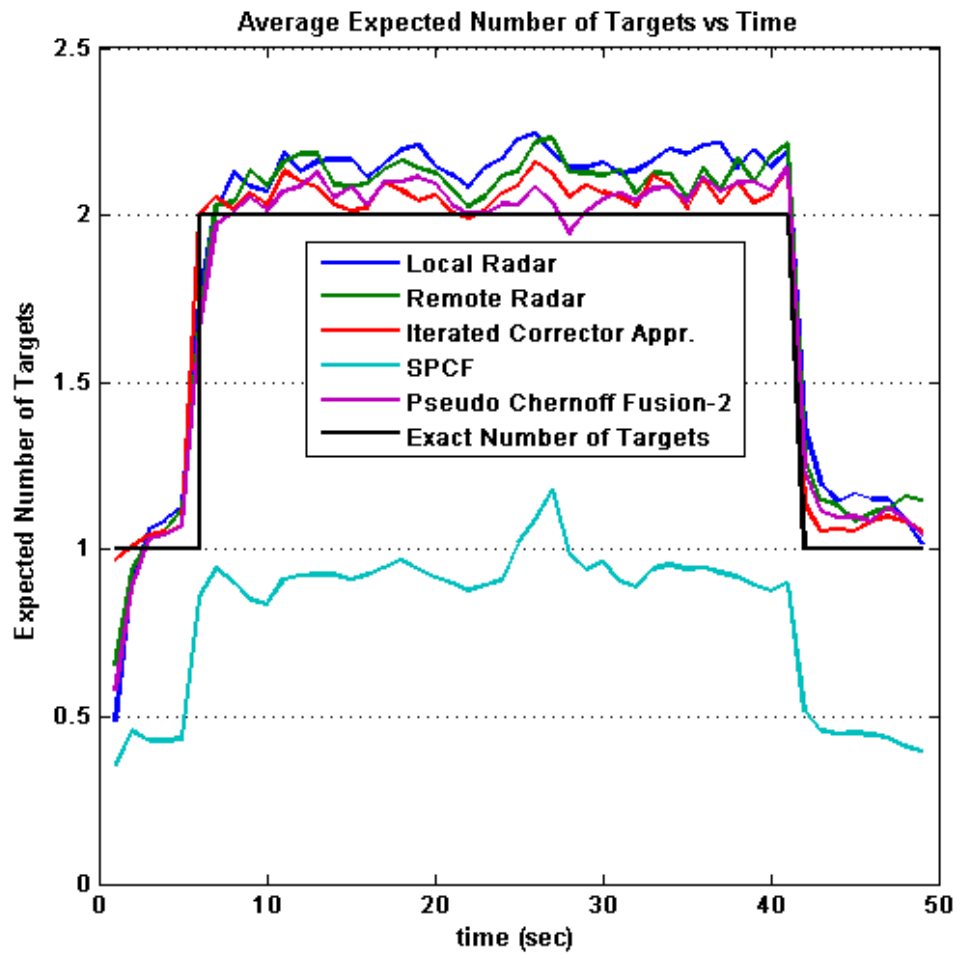


Figure 4.18: “Scenario-1”, “Method-1 without feedback”: Ensemble averaged expected number of targets of the trackers and the fusion techniques.

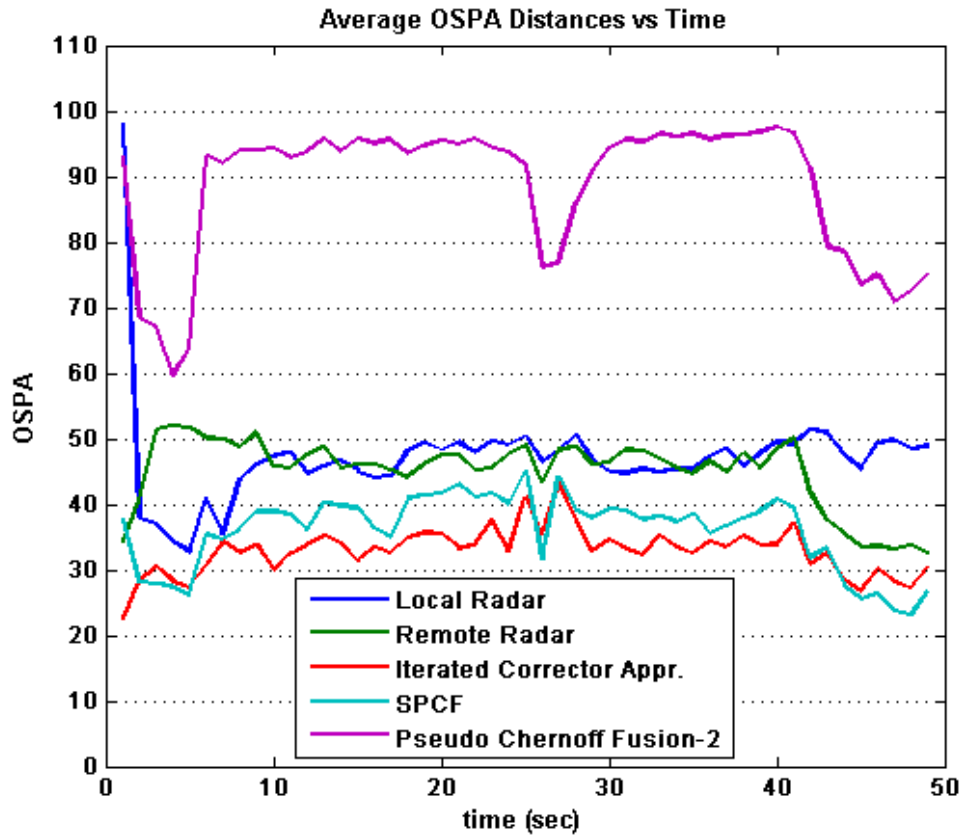


Figure 4.19: “Scenario-1”, “Method-2 without feedback”: Ensemble averaged OSPA distances of the trackers and the fusion techniques.

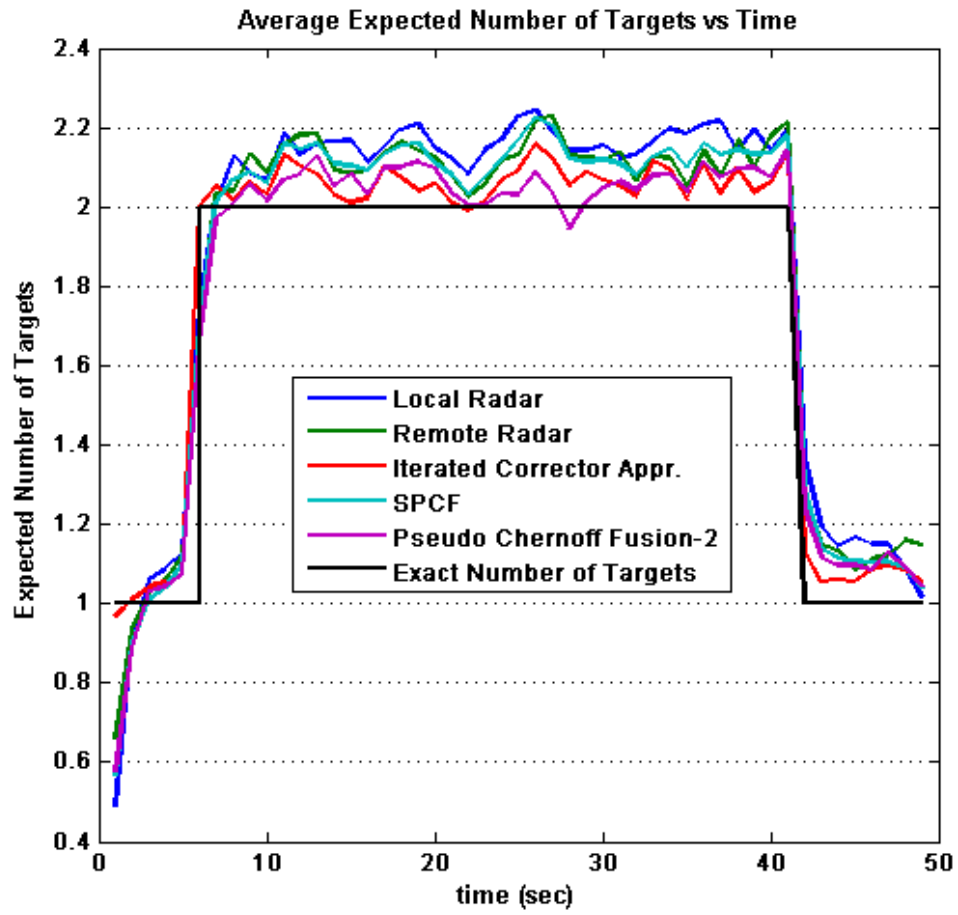


Figure 4.20: “Scenario-1”, “Method-2 without feedback”: Ensemble averaged expected number of targets of the trackers and the fusion techniques.

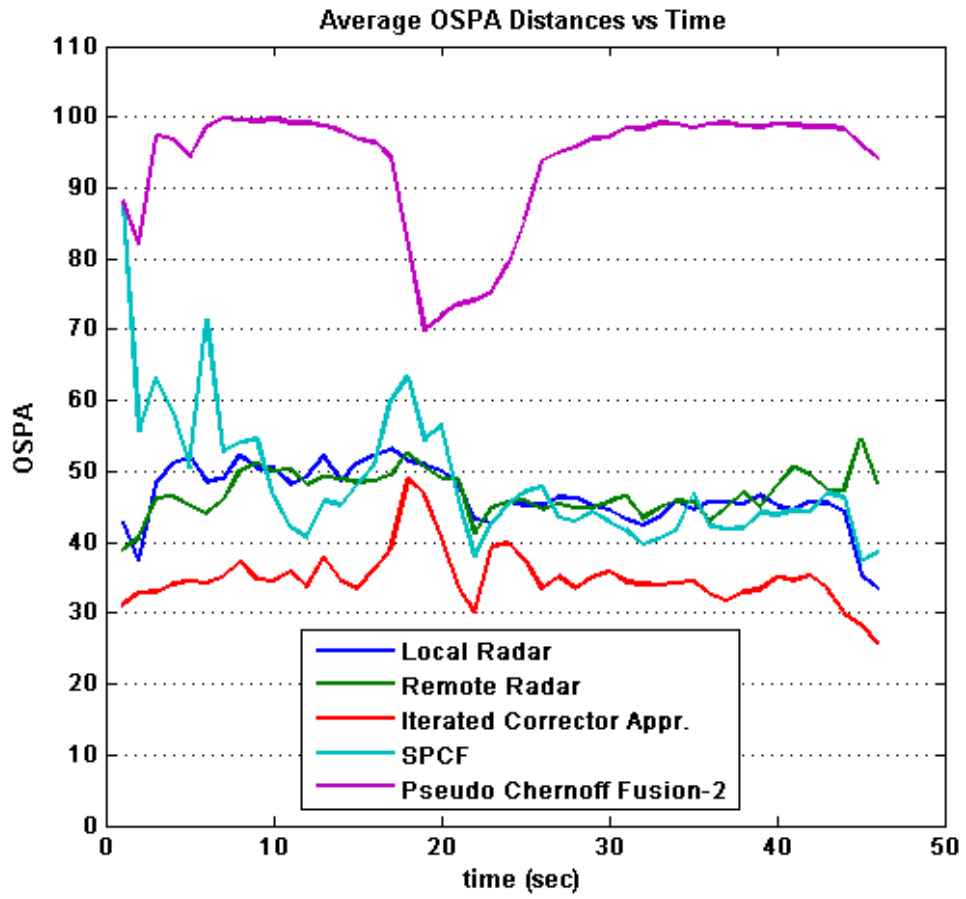


Figure 4.21: “Scenario-2”, “Method-1 with feedback”: Ensemble averaged OSPA distances of the trackers and the fusion techniques.

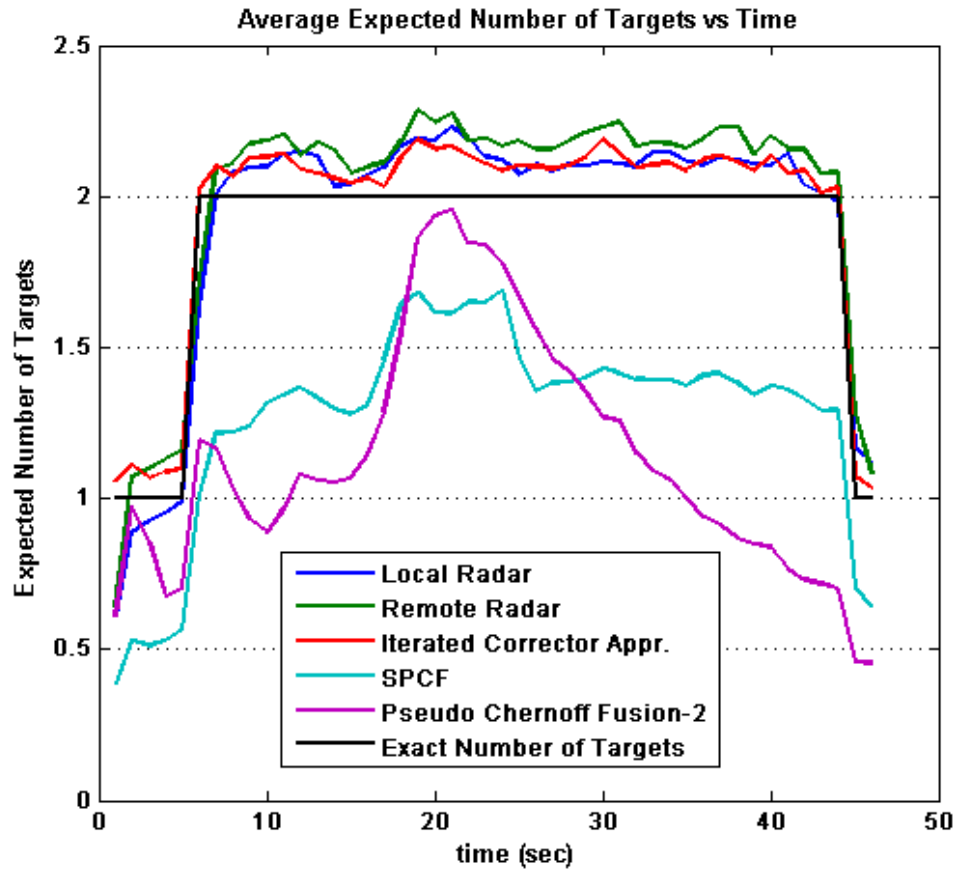


Figure 4.22: “Scenario-2”, “Method-1 with feedback”: Ensemble averaged expected number of targets of the trackers and the fusion techniques.

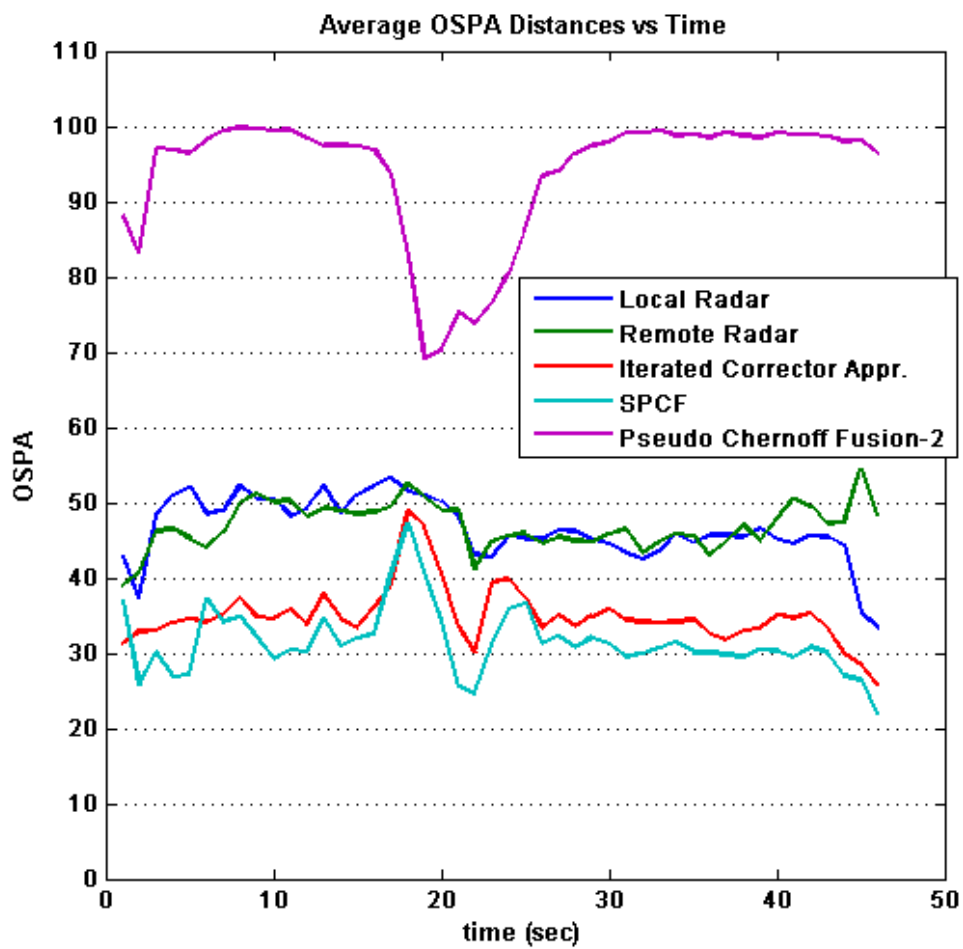


Figure 4.23: “Scenario-2”, “Method-2 with feedback”: Ensemble averaged OSPA distances of the trackers and the fusion techniques.

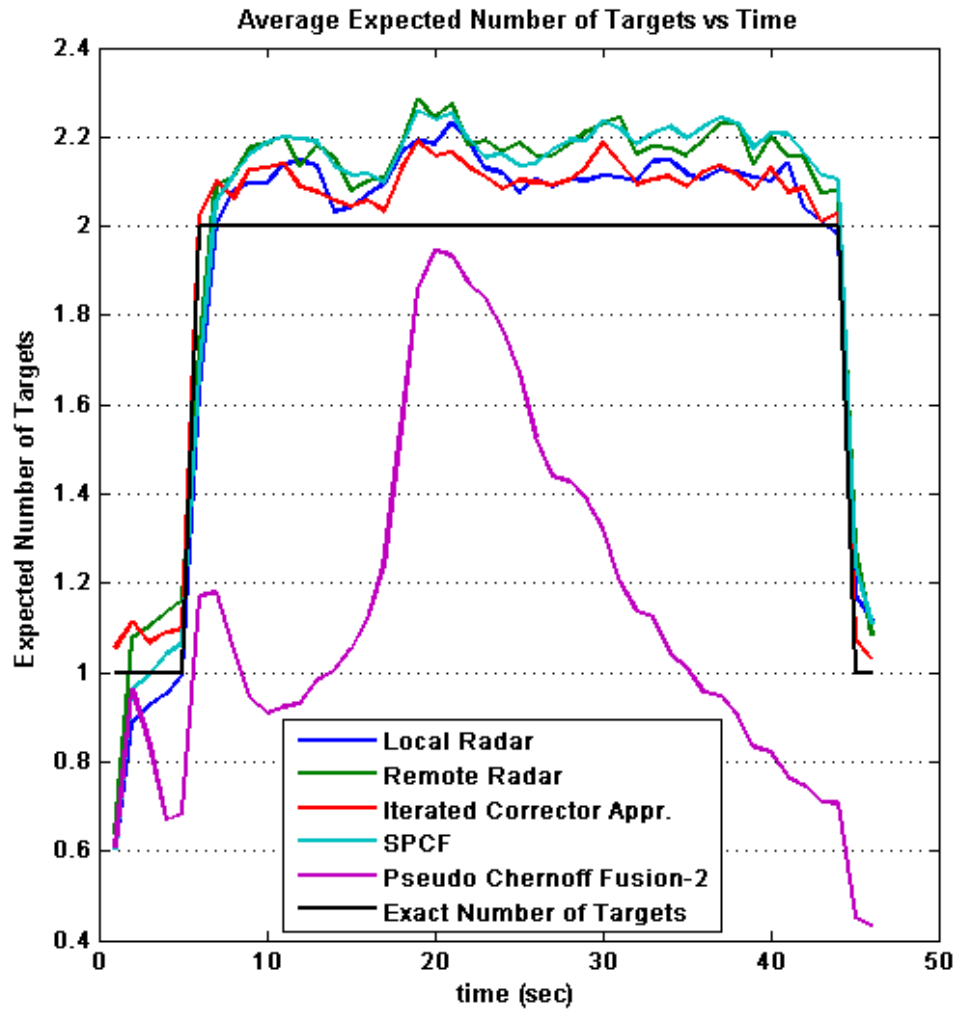


Figure 4.24: “Scenario-2”, “Method-2 with feedback”: Ensemble averaged expected number of targets of the trackers and the fusion techniques.

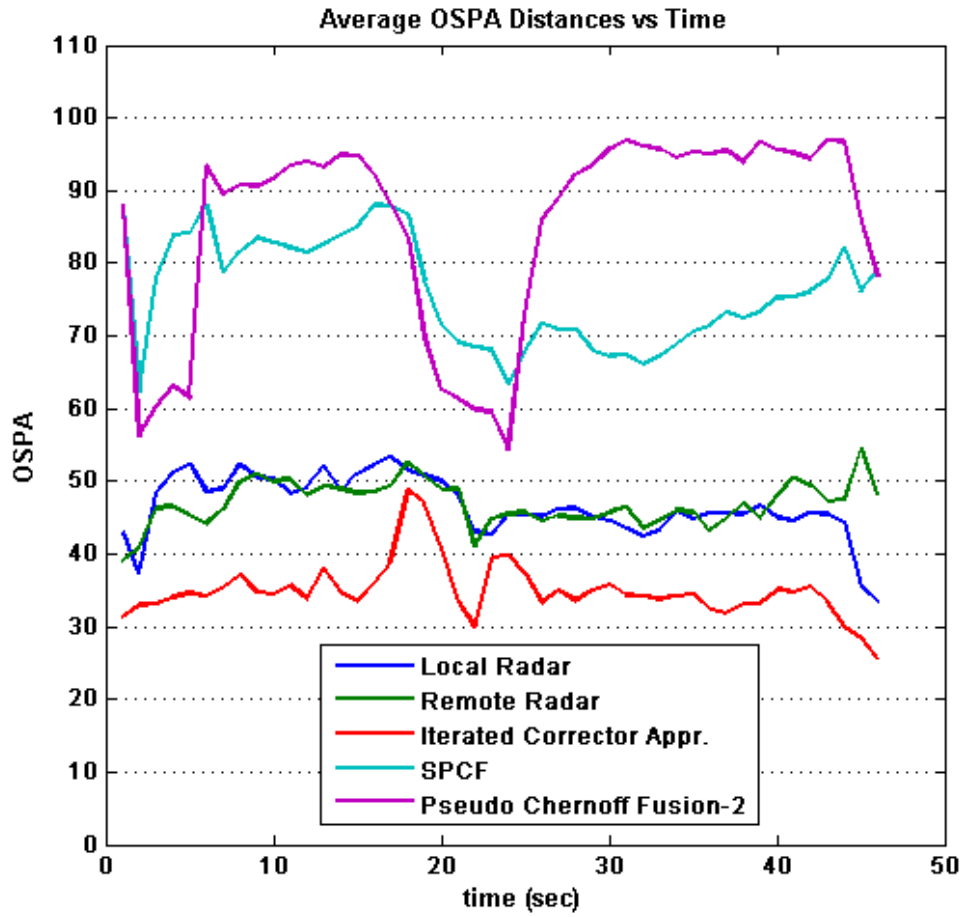


Figure 4.25: “Scenario-2”, “Method-1 without feedback”: Ensemble averaged OSPA distances of the trackers and the fusion techniques.

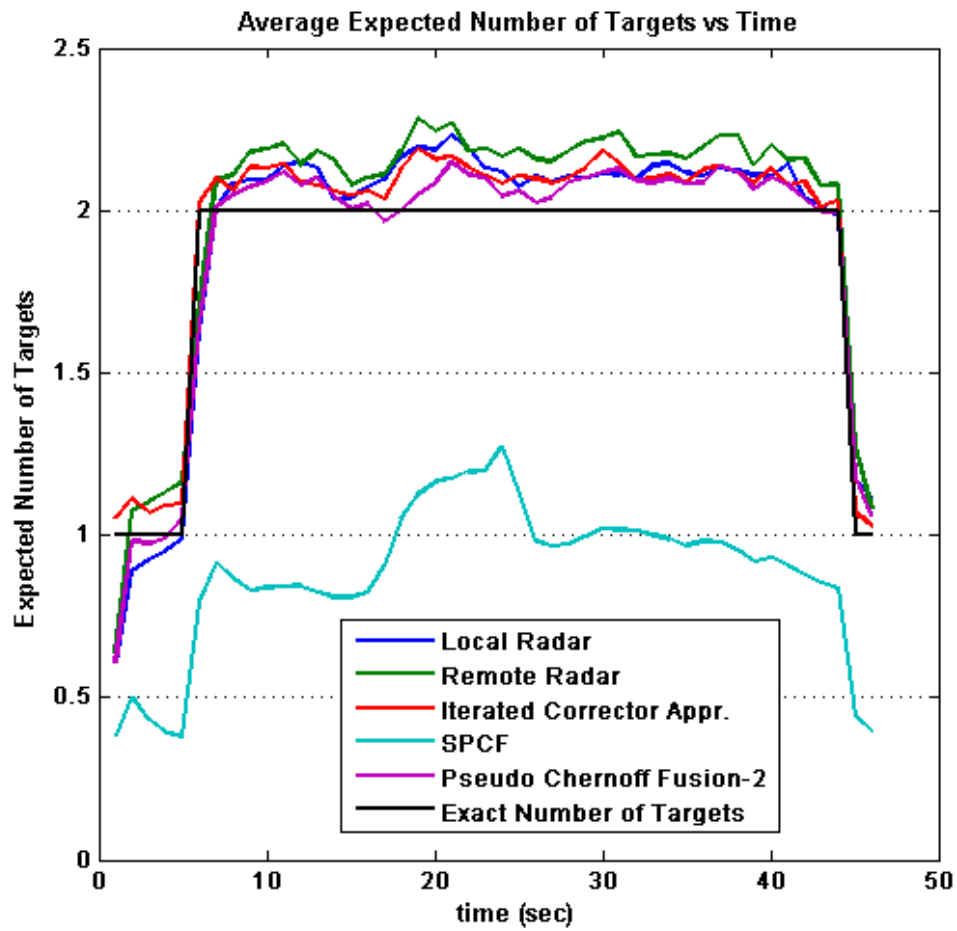


Figure 4.26: “Scenario-2”, “Method-1 without feedback”: Ensemble averaged expected number of targets of the trackers and the fusion techniques.

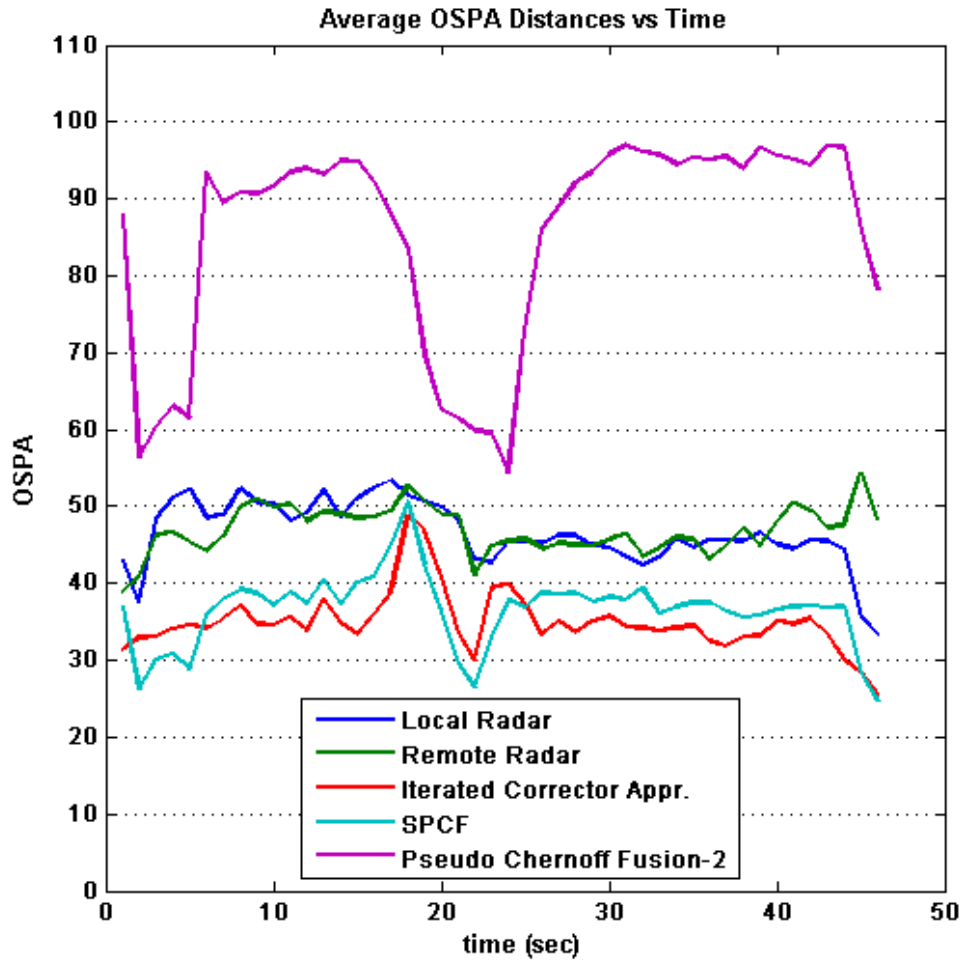


Figure 4.27: “Scenario-2”, “Method-2 without feedback”: Ensemble averaged OSPA distances of the trackers and the fusion techniques.

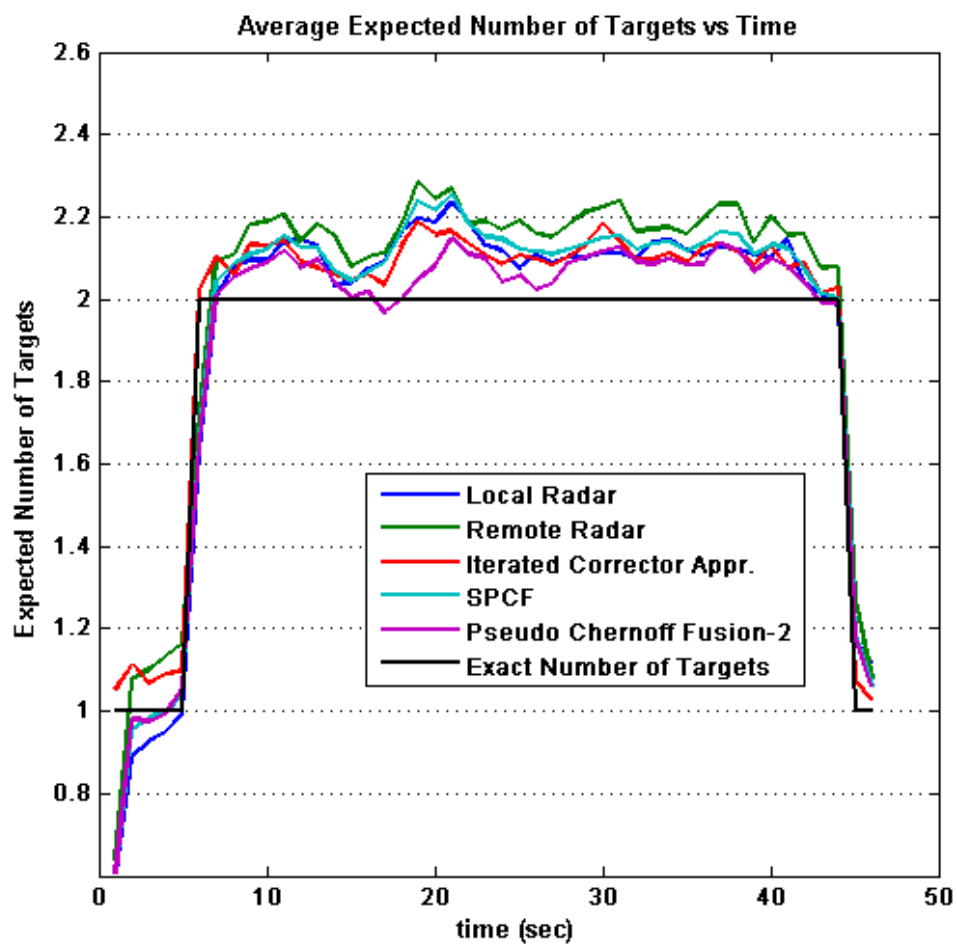


Figure 4.28: “Scenario-2”, “Method-2 without feedback”: Ensemble averaged expected number of targets of the trackers and the fusion techniques.

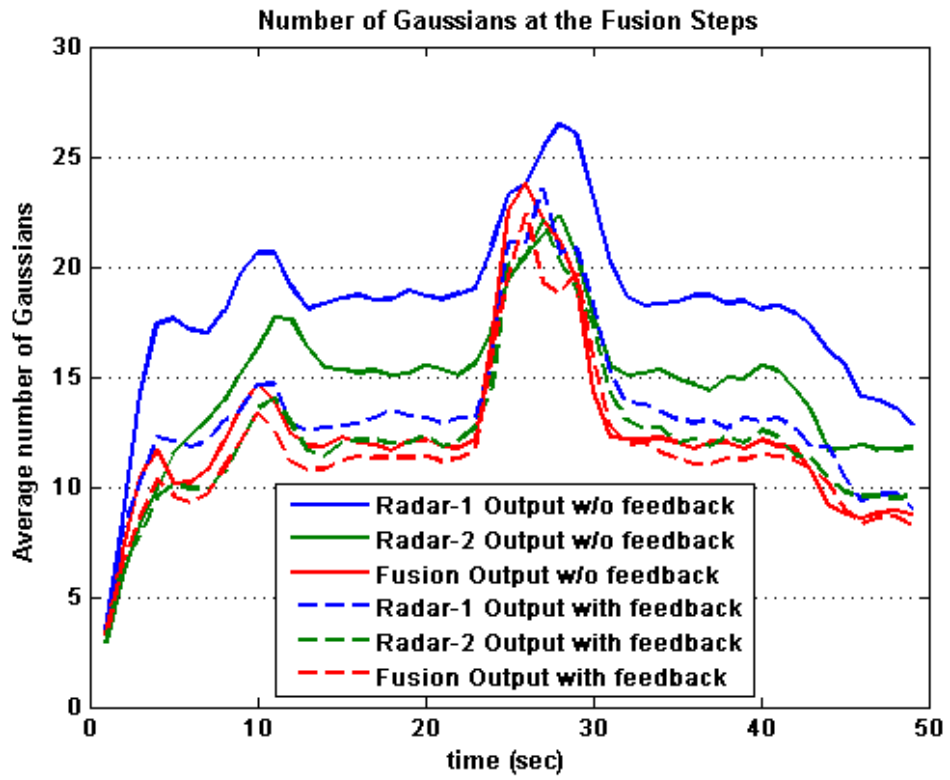


Figure 4.29: “Scenario-1”, “Method-2 with and without feedback”: Ensemble averaged number of Gaussians generated in SPCF fusion technique.

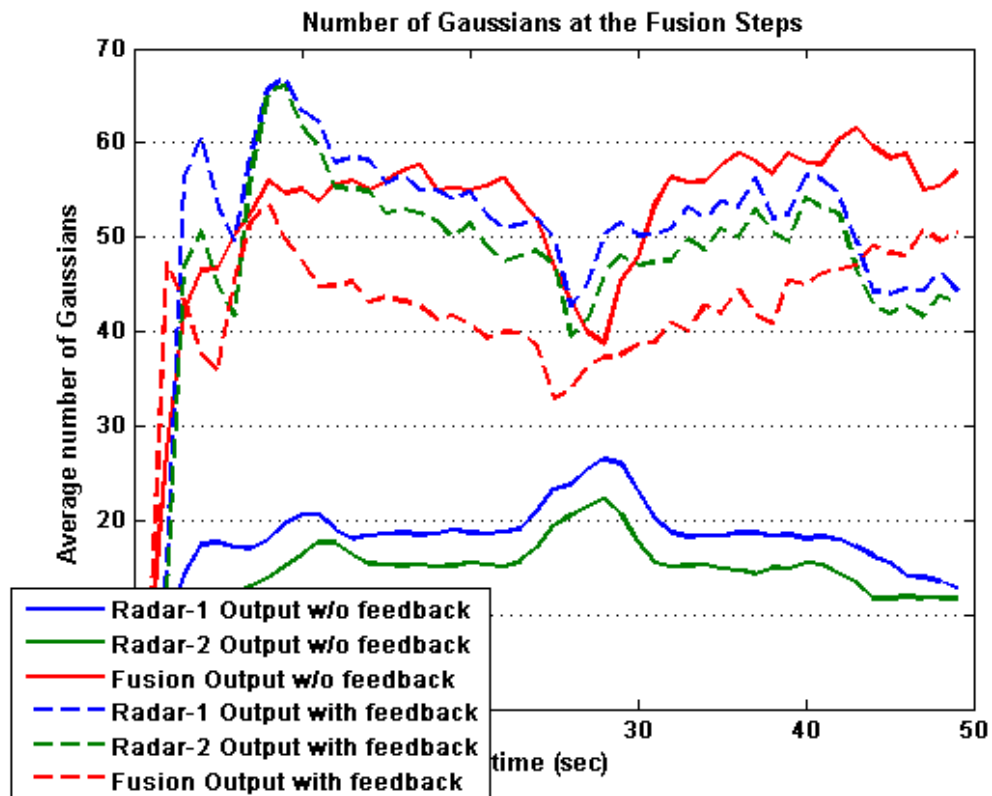


Figure 4.30: “Scenario-1”, “Method-2 with and without feedback”: Ensemble averaged number of Gaussians generated in Pseudo Chernoff-2 fusion technique.

CHAPTER 5

CONCLUSION

Unknown correlation in the data to be fused may cause in producing inconsistent results or even divergence of the over-all system. So, elimination of the commonality becomes a mandatory problem in decentralized data fusion systems. Several methods are proposed in the literature and Chernoff fusion is considered to be one of the effective techniques among all, since it brings conservativeness to the fusion operation. However, implementation of this technique is tricky because of the exponentiation of the underlying densities when these densities are not Gaussian.

Statement of this non-solved problem has been the driving force of this thesis together with its possible applications to target tracking field. Studying on the solutions to this problem and possible applications of it has resulted in three main contributions provided by this thesis to the decentralized data fusion area:

- Sigma Point Chernoff Fusion (SPCF) Technique
- Fusion of Target “Density” Functions in Track Fusion Systems
- Fusion of Target “Intensity” Functions in Track Fusion Systems

As the first contribution, SPCF, is proposed as an approximate method for Chernoff fusion of Gaussian mixtures which requires exponentiation of these functions. An arbitrary power of a Gaussian mixture is first approximated as an unnormalized Gaussian mixture by preserving the means and scaling the covariances of the original mixture. The weights of the approximating mixtures

on the other hand are found by an optimization which turns into a weighted least squares problem when a sigma-point approximation of the original density is used. The resulting Chernoff fusion formula for Gaussian mixtures then basically boils down to applying naive fusion on approximated exponentiated versions of the individual densities and therefore an analytical formulae can be obtained for the fused density which can be important in subsequent estimation stages in many practical target tracking applications. This result is important in that applying Chernoff fusion to Gaussian mixtures inevitably requires resort to numerical approaches due to the exponentiation of the mixtures. This would especially be critical in high dimensional state-spaces. The new fusion formulae, SPCF, enables the analytical evaluation of the objective function involved in the fusion if the variance is used as the corresponding uncertainty measure. Briefly, this novel technique

- provides an analytical fused density which is consistent,
- is easy to implement,
- has low computational cost compared to numerical integration.

The new fusion technique provides some new solutions to different decentralized track fusion problems. By using the proposed technique, SPCF, it is now possible to apply Chernoff fusion to a track fusion system because of the ease of its implementation for high state dimensions.

In light of this description, second contribution of the thesis is mainly raised from the application of SPCF to an IMM fusion system. The thesis analyzes the boundaries of the fusion performances of all applicable techniques and demonstrates that SPCF is a good candidate for realistic target scenarios and radar systems. In short, the analysis of the IMM fusion in this thesis brings following novelties to the literature:

- presenting a new perspective of fusing pdf's at different stages of IMM,
- proving the possibility of using Chernoff fusion for combining target state

density functions produced by IMM filter by approximating it by the SPCF technique,

- proposing and comparing different applicable IMM fusion architectures,
- determining the performance boundaries of decentralized fusion techniques for different IMM fusion architectures,
- showing that the proposed fusion technique augments the combined state estimates for also realistic target scenarios.

Third contribution mainly relies on the fusion of multiple GM-PHD filters with unknown correlation where target intensity must be fused. Fusion of PHD filters is considered for four different fusion architectures in a decentralized fusion system. These architectures include both fusion of single-object density functions and multitarget intensity functions and these are compared with each other based on the OSPA metric and expected number for targets. Following novelties are provided to the tracking world by this part of the thesis:

- bringing forward a method to fuse PHD's without referring to measurements,
- proving that it is possible to use Chernoff fusion for combining target intensity functions produced by a GMPHD filter by approximating it by the SPCF technique,
- proposing the fusion of spatial single object densities instead of multitarget intensities,
- proposing and comparing different applicable GMPHD fusion architectures.

To sum up, according to the author's opinion, this thesis has brought forward a strong tool to deal with correlated information and demonstrated its effectiveness in two main tracking applications. Certainly, there still exist some ideas given below that may improve its performance and reduce the computational demands of the algorithm:

- A closer work and deeper analysis of the basic assumptions of the SPCF method is planned. The assumptions are author's intuitive assumptions and relaxation of these assumptions and redefining the problem may lead to better Chernoff approximations, which may provide the fusion systems with higher performance.
- Grid search for the optimum w parameter in the Chernoff fusion operation may be modified so as to decrease the computation time of the SPCF algorithm. Selection of this parameter based on the past values of it sounds as a good idea yet detailed analysis on the best selection has to be performed.
- Hybrid fusion structures including various types of fusion methods seem to be a promising approach for fusion applications. Detailed investigation and further experimentation on hybrid structures is a future work for the authors.

REFERENCES

- [1] S. Arulampalam, S. Maskell, N. Gordon, and T. Clapp. A tutorial on particle filters for on-line non-linear/non-Gaussian Bayesian tracking. *IEEE Transactions on Signal Processing*, 50(2):174–188, Feb. 2002.
- [2] T. Bailey, S. Julier, and G. Agamennoni. On conservative fusion of information with unknown non-Gaussian dependence. In *Proceedings of the International Conference on Information Fusion*, pages 1876 –1883, July 2012.
- [3] Y. Bar-Shalom. On the track-to-track correlation problem. *IEEE Transactions on Automatic Control*, 26(2):571–572, Apr. 1981.
- [4] Y. Bar-Shalom and X. R. Li. *Multitarget-Multisensor Tracking: Principles, Techniques*. YBS Publishing, Storrs, CT, 1995.
- [5] Y. Bar-Shalom, X. R. Li, and T. Kirubarajan. *Estimation with Applications to Tracking and Navigation*. Wiley, New York, 2001.
- [6] A. Benaskeur. Consistent fusion of correlated data sources. In *Proceedings of the 28th Annual Conference of the Industrial Electronics Society (IECON 02)*, volume 4, pages 2652–2656, Nov. 2002.
- [7] W. Blair, G. Watson, T. Kirubarajan, and Y. Bar-Shalom. Benchmark for radar allocation and tracking in ECM. *IEEE Transactions on Aerospace and Electronic Systems*, 34(4):1097–1114, 1998.
- [8] H. A. P. Blom and Y. Bar-Shalom. The interacting multiple model algorithm for systems with Markov switching coefficients. *IEEE Transactions on Automatic Control*, 33(8):780–783, Aug. 1988.
- [9] K. Chang, C.-Y. Chong, and S. Mori. On scalable distributed sensor fusion. In *Proceedings of the 11th International Conference on Information Fusion*, June 2008.
- [10] K. Chang, C.-Y. Chong, and S. Mori. Analytical and computational evaluation of scalable distributed fusion algorithms. *IEEE Transactions on Aerospace and Electronic Systems*, 46(4):2022–2034, Oct. 2010.
- [11] L. Chen, P. Arambel, and R. Mehra. Estimation under unknown correlation: Covariance intersection revisited. *IEEE Transactions on Automatic Control*, 47(11):1879 – 1882, Nov. 2002.

- [12] C.-Y. Chong, S. Mori, W. Barker, and K.-C. Chang. Architectures and algorithms for track association and fusion. *IEEE Aerospace and Electronic Systems Magazine*, 15(1):5–13, Jan. 2000.
- [13] C.-Y. Chong, S. Mori, and K.-C. Chang. Distributed multitarget multisensor tracking. In Y. Bar-Shalom, editor, *Multitarget-Multisensor Tracking: Applications and Advances*, chapter 8. YBS, Storrs, CT, 1996.
- [14] D. Clark, A.-T. Cemgil, P. Peeling, and S. Godsill. Multi-object tracking of sinusoidal components in audio with the gaussian mixture probability hypothesis density filter. In *Proceedings of the IEEE Workshop on Applications of Signal Processing to Audio and Acoustics*, 2007.
- [15] D. Clark, S. Julier, R. Mahler, and B. Ristic. Robust multi-object sensor fusion with unknown correlations. In *Proceedings of Sensor Signal Processing for Defence (SSPD 2010)*, Sept. 2010.
- [16] D. Clark, S. Julier, R. Mahler, and B. Ristic. Robust multi-object sensor fusion with unknown correlations. In *Proceedings of the IEEE Sensor Signal Processing for Defence*, pages 1–5, September 2010.
- [17] D. Comaniciu, V. Ramesh, and P. Meer. Kernel-based object tracking. *IEEE Transactions on Pattern Analysis and Machine Intelligence*, 25(5):564–577, 2003.
- [18] E. Delande, E. Duflos, P. Vanheeghe, and D. Heurguier. Multi-sensor PHD: Construction and implementation by space partitioning. In *IEEE International Conference on Acoustics, Speech and Signal Processing (ICASSP)*, pages 3632–3635. IEEE, 2011.
- [19] M. Demirekler and E. Sarıtaş. Ortam simülâtörü algoritması. Technical report, Middle East Technical University, Electrical and Electronics Engineering Department, 2013.
- [20] N. J. Gordon, D. J. Salmond, and A. F. M. Smith. A novel approach to nonlinear/non-Gaussian Bayesian state estimation. In *IEE Proceedings on Radar and Signal Processing*, volume 140, pages 107–113, 1993.
- [21] B. K. Habtemariam, R. Tharmarasa, and T. Kirubarajan. PHD filter based track-before-detect for MIMO radars. *Signal Processing*, 92(3):667–678, 2012.
- [22] M. Hurley. An information theoretic justification for covariance intersection and its generalization. In *Proceedings of the International Conference on Information Fusion*, volume 1, pages 505–511, July 2002.
- [23] S. Julier and J. Uhlmann. A non-divergent estimation algorithm in the presence of unknown correlations. In *Proceedings of the American Control Conference*, volume 4, pages 2369–2373, June 1997.

- [24] S. Julier and J. Uhlmann. Unscented filtering and nonlinear estimation. *Proceedings of the IEEE*, 92(3):401–422, Mar. 2004.
- [25] S. Julier and J. K. Uhlmann. General decentralized data fusion with covariance intersection (CI). In D. Hall and J. Llinas, editors, *Handbook of Multisensor Data Fusion*, chapter 12. CRC Press LLC, Boca Raton, FL, 2001.
- [26] S. J. Julier. An empirical study into the use of Chernoff information for robust, distributed fusion of Gaussian mixture models. Technical report, DTIC Document, 2006.
- [27] S. J. Julier, T. Bailey, and J. K. Uhlmann. Using exponential mixture models for suboptimal distributed data fusion. In *Proceedings of IEEE Nonlinear Statistical Signal Processing Workshop*, pages 160–163, Sept. 2006.
- [28] C. L. Lawson and R. J. Hanson. *Solving Least Squares Problems*. Classics in Applied Mathematics. Society for Industrial and Applied Mathematics, 1995.
- [29] W. Li, Y. Jia, J. Du, and F. Yu. Gaussian mixture PHD filter for multi-sensor multi-target tracking with registration errors. *Signal Processing*, 93(1):86–99, 2013.
- [30] X. R. Li and V. P. Jilkov. Survey of maneuvering target tracking. part I dynamic models. *IEEE Transactions on Aerospace and Electronic Systems*, 39(4):1333–1364, 2003.
- [31] F. Lian, C. Han, W. Liu, J. Liu, and J. Sun. Unified cardinalized probability hypothesis density filters for extended targets and unresolved targets. *Signal Processing*, 92(7):1729–1744, 2012.
- [32] M. E. Liggins II, C. Y. Chong, I. Kadar, M. G. Alford, V. Vannicola, and S. Thomopoulos. Distributed fusion architectures and algorithms for target tracking. *Proceedings of the IEEE*, 85(1):95–107, Jan. 1997.
- [33] M. Longbin, S. Xiaoquan, Z. Yiyu, S. Z. Kang, and Y. Bar-Shalom. Unbiased converted measurements for tracking. *IEEE Transactions on Aerospace and Electronic Systems*, 34(3):1023–1027, 1998.
- [34] R. Mahler. *Statistical Multisource-Multitarget Information Fusion*. Artech House, Norwood, MA, 2007.
- [35] R. Mahler. The multisensor PHD filter: I. general solution via multitarget calculus. In *SPIE Defense, Security, and Sensing*, pages 73360E–73360E. International Society for Optics and Photonics, 2009.

- [36] R. Mahler. The multisensor PHD filter: II. Erroneous solution via Poisson magic. In *SPIE Defense, Security, and Sensing*, pages 73360D–73360D. International Society for Optics and Photonics, 2009.
- [37] R. Mahler. Approximate multisensor CPHD and PHD filters. In *13th Conference on Information Fusion (FUSION)*, pages 1–8. IEEE, 2010.
- [38] R. P. Mahler. Multitarget bayes filtering via first-order multitarget moments. *IEEE Transactions on Aerospace and Electronic Systems*, 39(4):1152–1178, 2003.
- [39] R. P. Mahler. Statistics 101 for multisensor, multitarget data fusion. *IEEE Aerospace and Electronic Systems Magazine*, 19(1):53–64, 2004.
- [40] R. P. S. Mahler. Optimal/robust distributed data fusion: a unified approach. In *Proceedings of the SPIE 4052, Signal Processing, Sensor Fusion, and Target Recognition IX*, pages 128–138, 2000.
- [41] C. Ouyang and H. Ji. Scale unbalance problem in product multisensor PHD filter. *Electronics Letters*, 47(22):1247–1249, 2011.
- [42] M. Roth, G. Hendeby, and F. Gustafsson. EKF/UKF maneuvering target tracking using coordinated turn models with polar/Cartesian velocity. In *17th International Conference on Information Fusion (FUSION)*, pages 1–8. IEEE, 2014.
- [43] D. Schuhmacher, B.-T. Vo, and B.-N. Vo. A consistent metric for performance evaluation of multi-object filters. *IEEE Transactions on Signal Processing*, 56(8):3447–3457, 2008.
- [44] H. W. Sorenson and D. L. Alspach. Recursive Bayesian Estimation Using Gaussian Sums. *Automatica*, 7(4):465–479, July 1971.
- [45] R. Streit. Multisensor multitarget intensity filter. In *11th International Conference on Information Fusion*, pages 1–8, June 2008.
- [46] R. L. Streit and L. D. Stone. Bayes derivation of multitarget intensity filters. In *11th International Conference on Information Fusion*, pages 1–8. IEEE, 2008.
- [47] B.-N. Vo and W.-K. Ma. The Gaussian mixture probability hypothesis density filter. *IEEE Transactions on Signal Processing*, 54(11):4091–4104, 2006.
- [48] B.-N. Vo, S. Singh, and A. Doucet. Sequential Monte Carlo implementation of the PHD filter for multi-target tracking. In *Proceedings of the International Conference on Information Fusion*, pages 792–799, 2003.

- [49] B.-T. Vo, B.-N. Vo, and A. Cantoni. The cardinalized probability hypothesis density filter for linear Gaussian multi-target models. In *40th Annual Conference on Information Sciences and Systems*, pages 681–686. IEEE, 2006.
- [50] L. Xiaodong, Z. Linhu, and L. Zhengxin. Probability hypothesis densities for multi-sensor, multi-target tracking with application to acoustic sensors array. In *2nd International Conference on Advanced Computer Control (ICACC)*, volume 5, pages 218–222. IEEE, 2010.
- [51] J. Yang and H. Ji. A novel track maintenance algorithm for PHD/CPHD filter. *Signal Processing*, 92(10):2371–2380, 2012.
- [52] Y. Zhou and J. Li. Data fusion of unknown correlations using internal ellipsoidal approximation. In *Proceedings of the 17th IFAC World Congress*, July 2008.

APPENDIX A

EK-GMPHD FILTER PSEUDO CODE

Pruning and state extraction steps required in the filter are also provided as in the Tables A.3 and A.4.

Table A.1: EK-GMPHD filter (Prediction of birth targets, prediction of existing targets, construction of PHD update components steps),(adopted from [47]).

given $\left\{w_{k-1}^{(i)}, m_{k-1}^{(i)}, P_{k-1}^{(i)}\right\}_{i=1}^{J_{k-1}}$ and the measurement set Z_k
step 1. (Prediction of birth targets)
$i = 0$ for $j = 1, \dots, J_{\gamma,k}$ $i := i + 1$ $w_{k k-1}^{(i)} = w_{\gamma,k}^{(j)}, m_{k k-1}^{(i)} = m_{\gamma,k}^{(j)}, P_{k k-1}^{(i)} = P_{\gamma,k}^{(j)}$ end for $j = 1, \dots, J_{\beta,k}$ for $l = 1, \dots, J_{k-1}$ $i := i + 1$ $w_{k k-1}^{(i)} = w_{k-1}^{(l)} w_{\beta,k}^{(j)}, m_{k k-1}^{(i)} = d_{\beta,k-1}^{(j)} + F_{\beta,k-1}^{(j)} m_{k-1}^{(l)}$ $P_{k k-1}^{(i)} = Q_{\beta,k-1}^{(j)} + F_{\beta,k-1}^{(j)} P_{k-1}^{(l)} [F_{\beta,k-1}^{(j)}]^T$ end end end
step 2. (Prediction of existing targets)
for $j = 1, \dots, J_{k-1}$ $i := i + 1$ $w_{k k-1}^{(i)} = p_{S,k} w_{k-1}^{(j)}, m_{k k-1}^{(i)} = \varphi_k(m_{k-1}^{(j)})$ $P_{k k-1}^{(i)} = G_{k-1}^{(j)} Q_{k-1} [G_{k-1}^{(j)}]^T + F_{k-1}^{(j)} P_{k-1}^{(j)} [F_{k-1}^{(j)}]^T$ where $F_{k-1}^{(j)} = \left. \frac{\partial \varphi_k(x_{k-1}, 0)}{\partial x_{k-1}} \right _{x_{k-1}=m_{k-1}^{(j)}},$ $G_{k-1}^{(j)} = \left. \frac{\partial \varphi_k(m_{k-1}^{(j)}, v_{k-1})}{\partial v_{k-1}} \right _{v_{k-1}=0},$ end $J_{k k-1} = i$
step 3. (Construction of PHD update components)
for $j = 1, \dots, J_{k k-1}$ $\eta_{k k-1}^{(j)} = h_k(m_{k k-1}^{(j)}, 0)$ $S_k^{(j)} = U_k^{(j)} R_k [U_k^{(j)}]^T + H_k^{(j)} P_{k k-1}^{(j)} [H_k^{(j)}]^T$ $K_k^{(j)} = P_{k k-1}^{(j)} [H_k^{(j)}]^T [S_k^{(j)}]^{-1}$ $P_{k k}^{(j)} = [I - K_k^{(j)} H_k^{(j)}] P_{k k-1}^{(j)}$ where $H_k^{(j)} = \left. \frac{\partial h_k(x_k, 0)}{\partial x_k} \right _{x_k=m_{k k-1}^{(j)}},$ $U_k^{(j)} = \left. \frac{\partial h_k(m_{k k-1}^{(j)}, \epsilon_k)}{\partial \epsilon_k} \right _{\epsilon_k=0},$ end

Table A.2: EK-GMPHD filter (Measurement update and outputting steps), (adopted from [47]).

step 4. (Update)
for $j = 1, \dots, J_{k k-1}$
$w_k^{(j)} = (1 - p_{D,k})w_{k k-1}^{(j)}$,
$m_k^{(j)} = m_{k k-1}^{(j)}, P_k^{(j)} = P_{k k-1}^{(j)}$
end
$l := 0$
for each $z \in Z_k$
$l := l + 1$
for $j = 1, \dots, J_{k k-1}$
$w_k^{(lJ_{k k-1}+j)} = p_{D,k}w_{k k-1}^{(j)}\mathcal{N}(z; \eta_{k k-1}^{(i)}, S_k^{(j)})$
$m_k^{(lJ_{k k-1}+j)} = m_{k k-1}^{(j)} + K_k^{(j)}(z - \eta_{k k-1}^{(j)})$
$P_k^{(lJ_{k k-1}+j)} = P_k^{(j)}$
end
end
$w_k^{(lJ_{k k-1}+j)} := \frac{w_k^{(lJ_{k k-1}+j)}}{\kappa_k(z) + \sum_{i=1}^{J_{k k-1}} w_k^{(lJ_{k k-1}+i)}}, \text{ for } j = 1, \dots, J_{k k-1}$
$J_k = lJ_{k k-1} + J_{k k-1}$
<hr/> output. $\left\{w_k^{(i)}, m_k^{(i)}, P_k^{(i)}\right\}_{i=1}^{J_k}$ <hr/>

Table A.3: EK-GMPHD filter (Pruning step), (adopted from [47]).

given $\left\{w_k^{(i)}, m_k^{(i)}, P_k^{(i)}\right\}_{i=1}^{J_k}$, a truncation period T , a merging threshold U , and a maximum allowable number of Gaussian terms J_{max} , Set $l = 0$, and $I = i = 1, \dots, J_k w_k^{(i)} > T$.
repeat
$l := l + 1$
$j := \arg \max_{i \in I} w_k^{(i)}$
$L := \left\{i \in I (m_k^{(i)} - m_k^{(j)})^T (P_k^{(j)})^{-1} (m_k^{(i)} - m_k^{(j)}) \leq U\right\}$
$\tilde{w}_k^{(l)} = \sum_{i \in L} w_k^{(i)}$
$\tilde{m}_k^{(l)} = \frac{1}{\tilde{w}_k^{(l)}} \sum_{i \in L} w_k^{(i)} x_k^{(i)}$
$\tilde{P}_k^{(l)} = \frac{1}{\tilde{w}_k^{(l)}} \sum_{i \in L} w_k^{(i)} (P_k^{(i)} + (\tilde{m}_k^{(l)} - m_k^{(i)})(\tilde{m}_k^{(l)} - m_k^{(i)})^T)$
$I := I \setminus L$
until $I = \emptyset$
if $l > J_{max}$ then replace $\left\{\tilde{w}_k^{(i)}, \tilde{m}_k^{(i)}, \tilde{P}_k^{(i)}\right\}_{i=1}^l$ by those of the J_{max} Gaussians with largest weights.
output $\left\{\tilde{w}_k^{(i)}, \tilde{m}_k^{(i)}, \tilde{P}_k^{(i)}\right\}_{i=1}^l$ as pruned Gaussian components.

Table A.4: EK-GMPHD filter (Multitarget state extraction), (adopted from [47]).

given $\left\{w_k^{(i)}, m_k^{(i)}, P_k^{(i)}\right\}_{i=1}^{J_k}$
Set $\hat{X}_k = \emptyset$
for $j = 1, \dots, J_k$
if $w_k^{(j)} > 0.5$
for $j = 1, \dots, \text{round}(w_k^{(j)})$
update $\hat{X}_k = [\hat{X}_k, m_k^{(j)}]$
end
end
end
output \hat{X}_k as the multi-target state estimate.

CURRICULUM VITAE

PERSONAL INFORMATION

Surname, Name: Günay, Melih

Nationality: Turkish (TC)

Date and Place of Birth: 06.05.1981, Konya-Ereğli

Marital Status: Married

Phone: +90-312-2863731 **Fax:** NA

EDUCATION

Degree	Institution	Year of Graduation
M.Sc.	METU Electrical and Electronics Eng.	2007
B.Sc.	METU Electrical and Electronics Eng.	2004
High School	İzmir Science High School	1999

PROFESSIONAL EXPERIENCE

Year	Place	Enrollment
2004-Present	ASELSAN Inc.	Systems Engineer

PUBLICATIONS

International Conference Publications

- M. Günay, M. Demirekler, U. Orguner, “Approximate Chernoff Fusion of Gaussian Mixtures Using Sigma Points”, 17th International Conference on

Information Fusion, Fusion-2014, July 2014, Salamanca-Spain

- H. I. Turan, M. Demirekler, M. Gunay, “A Novel Methodology for Target Classification Based on Dempster-Shafer Theory”, 3rd International Conference on Belief Functions, Belief-2014, September 2014, Oxford-UK

National Conference Publications

- M. Günay, M. Demirekler, “Quantization of Covariance Matrices” (in Turkish), National Automatic Control Conference, Ankara-Turkey, 2006, s.44-49.
- M. Günay, M. Demirekler, “Representation of covariance matrices in track fusion problems”, Signal Processing, Communication and Applications Conference, 2008. SIU 2008, IEEE 16th.
- M. Demirekler , E. Özkan, Y. Özbek, M. Günay, B. Özer, “Augmentation of Fusion Performance by Combining Different Levels of Fusion Layers in Decentralized Defence Systems” (in Turkish), Defense Technologies Conference, Ankara-Turkey, 2008
- M. Günay, O.S. Tapkan, M.A. Özgün, “Ground Based Air Defense Sub-Systems” (in Turkish), Defense Technologies Conference, Ankara-Turkey, 2008
- S. Özgen, U. Orguner, M. Günay, D. Acar, “Usage of Asynchronous Auction Algorithm in Track Fusion Systems” (in Turkish), Defense Technologies Conference, Ankara-Turkey, 2014
- H. İ. Turan, M. Demirekler, M. Günay, “Classification of Air Targets Based on Dempster Shafer Theory” (in Turkish), Defense Technologies Conference, Ankara-Turkey, 2014

AWARDS

- 2014 Middle East Technical University Electrical and Electronics Engineering Department Graduate Research Workshop 3rd Place Winner for the

study “Approximate Chernoff Fusion of Gaussian Mixtures Using Sigma Points”

PATENTS

- M. Günay, İ. Yüksel Ergün, “A test and analysis system and a method for threat evaluation and sensor/weapon assignment algorithms”, U.S. Patent Application No. 14/241,076, Patent Cooperation Treaty PCT/IB2013/052367 Unpublished (Filling date Mar. 25, 2013)